Control of GAbp Transcription Factor Activity Through Pro-Inflammatory Signalling

PhD Thesis submitted to the Combined Faculties for Natural Sciences and for Mathematics of the Ruperto-Carola University of Heidelberg, Germany, for the degree of Doctor of Natural Sciences

Presented by Anna Margareta Gail, Master of Science (Biochemistry) at the Technical University Munich, Germany, born on the 28th September 1979 in Wiesbaden, Germany

Reviewers: Prof. Dr. Peter Angel, DKFZ, Heidelberg, and Dr. Stephan Herzig, DKFZ, Heidelberg

Zusammenfassung

Eine systemische Entzündungsreaktion tritt häufig bei einer progressiven Krebserkrankung auf. Die auf den Entzündungsreiz hin aktivierte Immunantwort ist außer Kontrolle geraten und führt zur gravierenden Ausschüttung an pro-inflammatorischen Zytokinen, z.B. TNF-α. Diese dyfunktionale Immunreaktion führt zur Beeinträchtigung von bis dato gesunden Organen, wie z.B. dem Skelettmuskel. Die dem Prozeß der Muskelatrophie zugrundeliegenden molekularen Mechanismen sind insbesondere auf transkriptioneller Ebene weitestgehend unbekannt.

Aus diesem Grund wurde ein zellbasierter Screen im Hochdurchsatzverfahren durchgeführt, um jene transkriptionelle Regulatoren zu identifizieren, deren Aktivität sich unter atrophischen Bedingungen verändert. Eine Behandlung von HEK293T Zellen mit TNF-α führte zu einer deutlichen Erniedrigung der transkriptionellen Aktivität der DNA-bindenden Komponente des Ets Transkriptions Faktors GAbp, GAbpα. Die für die transkriptionelle Aktivität notwendige funktionale Interaktion von GAbpα mit der zweiten GAbp Untereinheit, GAbpβ, war in TNF-α behandelten C2C12 Zellen, einer murinen Muskelzelllinie, ebenfalls signifikant reduziert. Weiterhin konnte gezeigt werden, daß die Dissoziation des transkriptionell aktiven Heterodimers lediglich die minimalen Bindedomänen von GAbpα und GAbpβ benötigt, für TNF-α spezifisch ist und über eine intrazellulären Anhäufung von reaktiven Sauerstoff-Spezies (ROS) erfolgt. Im Muskel wird die Aktivität von GAbp durch den Wachstumsfaktor Neuregulin (NRG) erhöht und führt zur Expression von sub-synaptischen Genen (z.B. epsilon Untereinheit des Acetylcholin-Rezeptors (AChRε)), welche für die Innervation des Muskels durch motorische Nervenzellen unerläßlich sind. Die NRG-abhängige Aktivierung des AChRε-Promotors als auch der AChRε-mRNA Expression wurde in Gegenwart von TNF-α signifikant eingeschränkt, wobei diese Effekte spezifisch für TNF-α waren und über ROS erfolgten. Zudem war die Expression von sub-synaptischen GAbp Zielgenen in einem Mausmodel entzündlicher Tumorkachexie inhibiert.

Eine pro-inflammatorische Stimulation von Muskelzellen führt über intrazellulär aktivierte ROS zur Erniedrigung der transkriptionellen Aktivität von GAbp. Die daraus resultierende reduzierte Genexpression von sub-synaptischen GAbp Zielgenen könnte

zur Denervation des Muskels führen und somit wesentlich zur Muskelatrophie im Kontext systemischer Entzündungsreaktionen oder des Alterungsprozesses beitragen.

Summary

Cancer and the Metabolic Syndrome are debilitating human diseases being accompanied by a dysregulated immune response frequently resulting in systemic inflammatory processes. Circulating pro-inflammatory cytokines (e.g. TNF-α) target metabolic tissues, like skeletal muscle - a process leading to muscle atrophy. The molecular mechanisms of the underlying transcriptional control still remain elusive. Therefore, the identification of transcriptional regulators with altered transcriptional activity in response to atrophic conditions was addressed in this study.

In a cell-based high-throughput screen, the transcriptional activity of GAbpα, the DNA-binding component of the Ets transcription factor GAbp, significantly decreased upon TNF-α treatment. Subsequent analysis in the murine muscle cell line C2C12 revealed that reactive oxygen species (ROS) mediate TNF-α-dependet dissociation of GAbpα and GAbpβ, the transcriptional activation domain component of GAbp. This alteration of GAbp complex interaction was specific to TNF-α, and the minimal binding domains of GAbpα and GAbpβ were sufficient for TNF-α mediated dissociation. Moreover, TNF-α efficiently blocked the neuregulin growth factor (NRG) mediated activation of a GAbpα the DNA consensus motif of GAbpα, thus suggesting that dissociation of the transcriptional active GAbp heterodimer is implicated in GAbp target gene expression. This was further supported by the finding that NRG-induced expression of the sub-synaptic GAbp target gene, epsilon subunit of the acetylcholine receptor (AChRε), was restraint specifically by TNF-α. ROS inhibitors efficiently rescued this altered gene expression of AChRε under pro-inflammatory conditions.

Taken together, formation of ROS links pro-inflammatory TNF-α signalling in muscle cells to GAbp complex dissociation and thereby decreases the transcriptional activity of GAbp. This altered activity leads to decreased gene expression of GAbp sub-synaptic target genes; thus, suggesting that accumulation of ROS under atrophic conditions may lead to denervation of muscle cells causing muscle atrophy.

Acknowledgments

First, I would like to thank Stephan Herzig for giving me the opportunity to perform my PhD Thesis in his research group, for offering me the interesting screen as starting project, for his continuous support and significant input. In addition, I am grateful to Ulrike Hardeland, who had important impact on making this project happen, for technical advice, for revising the manuscript and for many helpful discussions. In addition, I am much obliged to Michael Dale Conkright from the Scripps Research Institute in Jupiter, Florida (USA), for collaboration on the Cell-Based High-Throughput Screen, crucial input and giving me the opportunity to join his lab for the screen. Furthermore, I would like to acknowledge Veit Witzemann from the *Max-Planck Institut für medizinische Forschung* for many interesting input and discussions regarding the neuromuscular junction.

Next, I thank all past and current lab members from the Molecular Metabolic Control Research Group at the DKFZ for providing an interesting scientific and social environment, in which advice was kindly provided at all times. In this context, I thank Anke Ostertag for cooperation on the lentivirus project, Alexander Vegiopoulos for useful input regarding the statistical analysis of the data and for providing muscle tissue from his mice experiments. Furthermore I am grateful to Antje Reuter, Joerg Schweitzer, and Daniela Strzoda for technical support.

I would also like to thank my thesis advisory committee, Renate Voit and Peter Angel, for their continuous support.

Last but not least, I am very grateful to my family and friends for supporting me throughout my studies and being always especially supportive and understanding. Many thanks go as well to Zita, Samson, Delilah and Herr Löw for being there.

Abbreviations

AChR	Nicotinic Acetylcholine Receptor
AChRε	Nicotinic Acetylcholine Receptor, epsilon subunit
AChREst	Nicotinic Acetylcholine Receptor Esterase
ANK	Ankyrin repeats
ß-gal	ß-galactosidase reporter
BSA	Bovine Serum Albumin
cDNA	Complementary DNA
CIP	Calf Intestine Phosphatase
CM-RAW	Conditioned RAW medium
CMV	Cytomegalovirus promoter
DBD	DNA binding domain
Dex	Dexamethasone
DM	Differentiating Medium
DMEM	Dulbecco´s Modified Eagle´s Medium
DNA	Desoxyribonucleic acid
EC	electrocompetent
EGF	Epidermal growth factor domain
ErbB	Tyrosine kinase-type cell surface receptor HER2
FCS	Fetal Calf Serum
FL	Full length protein
GAPDH	Glyceraldehyde-3-phosphate dehydrogenase
GAbpα	GA binding protein alpha
GAbpβ	GA binding protein beta
GFP	Green fluorescent protein
GM	Growth Medium
GR	Glucocorticoid Receptor
HEK	Human embryonic kidney cells
HRP	Horseradish Peroxidase
IFN-γ	Interferon-γ
IGF-1	Insulin-like growth factor 1
IL-1β, IL-6	Interleukin 1 beta, Interleukin 6
IκBα, NFKBIA	NF-κB inhibitory protein
IP	Immunoprecipitation
LB	Luria-Bertani

ABBREVIATIONS

LeuZip	Basic Leucine zipper domain
LPS	Lipopolysaccharides
Luc	Luciferase Reporter
miRNA	Micro RNA
MAFbx/ atrogin-1	Muscle Atrophy F-box
MCS	Multiple cloning site
miRNA	Micro RNA
MnTBAP	Mn(III)tetrakis(4-benzoic acid)porphyrin Chloride
MOI	Multiplicity of infection
MRF	Myogenic regulatory factor
MuRF1	Muscle RING Finger 1
MuSk	Muscle-specific tyrosine protein kinase receptor
NAC	*N*-acetycysteine
NC	Negative control
NF-κB	Nuclear factor κB
NLS	Nuclear localization signal
NMJ	Neuromuscular junction
NRG	Neuregulin (here: human NRG-β1/HRG- β1)
ORF	Open reading frame
ON	overnight
PCI	Phenol:Chloroform:Isoamylalkohol
PCR	Polymerase chain reaction
PhoSit	Phosphorylation sites
PNT	Pointed domain
PPI	Protein-Protein Interaction
P/S	Penicillin-Streptomycin
PSPC1	Paraspeckle component 1
qRT-PCR	Quantitative Real-Time PCR
RNA	Ribonucleic acid
ROS	Reactive oxygen species
RT	Room temperature
SDS-PAGE	Sodium dodecyl sulphate polyacrylamide gel electrophoresis
TAD	Transcriptional activation domain
TBP	TATA binding protein
TF	Transcription factor
TNF-α	Tumour necrosis factor-alpha
TU	Transforming units

ABBREVIATIONS

UTR	Untranslated regio
VCP	Valosin containing protein
Vp16	TAD from herpes simplex virus (HSV)
WB	Western-Blot

Contents

CONTENTS

CONTENTS

1 Introduction

1.1 Inflammation – an Adaptive Response to Severe Disturbances of Body Homeostasis

Inflammatory pathways of the innate and adaptive immune response are activated in response to infection or tissue injury and represent a disturbance of body homeostasis. The ultimate goal of the innate and adaptive immune response is to combat infection, to restore tissue structure and function, and regain thereby a vital body homeostasis. Much progress has been made in understanding the acute inflammatory reactions, being activated upon infection or tissue injury, and the localized chronic inflammation pathways, being triggered upon autoimmune diseases and chronic infections (Medzhitov 2008). However, the events leading to subacute or chronic inflammation still await their detailed understanding. In these cases, the immune response is incapable to clearly resolve the inflammation process at the site of origin. Moreover, a persistent inflammation response may even emanate to other tissues by circulating inflammatory mediators, a progress named systemic inflammation. Cancer and the Metabolic Syndrome (including obesity, insulin resistance, atherosclerosis, etc.) are often accompanied by a systemic inflammation response. Since the abundance of food and increased life expectancy are no more solely characteristics of the western industrialized nations, the prevalence for developing cancer and/ or the Metabolic Syndrome increases worldwide (Popkin 2007). In this context, several epidemiological studies indicate that several types of cancer are obesity related suggesting a correlation between these two diseases (Calle & Kaaks 2004).

The inflammatory pathway is characterized by coordinated reactions of the innate and adaptive immune response. The innate immune system, being activated within minutes to hours, consists of phagocytes, antigen-presenting cells, the complement system and natural killer cells. It functions to recognize, label and neutralize - by binding or destruction - the noxious stimulus. Most importantly, the innate immune response informs the adaptive immune response, so that the latter can mount an adequate reaction. A “classical” inflammatory reaction can be functionally categorized into four

participating classes: inducers, sensors, mediators, effectors (Medzhitov 2008) (Figure 1). The release of cellular constituents, ATP and K^+ ions for instance, from a necrotic cell represents an endogenous inducer. These components may be detected by tissue-resident macrophages (sensors), which in turn produce cytokines (mediators). Macrophages are able to distinguish whether the surrounding tissue cells are in a basal or malfunctioning state and report accordingly to the immune system. Finally, the released cytokines act on tissues and organs (effectors) leading to diverse reactions as further recruitment and activation of the components of the innate immune response and the development of a highly specific memory by the adaptive immune response. A chronic inflammation response is characterized by abnormal cytokine production, increased acute-phase reactants, activation of a cascade of inflammatory signalling pathways and the dominating presence of macrophages in the injured tissue (Hotamisligil 2006). These activated macrophages release inflammatory mediators which may act on otherwise healthy tissue turning the inflammation response into a systemic inflammation process.

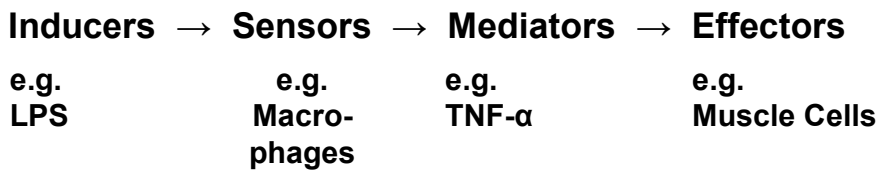

Figure 1: Inducers, sensors, mediators and effectors are involved in the course of a generic inflammatory pathway. LPS, an exogenous inducer, causes activation of macrophages, which act hereby as sensors. This process triggers the secretion of TNF-α from macrophages and finally effects tissues as the muscle. However, inducers such as LPS can also act directly on effectors (Medzhitov 2008).

On the molecular level, two signalling pathways have emerged as important regulators of the coordinated immune response with yet opposing reactions (Figure 2). While the pro-inflammatory nuclear factor (NF)-κB pathway promotes expression of cytokines and acute phase proteins, the glucocorticoid-mediated signalling pathway causes an inhibition of pro-inflammatory cytokine expression (McKay & Cidlowski 1999). The NF-κB signalling cascade is activated via extracellular stimuli, such as pro-inflammatory cytokines (e.g. tumor necrosis factor (TNF)-α), lipopolysaccharide (LPS) or oxidative stressors. NF-κB is a dimeric transcription factor with the p65/p50 heterodimer representing the "classical" NF-κB heterodimer. Under unstimulated

conditions NF-κB resides in the cytoplasm while bound to the NF-κB inhibitory protein (IκBα). Upon activation of the pathway, IκBα is phosphorylated and targeted to protein degradation via ubiquitylation. Thereby, the nuclear localization signal (NLS) on the p65 subunit gets exposed, and the dimer shuttles into the nucleus where it binds to κB-responsive elements in promoter sequences of target genes (Figure 2).

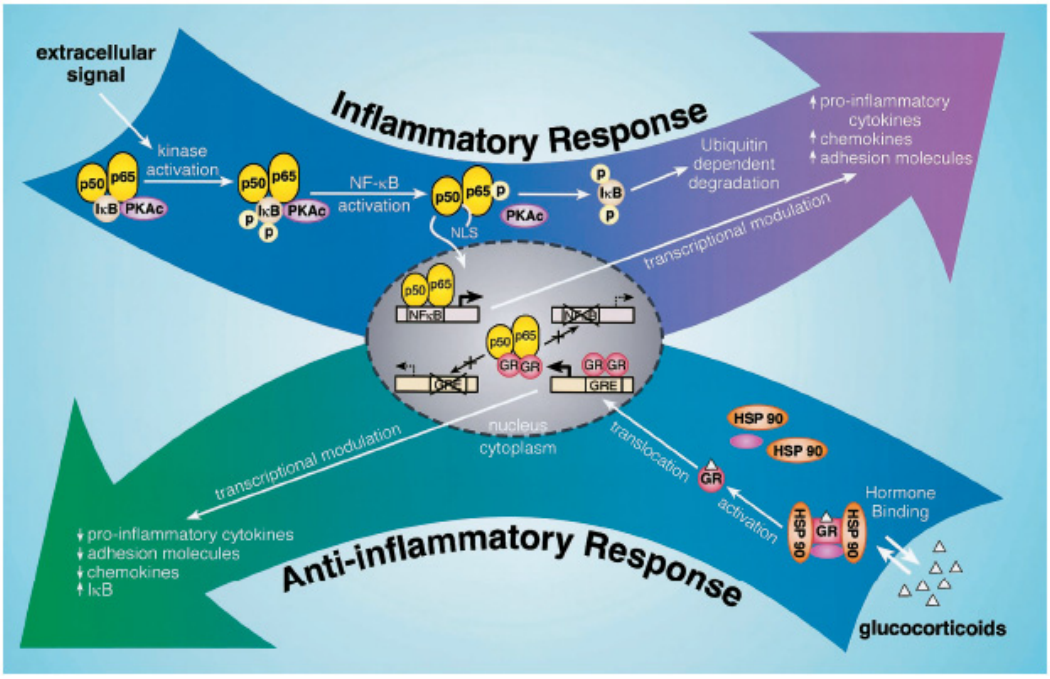

Figure 2: The NF-κB and glucocorticoid receptor (GR) pathway act as physiological antagonists during an inflammation response. While the NF-κB pathway drives production of pro-inflammatory cytokines, the GR pathway suppresses this effect. See text for details (McKay & Cidlowski 1999).

The anti-inflammatory response via glucocorticoid signalling is driven by binding of glucocorticoids to their cognate receptor, the glucocorticoid receptor (GR). GR is also anchored in the cytoplasm in complex with inhibitor proteins (Hsp90). The canonical GR pathway is then activated by binding of the hormone ligand to its cognate receptor with subsequent translocation into the nucleus, homodimerization of the GR and binding to glucocorticoid response elements (GRE) in promoter sequences of respective target genes (Figure 2). Glucocorticoids are a class of steroid hormones which are involved in glucose metabolism. In this context, they stimulate hepatic gluconeogenesis by transcriptional activation of genes crucial for gluconeogenesis. Furthermore, they mediate the mobilization of amino acids from extrahepatic tissues, inhibit glucose uptake in muscle and adipose tissue, and stimulate lipolysis in adipose tissue. Due to

their potent anti-inflammatory properties, glucocorticoids are widely used as immune suppressive drugs. However, when used for a longer time period or at higher doses, the desired anti-inflammatory effects of glucocorticoids are opposed by its role in regulating glucose metabolism. In this setting, the degradation of amino acids from muscle tissue for hepatic gluconeogenesis can cause serious tissue damage to the muscle (Goldberg 1969).

A balanced action of both pro- and anti-inflammatory pathways is a prerequisite for a controlled inflammation response. Usually, this response continues until the affected tissue-site is restored in its functionality. However, a dysregulated or chronic inflammation response can become detrimental resulting in serious tissue damage of otherwise healthy tissues, which did not contain the primary site of origin for the inflammation process. The skeletal muscle is one putative secondary effector site in the context of a systemic subacute or chronic inflammation.

Moreover, skeletal muscle atrophy and insulin resistance of the muscle have been reported to be associated with certain types of cancer and the Metabolic Syndrome (Tisdale 2002; Wei et al. 2008). However, the detailed understanding of these pathological states of muscle tissue is still unresolved.

1.2 Muscle Atrophy – a Dysregulation of Muscle Mass Homeostasis Occurring under Chronic Inflammation

The main function of the skeletal muscle is contraction, which is accomplished on the molecular level by the interaction between two muscle specific proteins, myosin and actin. In addition to this actomyosin complex, the neuromuscular junction (NMJ) represents another structural prerequisite for muscle contraction. The neuromuscular junction includes the nerve terminal of a motor neuron and the sub-synaptic membrane of an innervated skeletal muscle cell, both cells being separated from another through the synaptic cleft (Mejat et al. 2003). Secretion of the neurotransmitter acetylcholine from the nerve cell and binding to the nicotinic acetylcholine receptor (AChR), a heteropentameric ($AChR\alpha_2\beta\gamma/\varepsilon\delta$) ligand-gated ion-channel, at the muscle cell induces a structural conformation change, which results finally in muscle contraction. During

early neonatal development, the fetal γ-subunit of the AChR is replaced by the ε-subunit. The latter has been shown to be crucial for the NMJ, since *in vivo* deletion lead to muscle weakness and atrophy (Witzemann et al. 1996). Besides the function to innervate the muscle, the motor neuron exerts also a trophic influence on the skeletal muscle by secreting growth factors, as for instance neuregulins, which induce muscle specific transcription of sub-synaptic target genes.

The healthy state of muscle metabolism is tightly regulated by anabolic and catabolic processes. A dysregulation of this homeostasis results in either increase or decrease of muscle mass, named accordingly hypertrophy or atrophy. Skeletal muscle atrophy is most often characterized by a reduced protein synthesis and augmented proteolysis. Fasting, tissue injury, denervation or disuse are known triggers for skeletal muscle atrophy. In addition, muscle atrophy has been also observed in the context of systemic diseases, such as insulin resistance and certain types of cancer. Upon association with chronic diseases this pathology is called cachexia (McKinnell & Rudnicki 2004). Since augmented proteolysis is a hallmark of skeletal muscle atrophy, focus has been put on elucidating this catabolic pathway in skeletal muscle tissue. The degradation of proteins in muscle cells is accomplished by lysosomal proteolysis, calpains or the ATP ubiquitin-dependent proteasome. While extracellular proteins are degraded by the lysosomal system, intracellular proteins are substrates to the calpains and the proteasome (Tisdale 2002). Of these three pathways, the ATP ubiquitin-dependent proteolytic pathway was shown to be predominant in muscle atrophy. Proteins destined for degradation are recognized by ubiquitin ligases and accordingly covalently conjugated to multiple chains of the 76-amino acid polypeptide ubiquitin. Such posttranslationally modified proteins are terminally targeted to the proteasome for proteolysis.

In the past decade, two ubiquitin protein ligases have been discovered to play a crucial role in different states of muscle atrophy: Muscle RING Finger 1 (MuRF1) and Muscle Atrophy Factor F-box (MAFbx). Bodine *et al.* identified both ubiquitin protein ligases to be upregulated in three *in vivo* models of skeletal muscle atrophy, denervation, immobilization and hindlimb suspension (Bodine et al. 2001). In another study, the

mRNA levels of MAFbx were found to be augmented in a fasting model of atrophy and hence this protein was also named atrogin-1 (Gomes et al. 2001). Moreover, the expression of MuRF1 and MAFbx was increased in two further *in vivo* models of muscle atrophy: systemic treatment with either the pro-inflammatory cytokine interleukin-1 (IL-1) or the synthetic glucocorticoid dexamethasone (Dex) (Bodine et al. 2001). Additionally, activation of the inflammatory nuclear factor (NF)-κB pathway was found to enhance MuRF1 promoter activity in C2C12 cells, a murine muscle cell line (Cai et al. 2004). These diverse *in vivo* and *in vitro* models, suggest that the up-regulation of ubiquitin ligases, which are implicated in proteolysis via the ATP-dependent proteasome pathway, represents a common feature of muscle atrophy. Furthermore, the increased catabolism in muscle tissue undergoing atrophy seems to be mediated by both NF-κB- and glucocorticoid-signalling.

1.3 Molecular Mechanisms Leading to Muscle Hypertrophy and Atrophy

Following the initial discovery of the two ubiquitin protein ligases being implicated in skeletal muscle atrophy, the detailed understanding of the molecular events was of significant interest. More precisely, the question to answer was, if anabolic pathways were likewise dysregulated as catabolic pathways. Insulin and insulin-like growth factor I (IGF-1) are known to counteract the effects of glucocorticoids by promoting protein synthesis and growth (Ma et al. 2003). IGF-1 mediated activation of Akt by phosphorylation results in augmented protein synthesis promoted mainly by Akt targets such as Glycogen synthase kinase 3 (GSK3) or the mammalian target of rapamycin (mTOR). In addition, IGF-1 was shown to reduce atrogin-1 expression via the IGF-1/PI3K/Akt pathway (Sacheck et al. 2004; Stitt et al. 2004). In this context, Sandri *et al.* have shown that upon inhibition of Foxo3, this transcription factor is unable to induce expression of MAFbx/atrogin-1 mRNA (Sandri et al. 2004). In parallel, Akt phosphorylates FOXO transcription factors thereby excluding them from entry into the nucleus and rendering them transcriptionally inactive (Stitt et al. 2004). Thus, the up-regulation of the ubiquitin ligase MAFbx/atrogin-1 is inhibited under anabolic conditions providing a molecular mechanism for decreased catabolism in muscle hypertrophy.

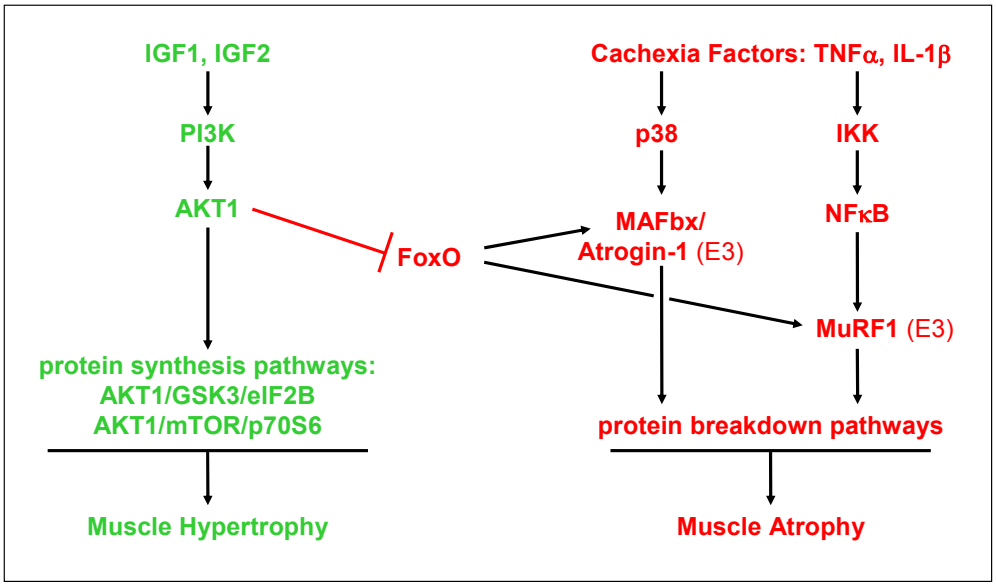

Figure 3: The PI3K/Akt signal transduction pathway in muscle hypertrophy and atrophy (McKinnell & Rudnicki 2004). Binding of the insulin growth factor (IGF-1) to its cognate receptor on the cell membrane activates the PI3Kinase pathway resulting finally in phosphorylation of the Foxo transcription factor. Such modified Foxo remains in the cytoplasm and is prevented from inducing expression of MAFbx/atrogin-1 mRNA within the nucleus. This molecular mechanism causes most probably muscle hypertrophy. In contrast, muscle atrophy is triggered by factors such as TNF-α, and the NF-κB pathway. In this context, expression of the ubiquitin ligases is increased and leads to protein breakdown. In conditions of disuse or cachexia, this pathway is dysregulated and an inactive Akt protein unable to phosphorylate Foxo allowing Foxo to enter the nucleus and driving expression of the ubiquitin ligase atrogin-1. (Illustration by courtesy of U.Hardeland, DKFZ, Heidelberg)

Along with the discovery that a dysregulated PI3K/Akt pathway contributes to skeletal muscle atrophy *in vitro* and *in vivo*, the involvement of the NF-κB pathway in muscle atrophy was addressed in detail (McKinnell & Rudnicki 2004). Similarly to the implication of Foxo proteins in ubiquitin-dependent proteolysis, the transcription factor NF-κB was shown to induce the expression of the ubiquitin protein ligase MuRF1 (Cai et al. 2004). However, the expression of MAFbx/atrogin-1 was not altered in this mouse model of muscle atrophy. Thus, while both ubiquitin ligases are targets of Dex mediated muscle atrophy, the NF-κB pathway targets specifically MuRF1.

While IGF-1 stimulates the PI3K/Akt pathway, the NF-κB pathway is activated by TNF-α or other pro-inflammatory cytokines. Chronic exposure of mice to TNF-α resulted in a dramatic reduction of body weight (Oliff et al. 1987). TNF-α was also shown to cause atrophy *in vitro*: TNF-α stimulation of differentiated C2C12 myocytes stimulated loss of myosin heavy chain most probably by activation of the NF-κB pathway (Li et al. 1998). Along with this, TNF-α has been implicated in obese humans

undergoing a chronic inflammation (Hotamisligil 2006). A similar observation, impaired insulin signalling, was also made in TNF-α treated C2C12 myotubes (del Aguila et al. 1999). To conclude, while IGF-1 promotes muscle hypertrophy, TNF-α induces muscle atrophy. In the course of an inflammation response, TNF-α is secreted from macrophages upon activation with LPS, and functions by activating neutrophils and mobilizing energy stores (Renz et al. 1992) (Figure 1). However, once released in larger quantities during a chronic or systemic inflammation, the otherwise beneficial effects turn to a debilitating threat for body homeostasis. Since this protein was found to play a role in cachexia, TNF-α was originally named cachectin, (Beutler & Cerami 1986).

As targets for the ubiquitin protein ligases several muscle specific proteins were found in C2C12 cells. Among those, MyoD was shown to be ubiquitinated by MAFbx/atrogin-1, while MuRF1 was responsible for degradation of the myosin heavy chain protein (Clarke et al. 2007; Tintignac et al. 2005). Myosin is a component of the actomyosin complex which allows muscle fibers to contract. Hence, its degradation results in the destruction of the actomyosin complex and loss of muscle movement. MyoD is a transcription factor belonging to the family of myogenic regulatory factors (MRFs), which is responsible for the differentiation of muscle precursor cells (satellite cells) into muscle cells during normal growth or regeneration of muscle tissue. The proteolysis of this transcription factor under atrophic conditions suggests that the differentiation of satellite cells is likewise affected. TNF-α was also found to decrease mRNA and protein levels of muscle specific proteins, such as MyoD and myosin heavy chain, via the activation of the NF-κB pathway in C2C12 cells (Acharyya et al. 2004; Guttridge et al. 2000; Langen et al. 2004).

1.4 Assembly of Multiprotein Complexes on Eukaryotic Promoter Sequences drives Gene Transcription

The molecular events leading to muscle atrophy may in fact involve also other intracellular signalling pathways than the two “classical” pathways for NF-κB- and GR-mediated signalling. In addition to excessive glucocorticoid or TNF-α levels, other pro-inflammatory cytokines, such as Interleukin (IL)-6, IL-1 and Interferon (IFN)-γ have

been shown to be implicated in different models of muscle atrophy (Guttridge et al. 2000; Strassmann et al. 1994). Binding of these cytokines to their cognate receptors drives intracellular signalling cascades, finally resulting in altered expression of several target genes in muscle tissue. Ubiquitin ligases, myosin heavy chain, and MyoD are examples for such regulated target genes. However, the molecular events, namely on the transcriptional level in the nucleus remain elusive with the FoxO family of transcription factors representing so far the only exception (Accili & Arden 2004).

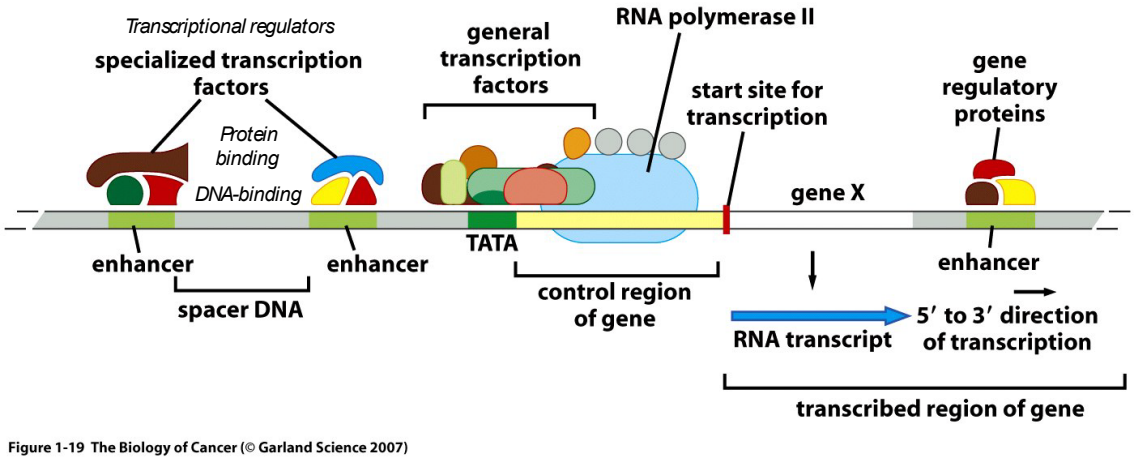

Figure 4: Eukaryotic transcriptional complexes assemble on DNA promoter sequences of target genes (Adapted for modification from Garland Science 2007). The promoter sequences may encompass several kilobases DNA. In addition, DNA transcription control elements which are then bound by proteins from the transcriptional complex may also be located many kilobases upstream or downstream from the start site of transcription within enhancer sequences. The transcriptionl complexes are composed of three levels of proteins: Specialized transcription factors, which can be further distinguished into DNA-binding and protein-binding proteins, co-regulators, and basal or general transcriptional proteins. Both, DNA-binding proteins and co-regulators can either activate or repress transcription of target genes and are hence named also activators or repressors.

A cell within a multicellular organism continuously receives signals, such as cytokines in the context of an inflammatory response. Part of these signals induces short-term responses, for instance modification of cellular metabolism. In addition, these signals can cause changes of gene expression patterns. These long-term responses are required for differentiation or division and are accomplished by formation of multiprotein transcriptional complexes on promoter sequences. Transcriptional complexes are composed of three different levels of proteins: DNA binding proteins, co-regulators and basal transcriptional proteins (Amelio et al. 2007). Basal transcriptional proteins can be further sub-categorized into the RNA polymerase, the general transcription factors,

chromatin remodelers, histone acetylases, deacetylases, kinases, and methylases. These proteins are along with the co-regulators ubiquitously present in all eukaryotic cells and crucial for the initiation of every RNA polymerase II primary transcript. However, regulation of gene transcription depends on DNA binding proteins. DNA binding proteins contain a DNA binding domain enabling them to bind characteristic nucleotide sequences on the DNA (e.g. GRE). In addition, these proteins contain one or two (e.g. GR) activation domains which interact with other proteins thereby stimulating transcription of the corresponding target gene. In contrast, co-regulators interact via protein-protein-interaction domains (e.g. ankyrin repeats) with DNA binding proteins and proteins of the basal transcriptional machinery (Figure 4). In this study, both DNA binding proteins and co-regulators are referred to as transcriptional regulators. They can either activate or repress transcription of genes and are accordingly named activators or repressors, respectively. Interestingly, the modular structure of DNA binding proteins can be shared between partner proteins with one protein containing the DNA binding domain and the other containing the transcription activation domain. The Ets transcription factors GAbp, which stands for "GA binding protein", is an example of such a protein. While GAbpα contains an Ets DNA binding domain, a variant of the winged-helix-turn-helix motif, the transcriptional activation domain resides on GAbpβ, a Notch-related protein containing several ankyrin repeats at its N-Terminus (Figure 5).

The activity of transcription factors can be either regulated by expression or indirectly through cell signalling. As mentioned earlier, the activity of the transcription factor GR is for instance activated by binding of its ligand. In this case, ligand binding and transcriptional activation are two functions of the same protein, a feature which all nuclear receptors share. The activity of the remaining classes of signal dependent transcription factors is also regulated by extracellular signals, yet, in these cases, the signal binds to a membrane-receptor thereby inducing intracellular signal pathways. These pathways and the gene expression changes they induce play a crucial role for the functional integrity of certain tissues. For example, a crucial function of the transcription factor GAbp in muscle tissue is to activate transcription of sub-synaptic targe genes, as for instance the epsilon-subunit of the AChR (AChRε). Congenital myasthenic syndrome, a muscular disorder affecting the NMJ, is correlated with a

mutation in the Ets-binding site of the AChRε promoter region thus underlying the importance of a functional gene expression for the integrity of muscle tissue (Ohno et al. 1999).

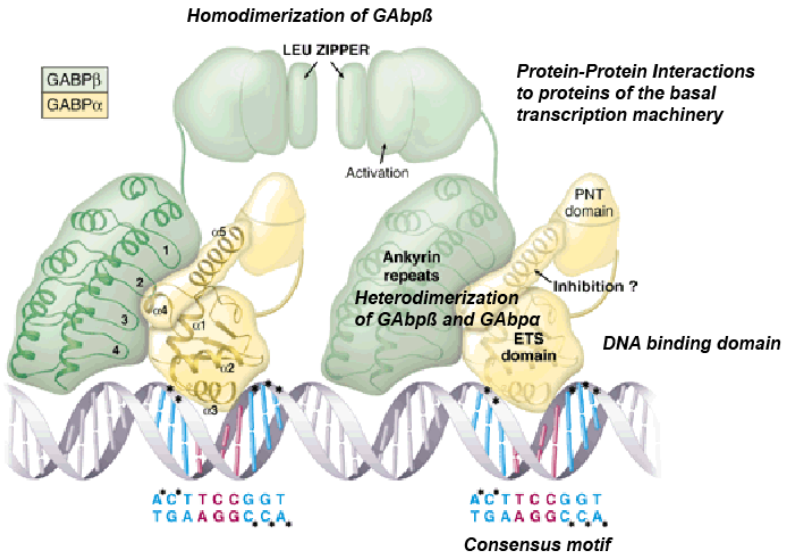

Figure 5: Binding of the heterotetrameric GAbp protein ($\alpha_2\beta_2$) to DNA sequences containing two 5´-GGA-3´ cores. GAbpα (yellow) binds via its Ets domain directly to the DNA. GAbpβ (green) binds via its ankyrin repeats to GAbpα and heterodimerizes throught its Leucine Zipper domain. In addition, the pointed (PNT) domain of GAbpα and Ankyrin repeats and Leucine Zipper of GAbpβ can undergo further protein-protein interactions to proteins of the basal transcription machinery (Modified illustration by K. Sutliff for Science, *Science* 13 February 1998:Vol. 279. no. 5353, pp. 1000 - 1002)

1.5 Aim of this study

The aim of this study was to identify novel transcriptional regulators with dysregulated transcriptional activity in response to atrophic stimulation. Furthermore, the analysis of the underlying molecular mechanism of a dysregulated transcription factor and its impact on gene transcription in muscle cells was focus of interest.

2 Methods

2.1 Cell Culture

2.1.1 Cultivation of Mammalian Cells

All cell lines were kept in incubators at 37°C, 95% humidity, and an atmosphere of 5% CO_2.

The murine muscle cell line C2C12 was grown in growth medium (GM). Cells were not allowed to reach confluency and passaged at ~ 60% confluency by trypsinization (3 mL per 15 cm plate). The detachment of cells occurred within 5 min at 37°C and was monitored by microscopic analysis. The reaction was stopped by addition of 9 mL GM and cells were pelleted by centrifugation (4 min, RT, 2500 rpm). The cell pellet was resuspended in GM (dilution 1:20 -1:30) and the cells seeded on fresh tissue culture dishes. C2C12 cells were used for a maximum of 10 passages. The differentiation of C2C12 myoblasts into myotubes was induced by serum withdrawal. Upon reaching > 95% confluency, the growth medium was replaced by differentiation medium and replaced every 48 h during the course of differentiation.

HEK293 and HEK293T cells were grown in DMEM supplemented with 10% FCS and 1% P/S. For passaging, cells were rinsed off the plate by pipetting up and down and diluted as described for C2C12 cells.

HEK293FT cells were also cultivated in DMEM supplemented with 10% FCS and 1% P/S. In addition, the medium was supplemented with 500 µg/mL Geneticin, 0.1 mM MEM Non-Essential Amino Acids, 1 mM Sodium Pyruvate, and 6 mM L-glutamine. Passaging of HEK293FT cells was performed as described for HEK293T cells.

RAW 264.6 cells, a mouse leukaemic monocyte macrophage cell line, were also kept in DMEM supplemented with 10% FCS and 1% P/S and cultivated as described with C2C12 cells.

2.1.2 Thawing and Freezing of Cell Lines

For preservation, tissue culture cell lines were stored in liquid nitrogen. The cells were washed once with PBS and collected by centrifugation (5 min at 2500 rpm). Then the cell pellet was resuspended in 1 mL freezing medium and the solution transferred directly into a cryovial. The cryovials were then positioned into a freezing device, which had been filled with isopropanol, thus allowing relatively slow freezing rates of ~ 1°C per minute upon transfer to a -80°C freezer. After overnight incubation the container had reached -80°C, so that the cryovials were transferred to the liquid nitrogen tank for long term storage.

For thawing cells, cryovials were removed from the liquid nitrogen tank and incubated immediately after in a 37°C water bath by slow agitation for 30 sec. 1 mL of appropriate growth medium was then applied to the vial and the cells were resuspended by pipetting up and down. Finally, the cell slurry was seeded on a fresh tissue culture dish containing pre-warmed growth medium.

Dish format	Area / well [cm^2]	Total area [cm^2]
10 cm	-	55
6-well plate	9.6	57.6
12-well plate	3.8	45.6
24-well plate	1.9	45.7

Table 1: Tissue culture dish formats used for transfection and corresponding area per well.

2.1.3 Generation of Conditioned RAW-Medium

Generation of conditioned RAW-medium was performed by seeding 20 x 10^6 cells on individual 15 cm dishes. These cells were cultivated for 48 h. On day 3, the cells had reached ~ 95 % confluency and were stimulated for 6 h with 100 ng/mL

Lipopolysaccharides (LPS) in growth medium. Such generated medium was collected and stored at -20°C. Prior to use, the medium was centrifuged (3 min at 2500 rpm) and the supernatant 0.45 µm filtered.

2.1.4 Transfection of Mammalian Cells

In this study, two different cell lines were used for transfection studies. Due to the different transfection efficiency of HEK and C2C12 cells, two different transfection protocols were employed.

2.1.4.1 Calcium Phosphate Transfection of HEK293(T) Cells

For efficient transfection of HEK293 and HEK293T cells, the "Calcium Phosphate Transfection" protocol was employed as follows. The day before transfection, cells were seeded at a density of 2x 10^4 cells per cm^2 dish surface. For overexpression studies cells were cultivated and transfected on 6-well plate format. In this context, cells were transfected with 2-3 µg DNA per well on 6-well plate format (2.6.3). In the course of a one-hybrid assay, 12-well plates were used instead and a maximum of 1.5 µg DNA was transfected per well. The DNA for transfection was mixed in an appropriate volume of 0.25 M $CaCl_2$ followed by adding an equal volume of 2x BBS and inverting the tube containing the reaction mix several times. The total volume of such generated DNA-Calcium Phosphate Mix corresponded to 10% (v/v) of the medium volume per well in transfection. For instance, provided a 12-well plate was used with 1 mL medium per well, the respective DNA was diluted in 50 µL $CaCl_2$, followed by addition of 50 µL 2x BBS. The DNA-Calcium Phosphate Mix was incubated at RT for 15 min and then added drop-wise to each well containing complete growth medium. The transfection was allowed to proceed for 8-16 h and was stopped by aspirating off the medium and replacement with new medium.

2.1.4.2 Lipofectamine-Mediated Transfection of C2C12 Cells

Since C2C12 cells were not efficiently transfected by using the "Calcium Phosphate Transfection" protocol, a Lipofectamine-mediated transfection was chosen instead and performed as follows. The day before transfection, cells were seeded at a density of 20x 10^4 cells/well on a 12-well plate format. The next day, 3.3 µg/cm^2 (here: 12.6 µg)

Lipofectamine were diluted in 25 µL Opti-MEM I. The DNA was diluted in 25 µL Opti-MEM I per well in a separate tube. The DNA and Lipofectamine solutions were then mixed and incubated at RT for 30 min. Finally, 350 µL serum-free DMEM was added to the DNA-Lipofectamine mix per well and the final mix applied a tissue culture well. The transfection was allowed to occur over 6 h in the incubator. Thereafter, cells were washed once with serum-free DMEM and differentiated by switching to DM.

2.1.5 Stimulation of Mammalian Cells

Cells were stimulated in complete growth medium by aspirating off the medium and replacing it with medium supplemented with corresponding stimuli. The duration of stimulation as well as final concentration of stimuli are indicated in the Results section. The various stimuli used in this study are listed in the Materials section.

2.1.6 Mammalian One- and Two-Hybrid Assay

For Mammalian One- and Two-Hybrid assays in HEK293T cells, the cells were seeded on 12-well plate formats, and transfected with 400 ng Gal4-Luc, 50 ng CMV-ß-gal, and 400 ng Gal-X per well (2.1.4). On the next day, cells were stimulated for 24h (2.1.5), harvested (2.6.5) and targeted to luciferase- and ß-galactosidase-assays (2.6.7, 2.6.8). For transfection of C2C12 cells in the course of a mammalian one- or two-hybrid assay, 100 ng Gal4-Luc, 20 ng CMV-ßGal and 100 ng Gal4-X or 1-5 ng Gal4-X and 1-5 ng Vp16-X were used for transfection (2.1.4). When using domain truncations of Gal4-GAbpα (dOST, dPNT, dT280, dEts) and Vp16-GAbpβ (dLeuZip, dTAD, dPhoSit) in a mammalian two-hybrid assay, 50 ng of these deletions constructs were used. All other plasmids were used as described before in these assays.

2.1.7 3xNBox and AChRε-Promoter Assays in C2C12 Cells

For analysis of AChRε promoter activity in C2C12 cells, which were seeded on 12-well plate format, C2C12 myoblasts were transfected with 20 ng CMV-ßGal, 100 ng pCDNA3.1(-)GAbpα, 100 ng pCDNA3.1(-)GAbpβ and 200 ng pGL3, pGL3-AChRε or pGL3-AchRε-NBox*mut*. Analysis of 3xNBox promoter activity in C2C12 cells was performed without co-expression of GAbp. The next day, cells were stimulated in DM with 5 nM NRG (human NRG-β1/HRG-β1 EGF domain) or vehicle (PBS + 0.1% BSA)

in the presence or absence of cytokine for 48 h (2.1.4, 2.1.5). Finally, cells were assayed for relative luciferase activity (2.6.5, 2.6.7, 2.6.8).

2.2 Cell-Based High-Throughput Screen

2.2.1 Reverse Transfection of HEK293T Cells

In this study a library of transcriptional regulators was used that had been cloned in frame with an N-terminal Gal4 DNA-binding domain. This library had been spotted beforehand on individual 384-well plates (10 ng DNA/well). On the day of transfection, the control plasmids (Gal4, Gal4-GR, Gal4-p65, and Gal4-Vp16) were spotted on corresponding wells of each 384-well plate (10 ng/well). Then, the reporter construct Gal4-Luciferase (20 ng/well) was diluted in serum-free DMEM. This mix was supplemented with transfection lipid (100 ng/well corresponding to a ratio of 2.5:1) and the DNA-Lipid complexes were allowed to form within 5 min at RT. Using a "Multidrop 384" apparatus, 20 µL of this DNA-lipid mix were then added to each well. The HEK293T cells were collected from 15 cm dishes, diluted accordingly, and finally added to each well (9500 cells per well) for reverse transfection. These plates were then covered and incubated overnight at 37°C.

2.2.2 Stimulation of Transfected HEK293T Cells

The next day, cells were stimulated with vehicle (here: ethanol), 1 µM Dexamethasone, 100 ng/mL human TNF-α, or both stimuli together for 24 h at 37°C.

2.2.3 Luciferase-Assay

Following stimulation, cells were lysed by addition of 40 µL BrightLite (PerkinElmer) reagent per well. Directly after, the luciferase-assay was performed on a "PerkinElmer (Wallac) 1430 ultraHTS microplate Imager ViewLux Station". For each individual factor of the Gal4 library, the fold change was calculated over vehicle treatment.

2.3 Bacterial Culture Methods

2.3.1 Cultivation of Bacteria

Transformed *E.coli* cells were grown either in LB medium or on LB agar plates supplemented with antibiotics (50 µg/mL ampicillin, 50 µg/mL kanamycin, 30 µg/mL chloramphenicol). All plasmids from the Gal4 screen were amplified in *E.coli* grown in low salt LB medium supplemented with 25 µg/mL zeocin.

2.3.2 Electroporation of Electrocompetent *E.coli* XL1-blue

Electrocompetent *E.coli* XL1-blue cells were prepared routinely by technicians. For amplification of plasmid DNA, electrocompetent XL1-blue cells were used for electroporation. Initially, an electroporation cuvette was pre-chilled on ice. After thawing 50 µL of the electrocompetent cells on ice, 200 - 400 ng of plasmid DNA or 1 µL of a ligation mix were added to the bacteria and the solution mixed by pipetting up and down. Upon transfer of the mix into a cuvette, a brief pulse of 2.5 kV was applied using the "Gene Pulser II". Following this, the mix was supplemented with 300 µL of chilled LB medium and transferred to a reaction tube for a 30 min incubation step at 37°C while shaking (650 rpm). Finally, 100-300 µL of such electroporated *E.coli* cells were plated on antibiotic-selective LB agar plates and incubated overnight at 37°C.

2.3.3 Inoculation of *E.coli*

Growth medium for *E.coli* (e.g. LB, NZY) was supplemented with antibiotic directly before use. Thereafter, a fresh overnight colony of *E.coli* was picked from an agar plate and transferred to 4 mL or 200 mL growth medium for mini- or maxi-preparation of plasmid DNA. Cells were grown overnight (14 - 18 h) under vigorous shaking at 37°C.

2.4 DNA Methods

2.4.1 Isolation of Genomic DNA

Genomic DNA was extracted from mouse tissue as follows. About 20 mg of tissue were cut on dry ice at 4°C and transferred to pre-chilled 2 mL-tube containing steal beads on

dry ice. Homogenization of tissue was achieved by using the tissue lyser for 2 min (pulse frequency set to 30 Hertz). The sample was vortexed and allowed to chill for 5 min at RT and supplemented with 0.5 mL lysis buffer for genomic DNA extraction. Proteinase K was added to the buffer directly before use. The proteins were digested for 3 h at 60°C while shaking. Next, the tissue lysate was incubated under shaking at 56°C overnight. The next day, genomic DNA was extracted by two successive extraction steps with a 25:24:1 solution of Phenol: Chloroform: Isoamylalcohol (PCI). After adding 0.5 mL PCI to the cell lysate, the reaction tube was vortexed, centrifuged (10 min, 4°C and 13,000 rpm), and the supernatant was transferred to a new tube. The next extraction step was performed with 0.5 mL Chloroform. The supernatant was again transferred to a fresh tube, followed by adding 0.5 mL Isopropanol and precipitating the genomic DNA for 1 h or overnight at -20°C. The genomic DNA was collected by centrifugation (45 min, 4°C and 13,000 rpm) and the supernatant discarded. The pellet was washed with 1 mL 75% Ethanol and centrifuged again (15 min, 4°C and 13,000 rpm). Finally, the pellet was air-dried for 10 min and resuspended in 100 - 200 µL TE buffer. In order to complete resuspension, the reaction tube containing the DNA-pellet was incubated for 2 h at 60°C. Genomic DNA was stored at 4°C.

2.4.2 Polymerase Chain Reaction

2.4.2.1 PCR for Cloning

Amplification of DNA in the course of a cloning procedure was routinely performed by PCR. Templates, primers and resulting plasmids are listed in the Materials Section. The Phusion polymerase was used routinely and each PCR reaction with a total volume of 50 µL was composed of following components: 1x Phusion Buffer, 200 µM dNTPs, 10-100 ng template DNA, 1 µM of sense and antisense primer, 0.01 U Phusion DNA polymerase.

The initial denaturation was routinely performed for 3 min at 98°C followed by DNA-amplification during 20-25 cycles of denaturation (10 sec 98°C), annealing (30 sec, Ta primer dependent) and elongation (time/kb, 72°C). Final elongation at 72 °C occurred over 10 min. Thereafter, 5-10 µL per PCR reaction were analyzed on an agarose gel.

2.4.2.2 Real-Time Quantitative PCR

In order to quantify mRNA from mammalian cells or muscle tissue samples, the complementary DNA (cDNA) was targeted to real-time quantitative PCR (qRT-PCR). In this study, the *Taq*Man-Method (Livak et al. 1995) was employed.

The cDNA samples obtained as described in paragraph 2.4.9 were diluted 10-fold with DNase/RNase free water. Per reaction 5 µL of such diluted cDNA was used. In addition, each reaction mixture was supplemented with 10 µL Platinum® Quantitative PCR Supermix, 0.4 µL ROX dye, 3.6 µL DNase/RNase free water and 1 µL of a specific TaqMan-Probe (see Materials Section). The subsequent PCR was performed routinely in duplicates for each gene of interest and in triplicates for housekeeping genes (TBP, GAPDH). GAPDH was used as housekeeping gene for the relative quantification of mRNA levels in gastrocnemius muscle samples of Colon26 mice. In all other experiments, TBP was used instead. All PCR reactions were pipetted on a 96-well plate and the PCR was run on a "7300 Real Time PCR System". The thermal profile consisted of an initial heating step at 50°C for 2 min followed by initial denaturation for 2 min at 95°C. Thereafter, DNA was amplified during 40-45 cycles of denaturation at 95°C (15 sec) and annealing/elongation at 60°C. Data acquisition took place in the annealing/elongation step.

2.4.3 Restriction Digest of DNA

In the course of a cloning procedure a preparative restriction digest of DNA fragments was performed. After Mini- or Maxi-Preparation of plasmids and prior to sequencing, the identity of DNA was routinely confirmed by an analytical restriction digest. Usually, 3-6 units of each restriction endonuclease were used per 10 µL batch volume and ~ 500 ng of DNA. The restriction digest was performed in a suitable restriction enzyme buffer and 1x BSA for 1.5 – 2 h at 37°C. Following this, the presence and size of DNA fragments was analyzed by agarose gel electrophoresis (2.4.5).

2.4.4 Purification of DNA

DNA fragments resulting from PCR reactions for cloning were purified by using the "QIAquick PCR Purification Kit"[1]. In contrast, DNA fragments from restriction digests were purified over preparative agarose gels and subsequent use of a gel extraction kit. In the latter case, the total restriction digest reaction volume was supplemented with 1x Orange G DNA loading buffer, loaded onto a 1% agarose gel and DNA fragments were separated while applying 100 V for ~ 45 min to the gel. DNA fragments were then isolated from agarose gels by employing the "QIAquick Gel Extraction Kit" (for details, see manufacturers instruction).

2.4.5 Agarose Gel Electrophoresis of DNA

Following restriction digest or PCR, the DNA fragments were analyzed by gel electrophoresis. Agarose gels of suitable density (0.7 – 2 %) were poured in TBE buffer supplemented with 0.1 µg/ mL Ethidium Bromide. Orange G DNA loading buffer was then added to the DNA batches and samples were loaded to the hardened agarose gel. The DNA fragments of various sizes were resolved while applying a current of 100 V to the agarose gel and afterwards visualized in the "BioRad Gel Doc apparatus".

2.4.6 Determination of DNA Concentration

The DNA concentration was determined spectrophotometrically by using the NanoDrop Spectrophotometer. Thereby, the ratio of absorptions 260nm/280nm was also analyzed. A ratio of 1.92-2.00 indicated relative low protein impurities (0-30%).

2.4.7 Ligation of DNA Fragments

In the course of a cloning procedure, the vector and insert, which had been digested to obtain compatible ends, were ligated as follows. Usually, 250 ng vector DNA and a 3-5 fold molar excess of insert was used. Both, insert and vector, were mixed and the resulting volume was filled up with water to 10 µL. The DNA mixture was incubated for 5 min at 45°C and then chilled at RT. Afterwards, 2 µL 10x ligase buffer, 7 µL H_2O, and 1 µL T4-DNA ligase were added to obtain a total ligation volume of 20 µL. The

[1] For details, see manufacturers instruction

reaction was allowed to proceed for 2 h at RT followed by incubation for 14 - 16 h at 4°C. Finally, 1 µL of the ligation mix was used for electroporation into electrocompetent XL1-blue *E.coli* cells.

2.4.8 Preparation of Plasmid DNA

In the course of a cloning procedure, plasmid DNA was usually prepared by using the "QIAprep Spin Mini Prep Kit", while the "PureLink HiPure Plasmid Maxi Kit" was employed for obtaining larger amounts of plasmid DNA e.g. for transfection etc.

2.4.9 Synthesis of Complementary DNA

Complementary DNA (cDNA) was synthesized using the "First Strand cDNA Synthesis Kit"[1]. Usually, 1 µg of total RNA were used per cDNA reaction.

2.4.10 Dephosphorylation of Plasmid DNA

In the course of a cloning procedure, recircularization of vector DNA was minimized by dephosphorylation with the calf intestine phosphatase (CIP). The reaction containing 30 µL DNA template, 4 µL 10x NEB3 buffer, 1µL CIP, and 5 µL water was allowed to occur for 1 h at 37°C.

2.4.11 Sequencing of Plasmid DNA

The sequence of plasmid DNA was routinely analyzed by the AGOWA company and the presence of the correct nucleotide sequence was confirmed by sequence alignment using the Vector NTI software from Invitrogen.

2.4.12 Cloning of Plasmid DNA

The insert of interest was obtained by either restriction digest or PCR amplification from the template plasmid DNA (2.4.2), template cDNA pool or genomic DNA. The PCR product was confirmed subsequently via agarose gel electrophoresis (2.4.5). Next, the insert and the vector were digested in parallel with the respective restriction enzymes (2.4.3). Such generated DNA fragments with compatible restriction sites were isolated by preparative agarose gel electrophoresis (2.4.5) and gel extraction (2.4.5).

The DNA fragments were then ligated (2.4.7) and electroporated (2.3.2) into electrocompetent XL1-blue *E.coli* cells. Isolated colonies were picked and transferred to LB medium for amplification of plasmid DNA (2.3.3). Following mini-preparation of plasmid DNA (2.4.8), the presence and the sequence of the insert were confirmed by restriction digest and sequencing (2.4.11).

2.5 RNA Methods

2.5.1 Preparation of RNA from Tissue Culture Samples

All steps were performed routinely at RT using columns and buffers from the "RNeasy Mini Kit". Initially, cells were harvested in RLT buffer (300 µL per well on a 6-well plate format) supplemented with 1% ß-mercaptoethanol. Alternatively, cells were lysed in QIAzol and RNA purified by chloroform extraction. The cell lysate was then transferred to the - 20°C freezer for further storage, or loaded directly after on a QIAshredder column and centrifuged (13,000 rpm, 2 min). The eluate from this initial centrifugation step was mixed with an equal volume of 70% ethanol by pipetting up and down. The resulting reaction mixture was then transferred to an RNeasy column and centrifuged again (13,000 rpm, 1 min). After discarding the flow-through, the column was washed with 350 µL RW1 buffer by applying the buffer on the column and incubating the column for 5 min at RT. This step was directly followed by a centrifugation step (13,000 rpm, 1 min). Next, on-column-DNA-digestion was performed as follows: 15 µL DNase was gently mixed in 105 µL DNase buffer (RDD buffer) and then applied to each column. The reaction was allowed to proceed for 22 min at RT. Subsequently, 350 µL RW1 buffer were added to each column and incubated for 2 min. The column was finally washed twice with 500 µL RPE buffer and the RNA eluted in 30 µL of RNase free water. RNA was stored at -80°C.

2.5.2 Preparation of RNA from Mouse Muscle Tissue Samples

All steps involving handling with phenol reagents such as QIAzol were performed under a fume hood. At the beginning, tissue samples were cut on dry ice inside the cold room (4°C) into pieces of 30-60 mg. Such generated tissue samples were transferred to pre-chilled 2 mL tubes containing single strainless steal beads and 1 mL QIAZOL on

dry ice. Homogenization of tissue was achieved by using the tissue lyser for 2 min (pulse frequency set to 30 Hertz). The samples were vortexed and incubated for 5 min at RT. The RNA was purified by adding 0.2 mL chlorophorm to each tube and vigorous shaking at RT for 15 sec. Following an additional incubation time on ice for 5 - 10 min (until phase separation was visible), the tubes were centrifuged for 15 min at 4°C and 13,000 rpm. As next, the aqueous phase was transferred to a new tube and supplemented with 0.6 mL 75% ethanol. Finally, the reaction was mixed thoroughly, applied to an RNeasy column and RNA preparation continued as described in 2.5.1.

2.5.3 Determination of RNA Concentration

The RNA concentration was determined spectrophotometrically at 260 nm using the NanoDrop Spectrophotometer. In parallel, the ratio 260 nm/280 nm was detected in order to measure protein-impurities in the samples (see 2.4.6).

2.5.4 Agarose Gel Electrophoresis of RNA

In the course of RNA preparation from tissue culture and muscle tissue samples, the quality of the RNA was routinely analyzed by agarose gel electrophoresis. 1% agarose gels were poured with RNase-free agarose in 1x TBE buffer. The RNA samples were denatured in a formaldehyde/formamide solvent (RNA denaturing buffer). If not else mentioned, 1 µL per RNA sample were added to 10 µL RNA denaturing buffer and incubated for 10 min at 65°C. As next, the total volume (11 µL) was loaded onto the agarose gel and separated for at least 40 min at 100 V. The quality of the RNA was determined visually by examination of the ratio between 28S to 18S ribosomal RNA, which was 2:1 for intact RNA.

2.6 Protein Methods

2.6.1 Determination of Protein Concentration

For determination of protein concentration, two different methods were employed. Provided the cell lysate was prepared with the 2x SDS + 8 M Urea buffer, the protein content of such obtained denaturing protein extracts was determined by using the “2-D Quant Kit”. For this purpose, the proteins were precipitated and then targeted to an

absorption detection method. If, however, a native cell extract was prepared, the Bradford Assay was employed instead. The Bradford reagent was diluted 5-fold in water and 1 mL of such generated solution added to each single plastic cuvette. Then, a suitable volume of cell lysate (3-5 µL) was added to a cuvette and the solution subsequently mixed. The absorption of the various cell lysate samples was measured in a Spectrophotometer at a wavelength of 595 nm. In parallel, a BSA standard curve was determined, encompassing the range of ~ 5 - 20 µg protein.

2.6.2 SDS-Polyacrylamide Gel Electrophoresis of Proteins

For SDS-PAGE analysis of proteins, denaturing SDS gels were used. Usually, 15%, 10% or 8% resolving gels were poured in order to separate and analyze proteins of 10-60 kDa, 30-120 kDa or 50-200 kDa. In all cases, a 4% stacking gel was poured on top of the resolving gel. Proteins were denatured in SDS Reducing buffer and boiled at 95°C for 5-10 min. Finally, 10-50 µg protein was loaded per lane. As protein mass standard, 5 µL of the "PageRuler™ Unstained Protein Ladder" were used. The protein samples were allowed to enter the stacking gel while applying 100 V. As soon as the samples have entered the resolving gel, the current was increased up to 150 V.

2.6.3 Western-Blot

Proteins, which had been resolved by SDS-PAGE, were electrophoretically transferred to nitrocellulose membranes using the Wet-Blot principle for subsequent analysis of protein expression. Prior to use, the membrane was equilibrated for ~ 20 min with transfer buffer. All other components of the blotting apparatus, as for instance sponges, filter papers, and the gel, were also pre-chilled in transfer buffer. The efficient transfer of proteins was achieved by applying a current of 30 V to the apparatus at 4°C and overnight.

The expression of proteins was analyzed by Western-Blot. Following overnight blotting, the nitrocellulose membrane was rinsed in water and the protein transfer was confirmed by Ponceau S staining. The staining solution was then removed and unspecific antigen sites blocked by incubating the membrane under mild agitation for 1 h in blocking buffer. The primary antibody was diluted to the desired final

concentration (see Materials Section) in blocking buffer and the membrane incubated with the primary antibody for 1 h under mild agitation. Subsequently, the membrane was washed three times for 10 min with PBS-T buffer. The secondary antibody, a Horseradish Peroxidase (HRP) conjugate, was diluted likewise (1:3000 – 1:5000) and allowed to bind to the primary for 1 h under mild agitation. Again, the membrane was washed three times for 10 min with PBS-T buffer and incubated directly after with the "ECL™ Western Blotting Detection Reagents". The chemiluminescent reaction of the enzyme Horseradish Peroxidase was monitored on "Hyperfilm™ ECL" films.

2.6.4 Co-Immunoprecipitation of Proteins from C2C12 Cells

The C2C12 cells, destined for immunoprecipitation (IP) of endogenous proteins, were washed twice with ice-cold PBS on ice. Then, 0.5 mL of Larry-buffer was added per 10 cm dish and the cells were scraped off the plate. The cell slurry was transferred to a reaction tube and incubated on ice for 30 min. Every 5-10min, the reaction tube was vigorously vortexed in order to enable complete cell lysis. Thereafter, the cell debris was collected by centrifugation (15 min, 4°C, and 13,000 rpm). The supernatant was transferred into a new tube, thereby keeping an aliquot as input in a separate tube. The immunoprecipitation of endogenous proteins from the cell lysate was performed for 1 h on ice by using 1 µg of the respective antibody. Meanwhile, Protein A/G PLUS-Agarose (25%) was equilibrated in cell lysis buffer by two subsequent washing and centrifugation steps (5 min, 4°C and 2,500 rpm) and added to the antibody-cell lysate (final concentration: 4% of the total reaction volume). Such generated mix was allowed to rotate mildly at 4°C for 1 h. The agarose was collected thereafter by centrifugation (5 min, 4°C and 2,500 rpm). An aliquot of this first centrifugation step was kept as unbound protein fraction. The agarose was then subjected to three consecutive washing and centrifugation steps (5 min, 4°C and 2,500 rpm). At the end of the IP, 40-50 µL of 2x SDS reducing buffer were added to each tube in reaction and proteins denatured by boiling at 95°C for 5 min. The tubes were vigorously vortexed, centrifuged (5 min, RT and 13,000 rpm), and the supernatant was carefully transferred to a new tube. These eluates were finally separated by SDS-PAGE (2.6.2). Likewise, previously collected input and unbound protein fractions were diluted in an equivalent volume of 2x SDS reducing buffer and boiled for 5 min. 20 µL of each fraction were loaded onto SDS gels.

2.6.5 Harvesting Cells for Reporter-Assay

In the course of a promoter analysis or a mammalian one- or two-hybrid assay, accordingly transfected and stimulated cells were harvested from 12-well plates for subsequent determination of luciferase- (2.6.7) and ß-galactosidase-activity (2.6.8). The cells were washed once with PBS and then lysed in 0.15 mL harvest buffer by mildly agitating the multi-well plates for 5 min. The cell slurry was then transferred to a reaction tube and the cell debris collected by centrifugation for 5 min at 4°C and 13,000 rpm. Finally, the supernatant was used for determination of luciferase- and ß-galactosidase activity (2.6.7, 2.6.8).

2.6.6 Western-Blot Analysis of Proteins from Cell Culture Extracts

For Western-Blot analysis of overexpressed protein levels in cell culture extracts whole cell extracts (WCE) were prepared. If not else mentioned, cells were grown on a 6-well plate format and harvested in 0.3 mL buffer per well. Denaturing WCE for protein analysis were prepared by washing cells once with 1x PBS and lysing the cells on the plate in 2x SDS + 8 M Urea buffer. Immediately after, the samples were boiled for 10 min at 95°C. The concentration of these extracts was subsequently determined via "2-D Quant Kit" and the extracts stored at -20°C until further analysis. Provided, endogenous protein levels were analyzed, native or whole cell extracts were prepared. Thereafter, the protein content was determined (2.6.1) and 10 – 20 µg protein resolved via SDS-PAGE (2.6.2). Finally, the protein expression was analyzed by Western-Blot by using appropriate antibodies (2.6.3).

2.6.7 Assay for Luciferase Activity

Luciferase activity was routinely analyzed in the course of mammalian one- and two-hybrid or promoter assays. The assay was performed in triplicates on 12-well plates. The amount of luciferase correlated to the promoter activity and was determined by an enzymatic assay. Usually, 30 µL of cell lysate (see 2.6.5) were used per well. The cell lysates containing the luciferase enzyme were pipetted on a black 96 well plate. Prior to measurement, 100 µL assay buffer containing co-factors required for the reaction were added to each well. The plate was then loaded into the Luminometer and luciferase activity measured upon injection of 100 µL Luciferase buffer, which contained the

substrate. The relative luciferase activity per reaction mixture was calculated relative to ß-Galactosidase activity (2.6.8)

2.6.8 Assay for ß-Galactosidase Activity

The activity of the reporter enzyme ß-galactosidase was determined via an enzyme activity measurement. Briefly, 50 µL of supernatant from cell lysates (2.6.5) were pipetted into individual wells of a translucent 96-well plate. Then, 50 µL of ONPG buffer containing the substrate were added to each well. The amount of ß-galactosidase in the cell lysate was proportional to the amount of transformed substrate. The latter is measured by an absorption measurement at a wavelength of 480 nm.

2.7 RNAi Design and Cloning Methods

The "Block-iT™ Pol II RNAi Expression Vector Kit" from Invitrogen was employed for cloning a miRNA GAbpα expression vector.

2.7.1 Design of miRNAs Targeting Murine GAbpα

For RNAi-mediated knock-down of GAbpα in C2C12 cells, the online available "Invitrogen´s RNAi Designer" was used to design three different miRNAs targeting the 3' UTR within GAbpα mRNA by use of following parameters. The sequences of the miRNAs are listed in the Materials Section.

Gene Name	GAbpα	
Organism	Mus Musculus	
Definition	GA repeat protein, alpha, mRNA	
Accession	BC013562	NM 008065
ORF Region	151-1206	447-1811
Length	4266	5004

Table 2: This table illustrates the parameters used for the design of miRNAs targeting the 3' UTR within GAbpa mRNA by using the online available "Invitrogen´s RNAi Designer" software.

2.7.2 Cloning of the miRNA Expression Vectors

An expression vector for the miRNA was cloned according to the "Block-iT Pol II miR RNAi Expression Vector Kits" by using the buffers and components included in the kit. Initially, the single-stranded DNA (ssDNA) oligos were reconstituted with water to a final concentration of 200 µM. Following this, the bottom and top oligo were annealed for each miRNA target position (1256, 4216, 4682) by mixing 5 µL of each top and bottom strand ssDNA oligo with 2 µL 10x OligoAnnealing Buffer and 8 µL RNase/DNase free water in a 0.5 mL sterile microcentrifuge tube at RT. The mix was then boiled for 4 min at 95°C. The annealing occurred during the successive chilling of the tubes for 5 – 10 min at RT. Such generated 50 µM stock solutions of double-stranded DNA (dsDNA) oligos were then diluted via serial dilutions to 10 nM solutions with water and 10x oligo annealing buffer. The integrity of the dsDNA oligos was checked via gel electrophoresis on a 4% agarose gel.

The ligation of the dsDNA oligos into the pCDNA6.2-GW/EmGFP vector was performed by mixing following components in the indicated order at RT:

Component (stock concentration)	**Volume [µL]**
5x Ligation Buffer	4
pCDNA6.2-GW/EmGFP (5 ng/µL)	2
ds oligo (10 nM)	4
H_2O	9
T4 DNA Ligase	1

Table 3: This table summarizes the components required for ligation of the dsDNA oligos with the pCDNA6.2-GW/EmGFP vector.

The ligation batch was mixed well by pipetting up and down, incubated at RT for 5 min and transformed into OneShot TOP10 competent *E.coli*. For chemical transformation, 2 µL of the ligation mixture were added into one vial of TOP10 *E.coli* cells and gently mixed by pipetting up and down. The tube was incubated on ice for 20 min, followed by a heat-shock for 30 sec at 42°C and immediate transfer of the tube to ice. Following this, 250 µL of chilled SOC medium were added to the bacteria and the tube shaked at 37°C for 1 h. Finally, the cells were plated on spectinomycin (50 µg/mL) selective agar

plates. The next day, single bacterial colonies were transferred into LB medium, grown overnight and subjected to plasmid-preparation (2.4.8). Plasmids were analyzed via sequencing. These miRNA expression vectors (pCDNA6.2-GW/EmGFP-miRNA) were tested thereafter using the pTarget system for knock-down efficiency of the target protein, GAbpα *in vitro* (2.7.4).

2.7.3 Cloning of GAbpα into the pTarget Vector

The validation of knock-down efficiency of miRNAs was performed by using the "GeneEraser™ Luciferase Suppression-Test System" by Stratagene. For this purpose, the Gabpα sequence containing the miRNA target site was cloned into the pTarget vector thus generating a fusion protein of Gabpα and the luciferase reporter. Here, a modified version of the pTarget vector containing a multiple cloning site (MCS) was used for cloning of the Gabpα DNA sequence. Two PCR reactions were performed to amplify two different Gabpα DNA sequences from a cDNA pool from C2C12 cells. For generation of the plasmid pTarget-GAbpα-ORF the forward primer GAbpα-pos447-for and the reverse primer GAbpα-pos2401-rev were taken. By using the primer pair GAbpα-pos2443-for and GAbpα-pos4767-rev, the plasmid pTarget-GAbpα-3'UTR was cloned. The PCR reactions were analyzed via agarose gel electrophoresis (2.4.5), purified (2.4.4) and digested - along with the vector - with *Not*I (2.4.3). Thereafter, the vector and inserts were resolved on a preparative agarose gel (2.4.5) and excised from the gel. Prior to ligation (2.4.7), the vector was dephosphorylated (2.4.10). The amplification of ligated vectors was performed in XL10-Gold ultracompetent cells: For each transformation, 40 µl of cells were transferred into a 15 mL polypropylene round-bottom tube followed by adding 1.6 µL of the XL10-Gold β-mercaptoethanol mix to each batch of cells. The mix was gently swirled every 2 min during a total incubation time of 10 min on ice. Then, 2 µL of the ligation reaction were added, directly followed by a further incubation period of 30 min on ice. The tubes were heat-pulsed for 30 sec at 42°C in a water bath and incubated thereafter for 2 min on ice. Finally, 0.45 mL pre-heated NZY^+ broth medium were added to each tube and the cells incubated in this medium for 1 h at 37°C while gently shaking (225 rpm). The cell slurry was spread on NZY^+ broth agar plates containing 50 µg/ mL kanamycin. The next day, isolated colonies were picked and transferred to NZY^+ broth medium for inoculation (2.3.3).

Following overnight amplification of *E.coli*, plasmid DNA was prepared (2.4.8), digested with *Not*I, *Bam*HI, *Eco*RI or *Hind*III (2.4.3) and analyzed via agarose gel electrophoresis (2.4.5). Positive clones were further analyzed by sequencing.

2.7.4 Validation of Knock-Down Efficiency of miRNAs with the "GeneEraser™ Luciferase Suppression System"

Following the cloning of the miRNA expression vectors (2.7.2) and the pTarget-GAbpα vectors (2.7.3), the "GeneEraser™ Luciferase Suppression System" was employed to validate the knock-down efficiency of the three designed miRNAs (1256, 4216, 4682) *in vitro*. The assay was performed on 24-well plates in HEK293 cells. Cells were transfected in triplicates with declining amounts (250, 100, 10 or 1 ng) of a negative control miRNA-expression vector (pCDNA6.2-GW/EmGFP-miRNA NC) or a Gabpα targeting miRNA-expression vector (pCDNA6.2-GW/EmGFP-miRNA 1256/4216/4682). The plasmid CMV-β-gal was used at a final concentration of 25 ng/well and the luciferase reporter gene plasmid was used at a final concentration of 100 ng/well. The plasmid pTarget-Gabpα-3'UTR was taken for analysis of miRNA 4216 and miRNA 4682, while pTarget-Gabpα-ORF was sued for analysis of miRNA 1256. For each well in transfection, 25 µL $CaCl_2$ and 25 µL 2x BBS were used (2.1.4.1). The next day, the transfection medium was aspirated off and replaced by new medium. The Luciferase- and ßGalactosidase-Assay (2.6.5) was performed 40 h after transfection start.

2.7.5 Validation of the Knock-Down Efficiency of miRNA on Overexpressed Protein Levels

The knock-down efficiency of the miRNA 1256 was assessed by overexpression along with a GAbpα expression vector in HEK293T cells. For this purpose, an overexpression vector for GAbpα containing the miRNA target site was required. The GAbpα sequence from the plasmid pTarget-Gabpα-ORF was obtainted via restriction digest with *Not*I (2.4.3) and cloned into the pCDNA3.1(-) vector. This overexpression vector for GAbpα was used for validation of knock-down efficiency of miRNA 1256 as well as for AChRε promoter assays (2.1.7).

HEK293T cells were seeded on a 6-multiwell dish (2.1.4.1). The next day, cells were transfected (2.1.4.1) with 2 µg pCDNA3.1(-)GAbpα overexpression plasmid per well. While one well was left untreated, four wells were concomitantly transfected with increasing amounts (0.5, 1, 2 and 4 µg) of the miRNA1256 expression plasmid (pCDNA6.2-miR1256). The last well was transfected with the highest plasmid amount used (4 µg) of an unspecific miRNA (pCDNA6.2-miRNC). The transfection medium was changed the next day and whole cell extracts were prepared 48 h after transfection start. The protein content of these prepared whole cell extracts was determined (2.6.1), 30 µg total protein of each sample were resolved by SDS-PAGE (2.6.2). GAbpα expression was analyzed via immunoblotting (2.6.3).

2.7.6 Cloning of a Lentiviral Destination Vector

A lentivirus based gene transfer system was employed for RNAi delivery into C2C12 cells. For the production of RNAi containing lentivirus, a lentiviral destination vector was required and cloned according to the "Block-iT™ Lentiviral Pol II miR RNAi Expression System" from Invitrogen.

The pCDNA6.2-GW/EmGFP-miRNA1256 and pCDNA6.2-GW/EmGFP-miRNANC expression vectors contained *att*B sites, which could not be directly used with the pLenti6/V5-DEST destination vector to generate a lentiviral expression vector. Instead, a BP reaction was performed as follows in order to generate an entry clone containing *att*L sites. Initially, the pCDNA6.2-GW/EmGFP-miRNA1256/NC expression vectors were linearized using *Eag*I: 6 µL of 1µg/µL expression vector were mixed with 2 µL 10x BSA, 2 µL NEB3, 1.25 µL *Eag*I, and 12.75 µL water and incubated for 90 min at 37°C. Next, the linearized DNA was precipitated with 0.1 volumes of 3 M sodium acetate (here: 2 µL were used) and 2.5 volumes of 100% ethanol. The DNA pellet was pelleted by centrifugation (5 min, 13,000 rpm), washed twice with 70% ethanol, and dissolved in TE buffer. Subsequently, the actual rapid BP/LR Recombination Reaction was performed at RT as follows: 40 fmol of linearized *att*B expression clone (miRNA1256 or miRNANC), 150 ng pDONR 221 vector were mixed in TE buffer to a final reaction volume of 8 µL. Then, 2 µL of the BP Clonase II enzyme mix were added to this reaction, mixed well by pipetting up and down, and incubated for 1 h at 25°C,

thereby generating pENTR 221/miR1256 and pENTR 221/miRNC. Next, 3 µL from each BP reaction were transferred to a new sterile 0.5 mL microcentrifuge tube and filled up with 150 ng pLenti6/V5-DEST vector and TE buffer to a final reaction volume of 8 µL. Finally, 2 µL of LR Clonase II enzyme mix were added to the reaction and the reaction was allowed to proceed for 2 h at 25°C. Following this, 1 µL of the Proteinase K solution were added to each reaction and incubated for 10 min at 37°C.

The LR recombination reaction was then transformed into "One Shot® Stbl3™ Chemically Competent *E.coli*". For each transformation reaction, one vial of these cells was thawn on ice followed by adding 3 µL of the LR recombination reaction to the competent cells. The reaction was gently mixed and incubated for 30 min on ice. The heat-shock occurred for 45 sec at 42°C directly followed by chilling the reaction on ice for 2 min. Next, 250 µL of pre-warmed SOC medium were added and the tube incubated at 37°C for 1 h while shaking (225 rpm). Finally, the transformation mix was spread on ampicillin selective agar plates and incubated overnight at 37°C. Single putative expression clones were tested in parallel for ampicillin-resistance and chloramphenicol-sensitivity. Such obtained pLenti6/miRNC and pLenti6/miRGAbpα vectors were then used for production of Lentivirus in HEK293FT (2.8.1) or HEK293T cells (2.8.2).

2.8 Lentivirus Methods

2.8.1 Production of Lentivirus in HEK293FT Cells

Two different Lentiviruses were produced here according to the "Block-iT™ Lentiviral Pol II miR RNAi Expression System" from Invitrogen. One lentivirus originating from plasmid NC contained the miRNA NC sequence while the other contained the miRNA GAbpα sequence.

DNA-Lipofectamine 2000 complexes were prepared as follows for both transfection samples individually (Lentivirus miR NC or miR Gabpα): 9 µg ViraPower™ Packaging Mix and 3 µg pLenti6/miRNC or pLenti6/miRGAbpα were diluted and gently mixed in 1.5 mL of Opti-MEM I medium without serum in a sterile 5 mL tube. In parallel, 36 µL

Lipofectamine™ 2000 were diluted in a separate 5 mL tube in 1.5 mL Opti-MEM I medium without serum, mixed, and incubated for 5 min at RT. Then, both, DNA and Lipofectamine™ 2000, were combined, again gently mixed, and incubated for 20 min at RT. Meanwhile, HEK293FT cells were collected and resuspended at a density of 1,2 x 10^6 cells/mL in growth medium containing serum, yet without antibiotics. The DNA-Lipofectamine™ 2000 complexes were added to a 10 cm tissue culture plate containing 5 mL of growth medium containing serum without antibiotics. Next, 5 mL of the HEK293FT cell suspension were added to the plate, mixed gently by rocking the plate back and forth and incubated overnight at 37°C. The next day, the transfection medium was replaced by normal growth medium containing sodium pyruvate plus antibiotics. The virus-containing supernatant was harvested 48-72 h post-transfection by transferring the supernatant to a 15 ml falcon tube and collecting the cell debris by centrifugation for 5 min at 4°C and 3,000 rpm. The supernatant was 0.45 µm filtered, aliquoted, and stored at - 80°C.

2.8.2 Production of Lentivirus in HEK293T Cells

As alternative packaging cell, HEK293T cells were utilized for production of Lentivirus-miRNC and Lentivirus-miRGAbpα according to (Tiscornia et al. 2006). One day before transfection, HEK 293T cells were seeded on 10 cm tissue culture plates at a density of 3x 10^6 cells/dish. The next day, the medium was changed to 9 mL per 10 cm dish 1h prior to transfection. Per 10 cm dish, the following plasmids were mixed in a reaction tube in 0.5 mL $CaCl_2$: 10 µg vector (pLenti6/miRNC or pLenti6/miRGAbpa), 6.5 µg pMDL g/p RRE, 3.5 µg pMD2.G, and 2.5 µg pRSVrev. Then, 0.5 mL 2x BBS were added to the $CaCl_2$-DNA mix and the transfection was continued as described in 2.1.4.1. The next day (~ 12 h later), the medium was replaced by fresh medium and the virus-containing supernatant was harvested another 24-48 h later. The cell debris was collected by centrifugation for 5 min at 1,000 rpm and the supernatant was 0.45 µm filtered. For scale-up, the same transfection protocol was performed on 15 cm dishes with accordingly larger amounts of plasmids and transfection media.

2.8.3 Concentration of Lentivirus via Ultracentrifugation

Lentivirus containing supernatant from HEK293T cells was concentrated via ultracentrifugation. Initially, the supernatant was centrifuged (2,500 rpm, 5 min, 4°C) and 0.45 µm filtered. Thereafter, the virus was collected via ultracentrifugation in ultraclear centrifugation tubes for 90 min at 25,000 rpm and 4 °C. The pellet was allowed to dissolve overnight at 4°C in 0.1 mL filtered (0.22 µM) PBS. The next day, aliquots were prepared and stored at -80 °C.

2.8.4 Transduction of C2C12 Cells with Lentivirus

C2C12 Sigma cells were transduced with lentivirus for titering of the lentiviral stock, assessment of knock-down efficiency or generation of stable knock-down clones. The transduction was performed either after or while cells were seeded on a 6-well plate format in 1-1.5 mL of GM. This transduction medium contained diluted lentiviral stock as indicated and was supplemented with 6 µg/mL polybrene. Provided that cells were transduced while being passaged, 3x 10^4 cells per well were added to each transduction batch. Untransduced cells served as control, hence named “mock”.

2.8.5 Titering of the Lentiviral Stock in C2C12 Cells

C2C12 cells were transduced on day 0 with lentivirus (2.8.4) by using a serial dilution of virus. The transduced cells were targeted to Blasticidin-selection (2-4 µg/mL) from day 4 on for ~ 10 days by changing the medium every 3-4 days. The medium was then aspirated off and cells were washed twice with PBS. For visualization of individual cell clone populations, 1 mL of crystal violet solution was added to each well. The cells were incubated for 10 min at RT, thereafter washed again twice with PBS and the stained colonies counted.

2.8.6 Generating Stable miRNA Expression C2C12 Clones

C2C12 cells were transduced on duplicate wells on day 0 with lentivirus as described under 2.8.4. Starting on day 3, efficiently transduced cells were selected with Blasticidin by supplementing GM with 2 µg/mL antibiotic. The medium was replaced by new medium every 3-4 days. On day 10 of selection, cells had reached ~ 70%

confluency and were passaged. For selection of monoclonal miRNA expression clones, cells were seeded on 96-well plate format with each well containing one cell clone. For generation of polyclonal miRNA expression clones, a cell pool was seeded on 10 cm dishes. The selection pressure was increased for the next 7 days by changing the antibiotic-concentration in GM to 4 µg/mL until all non-transduced cells on mock wells were killed. During selection for mono- and polyclonal miRNA expression C2C12 cells, cells were passaged and seeded on larger tissue culture dishes prior to reaching > 70% confluency. Finally, cells were allowed to differentiate into myotubes and tissue culture samples were prepared for mRNA (2.5.1) and protein (2.6.6) analysis.

2.9 Colon26 Murine Cachexia Model

For tumor induction in cachexia models, $1.5*10^6$ Colon-26 cells in PBS were injected subcutaneously into 10-week-old CD2F1 mice (Charles River Laboratories, Brussels). Control mice were injected with PBS. Mice were sacrificed approximately 3 weeks after injection.

3 Results

3.1 Identification of Novel Transcriptional Regulators with Altered Activity under Atrophic Signalling

In this study, a cell-based high-throughput screen was employed in collaboration with M.D. Conkright from the Scripps Research Institute in Florida (USA) in order to identify novel transcriptional regulators being dysregulated under atrophic signalling. The screen consisted of ~ 1450 transcriptional regulators from human (755) and mouse (695) origin, which had previously been cloned in frame with an N-terminal Gal4 DNA-binding domain (Gal4). Individual transcriptional regulators were transfected along with a GAL4 *UAS::*luciferase reporter construct into HEK293T cells (2.2.1).

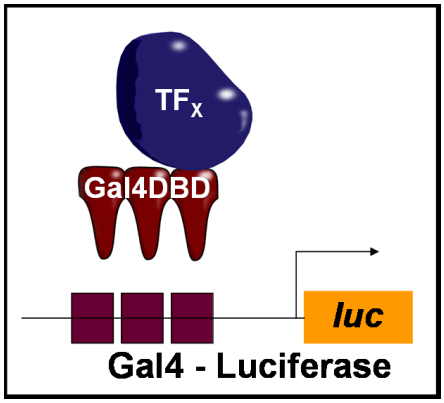

Figure 6: The cell-based high-throughput screen used in this study was based on the mammalian one-hybrid assay. Individual transcriptional regulators (TFx), which had been cloned in frame with an N-terminal Gal4 DNA-binding domain (Gal), were each transfected along with a *GAL4 UAS*::luciferase reporter (Gal4-Luciferase) into HEK293T cells. The screen consisted of ~ 1450 transcriptional regulators from human and mouse origin.

Following transfection, the Gal4 fusion proteins would bind to the Gal4 promoter thereby activating transcription of the luciferase reporter gene. The amount of expressed luciferase is determined by the ability of individual fusion proteins to recruit endogenous proteins from the basal transcription machinery or other transcriptional regulators and activate thereby transcription. Thus, under these conditions, each fusion protein has a basal transcriptional activity which can be monitored by luminescence

measurement. The molecular mechanisms underlying this screen design is identical with a mammalian one-hybrid assay (Figure 6).

Since the overall aim was, to find novel transcriptional regulators in two different *in vitro* models of muscle atrophy, cells were treated with TNF-α and Dex (2.2.2). These stimuli induced signal transduction pathways thereby changing the expression, localization or activity of endogenous proteins of the transcription machinery. Provided, these shift had an impact on individual Gal4 fusion proteins, the basal transcription activity of these Gal4 fusion proteins would either increase or decrease. Thus, focus of interest was to identify those transcriptional regulators with a significant change in relative luciferase activity upon pro-atrophic stimulation. Noteworthy, this screen design allowed monitoring changes in functional interactions between the Gal4 fusion protein and the proteins of the transcription machinery.

3.1.1 TNF-α Caused the Strongest Changes in Transcriptional Activity

In preparation for the actual screen, two Gal4 fusion proteins were validated as positive controls for the stimulation of cells with Dex and TNF-α, Gal4-GR and Gal4-NFKBIA, respectively. As negative control, the Gal4-DBD alone (Gal4) was used. Dex treatment induced significantly the transcriptional activity of Gal4-GR via the Gal4-Luc promoter-reporter construct (Figure 7). Thereby, a concentration of 1 µM Dex was sufficient and hence used for the screen. The fusion protein of Gal4 with IκBα (Gal4-NFKBIA) served as an ideal positive control for stimulation with TNF-α, since TNF-α increased the transcriptional activity of this fusion protein dose-dependently (Figure 7). Due to the potent apoptotic side effects of TNF-α, the mid-range concentration of 100 ng/mL TNF-α was chosen for the actual screen. In addition to the treatment with TNF-α or Dex, cells were also stimulated with both stimuli together in a third group, since the intracellular pathways induced by TNF-α and Dex are known to interact (McKay & Cidlowski 1999). Basically, the screen was performed as described in Amelio *et al.* 2007 (2.2).

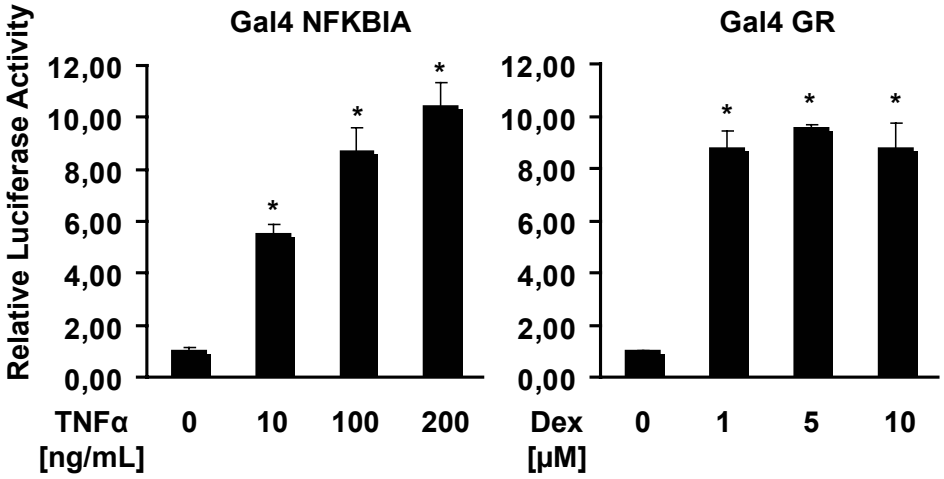

Figure 7: A concentration of 100 ng/mL TNF-α and 1 µM Dex was sufficient to induce relative luciferease activity of Gal4-NFKBIA and Gal4-GR, respectively. HEK29T cells were transfected with Gal4-Luc and CMV-ß-gal and Gal4-NFKBIA or Gal4-GR. Thereafter, cells were stimulated for 24 h with 10, 100, or 200 ng/mL TNF-α or 1, 5, or 10 µM Dex. Finally, relative luciferase activity was assayed and normalized to untreated control. (N = 3, mean ± SEM, * $p < 0.01$, one-way ANOVA with Dunnett´s posttest comparing each treatment group to untreated group)

Briefly, HEK293T cells were transfected with the promoter-reporter construct and individual Gal4 constructs from the library on 384 well plates (2.2.1). The next day, cells were stimulated for 24 h with 1 µM Dex, 100 ng/mL TNF-α, or both stimuli together and then subjected to measurement of reporter activity (2.6.7). The average of the luciferase activity from duplicate measurements was calculated. Fold changes of luciferase activity were calculated for each Gal4 fusion protein and stimulation condition over vehicle treatment. For each stimulation condition (Dex, TNF-α, Dex + TNF-α) and transcription factor species (human, mouse) the cut-off value for the fold change was determined graphically from a sorted rank. Above or underneath this value, the change in transcriptional activity was called significant. The sorted ranks of mouse and human transcription factors are depicted in Figure 8. The graph representing Dex-stimulation ran differently than the TNF-α and Dex + TNF-α graphs, with lower elevations towards the end of the graph, where the maximum fold changes were represented. The TNF-α and Dex + TNF-α graphs, however, resembled each other thus indicating that the TNF-α effects were dominant in the co-stimulation experiment. These graphs showed also the greatest elevation at the ends and hence the greatest fold changes. For example, by using TNF-α, a maximum fold increase of 7.8 was detected.

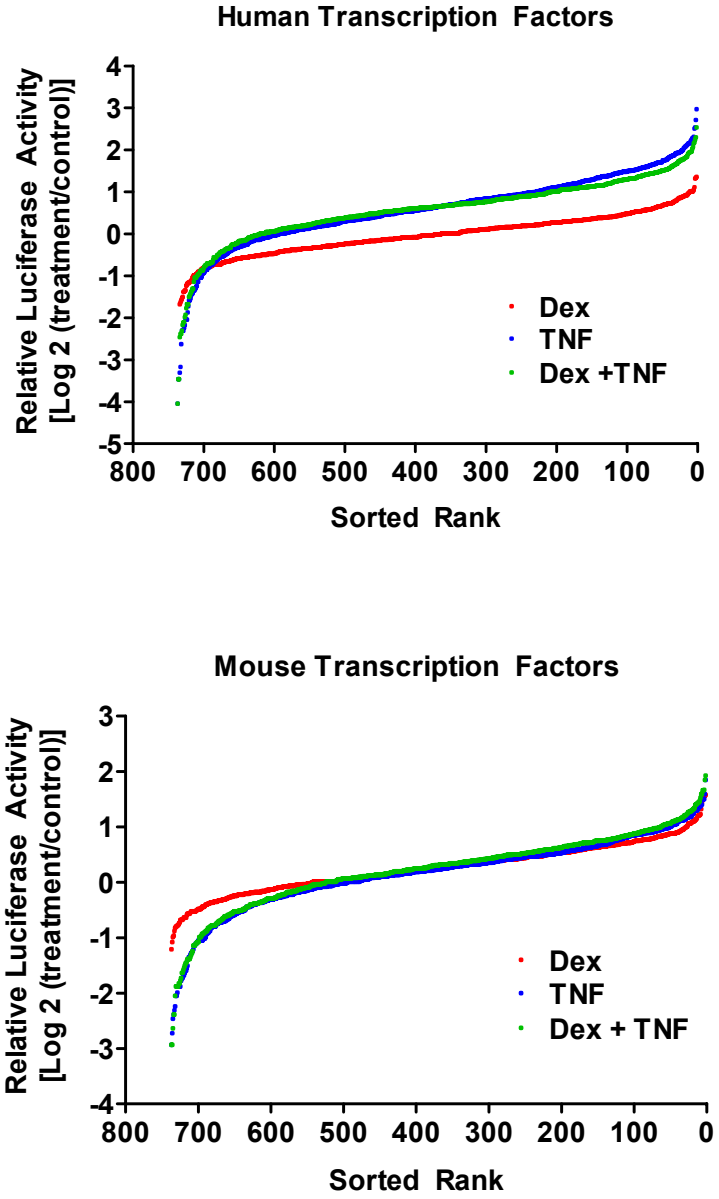

Figure 8: The pro-atrophic stimulus TNF-α induced the greatest fold changes in transcriptional activity. The cell-based high-throughput screen was performed as described in Amelio, 2007 #28. Gal4 constructs were transfected along with a Gal4 driven luciferase reporter into HEK293T cells as described in 2.2. Thereafter, cells were stimulated for 24 h with 1 µM Dex, 100 ng/mL TNF-α, or both stimuli together. Fold changes were plotted on a $\log_2$ scale against a sorted rank of fusion constructs from right to left. Fold changes are plotted over untreated control of relative luciferase activity from mouse and human transcription factors.

In total, 6.9% of all tested transcription factors had an altered transcriptional activity, whereas more transcriptional regulators were changed towards a fold increase (4.7%) than fold decrease (2.2%) (Figure 9). Furthermore, more human transcriptional regulators (60%) than murine transcriptional regulators (40%) responded by a change in

luciferase expression under these settings in this cell line. The comparison of the different stimulation conditions revealed, that TNF-α treatment had the strongest effect on transcription factors, since 40% of all significantly altered transcription factors changed during this stimulation condition.

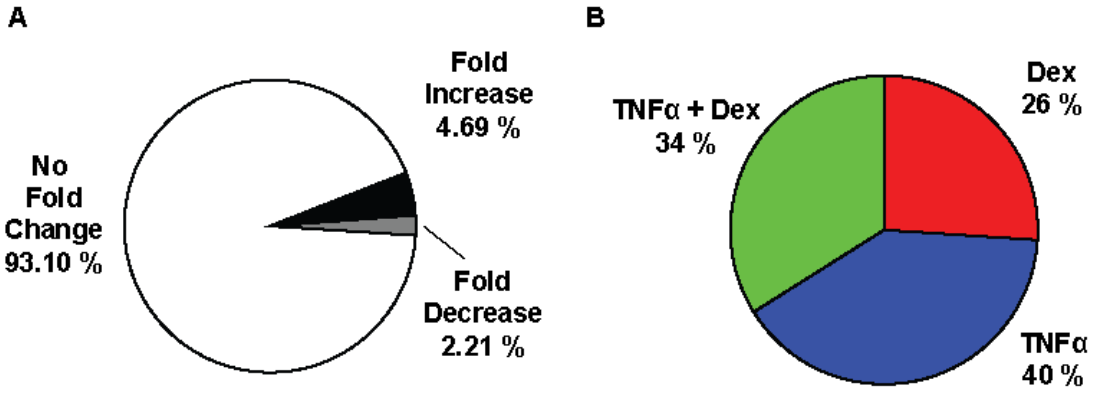

Figure 9: From all tested Gal4 fusion proteins, 6.9% showed a fold change upon pro-atrophic stimulation as determined by a Cell-Based High-Throughput Screen in HEK293T cells.

A) From 1450 tested Gal4 fusion proteins, 4.69 % responded via fold increase and 2.21% via a fold decrease towards pro-atrophic stimulation.

B) From these 100 Factors, 40%, 34% and 26% showed a change of transcriptional activity upon TNF-α, TNF-α + Dex, or Dex stimulation.

3.1.2 The Transcriptional Activity of Gal4-PSPC1 and Gal4-GAbpα was reproducibly altered

Putative TNF-α targets from the screen were retested in HEK293T cells growing on 12-well plates by using the mammalian one-hybrid assay. The cells were transfected with Gal4-Luc, Gal4 construct (Gal4-TF) and CMV-ß-gal (2.1.6), stimulated with 1 µM Dex, 100 ng/mL TNF-α, or both stimuli together for 24 h (2.1.5) and harvested for determination of relative luciferase activity (2.6.7). The changes of relative luciferase activity were calculated as mentioned before and plotted upon normalization to untreated control settings. A selection of tested transcription factors after stimulation with TNF-α is shown in Figure 10. The changes of relative luciferase activity for the majority of the TNF-α targets from the screen (USA) could not be reproduced on 12-well plate format (GER) (Figure 10). In addition, some of the screen targets had a relatively big standard deviation.

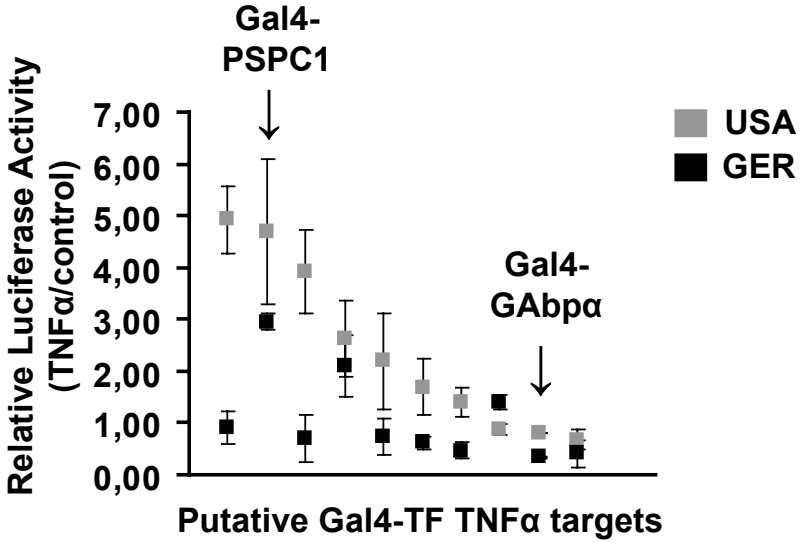

Figure 10: Relative luciferase activity of Gal4-PSPC1 and Gal4-GAbpα were reproducibly altered in TNF-α treated HEK293T cells as compared to putative Gal4-TF TNFα targets. For the manual setup, HEK293T cells were transfected with Gal4-Luc, pCMV-ß-gal, and Gal4-TFx and stimulated for 24 h with 100 ng/mL TNF-α. Thereafter, the luciferase activity was determined. Relative luciferase activity was plotted as fold change over untreated control by comparing screen settings (USA) on 384-well plates to a manual set-up on 12 well plates (GER). (N=2 (USA), N=3 (GER), mean ± stddev)

Based on these results, two candidates were chosen which showed a reproducible fold change in the screen settings and on 12-well plate format: Gal4-GAbpα showed a ~ 70%-fold decrease and Gal4-PSPC1 a 2.9-fold increase upon stimulation with TNF-α (Figure 11). "GA binding protein alpha" (GAbpα) is a transcriptional regulator identified from the mouse library, while PSPC1 is a factor from the human screen and stands for "Paraspeckle component 1".

In order to assess whether the fold change upon TNF-α stimulation was due to a change in protein expression, the protein levels of Gal4 fusion proteins were analyzed. First, HEK293T cells were transfected under assay settings (2.1.6) and treated with 100 ng/mL TNF-α, or left untreated for 24 h. Following this, overexpression of Gal4 fusion proteins was analyzed via western-blotting using the mouse Gal4-DBD antibody (2.6.3). Valosin containing protein (VCP) was used as loading control.

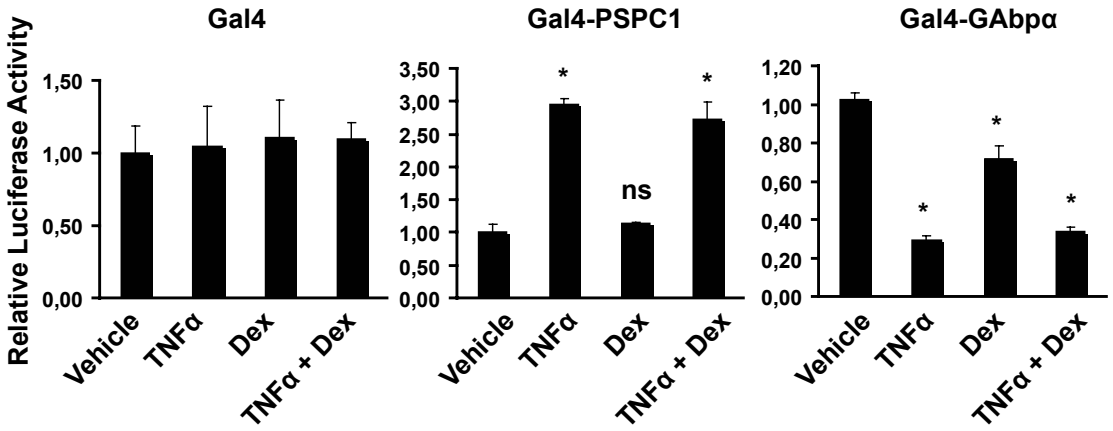

Figure 11: Alteration of relative luciferase activity of Gal4-PSPC1 or Gal4-GAbpα upon pro-atrophic stimulation. For the mammalian one-hybrid assay in HEK293T cells, cells were transfected with Gal4-Luc, pCMV-ß-gal, and Gal4, Gal4-PSPC1 or Gal4-GAbpα, respectively. Subsequent stimulation was carried out for 24 h with 100 ng/mL TNF-α, 1 µM Dex, or both stimuli together. Thereafter, relative luciferase activity was determined and normalized to untreated (vehicle) control. (N = 3-6, one (Gal4) and two independent experiments (Gal4-PSPC1, Gal4-GAbpα), mean ± SEM, * $p < 0.01$, one-way ANOVA with Dunnett´s posttest comparing each treatment group to control group)

The protein levels of Gal4-PSPC1 and Gal4-GAbpα were slightly up-regulated upon TNF-α treatment of HEK293T cells (Figure 12). Most importantly, no decreased protein levels of Gal4-GAbpα or increased levels of Gal4-PSPC1 were detected upon TNF-α treatment, thus, indicating that changes in luciferase activity were indeed due to a change in transcriptional activity and not because of a change in protein expression.

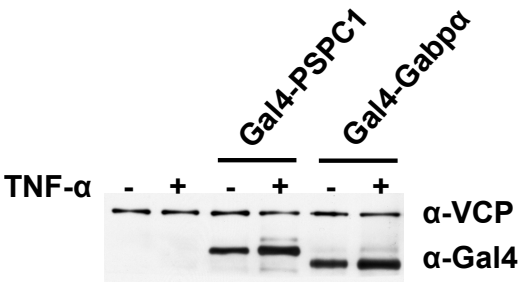

Figure 12: The activity of Gal4-GAbpα and Gal4-PSPC1 was not regulated via protein expression in TNF-α stimulated HEK293T cells. For western-blot analysis of overexpressed proteins in HEK293T cells, cells were transfected with indicated Gal4 fusion proteins and stimulated for 24 h with 100 ng/mL TNF-α or left untreated. Following this, whole cells extracts were prepared and subjected to western-blotting with the mouse antibody Gal4-DBD (2.6.3). Western-blot with VCP was used as loading control.

3.1.3 Validation of TNF-α targets in C2C12 cells

Since the aim of this study was to investigate the dysregulated transcriptional activity of novel transcriptional regulators under pro-inflammatory settings in muscle, C2C12 cells were employed in this study. These cells had previously been established as an *in vitro* muscle cell culture model (Yaffe & Saxel 1977). C2C12 cells can easily be propagated as muscle precursor cells, named myoblasts. Upon serum deprivation and after reaching > 95% confluency, these cells start to fuse into multinucleated myotubes which form within 2-4 days of the differentiation process (Figure 13). In parallel, the expression of the muscle specific protein myosin is increased (Figure 14).

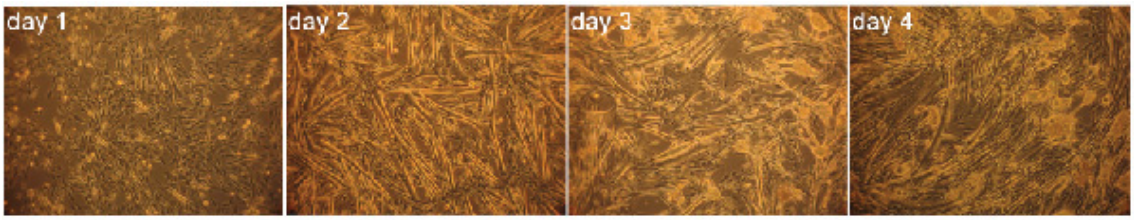

Figure 13: C2C12 LP myoblasts fuse into multinucleated C2C12 myotubes within the course of differentiation. Light microscopy images of C2C12 myoblasts which were allowed to reach > 95% confluency and thereafter induced to differentiate by switching from growth medium (GM) to differentiation medium (DM).

Initially, C2C12 cells were tested for their applicability as an *in vitro* model for Dex or TNF-α mediated muscle atrophy. Hence, C2C12 myotubes were stimulated for 24 h with 100 ng/mL TNF-α, 1 µM Dex or both stimuli together (2.1.5). Whole cell extracts were prepared and assessed for expression of myosin (2.6.6). This muscle-specific protein was found to be significantly decreased upon pro-atrophic stimulation with TNF-α and Interferon gamma (IFN-γ) (Figure 14) (Acharyya et al. 2004). However, no change in protein levels could be detected for Dex treatment or the TNF-α + Dex co-treated C2C12 myotubes. This suggests, that stimulation of C2C12 cells with TNF-α does indeed provide a suitable *in vitro* model for TNF-α mediated muscle atrophy.

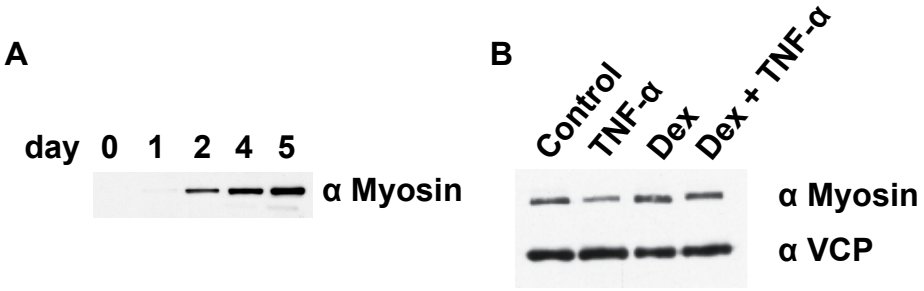

Figure 14: Myosin protein levels increased along with the differentiation process in C2C12 cells and decreased upon stimulation of C2C12 myotubes with TNF-α.

A) Western-blot analysis of endogenous myosin protein levels in differentiating C2C12 myocytes. C2C12 cells were allowed to differentiate over 5 days. Whole cell extracts were prepared from C2C12 myoblasts (day 0) and on each day of the differentiation process. Thereafter, myosin protein levels were analyzed by western-blot (2.6.3).

B) Western-blot analysis of endogenous myosin protein levels in C2C12 myocytes C2C12 myotubes were stimulated overnight with 100 ng/ mL TNF-α, 1 µM Dex or both stimuli at once in DM. Thereafter myosin protein levels were analyzed by western-blot (2.6.3) and VCP protein levels were detected as loading control.

The identified screen targets - PSPC1 and GAbpα - were tested for an alteration of transcriptional activity in C2C12 cells by the mammalian one-hybrid assay. For this purpose, C2C12 cells were transfected with Gal4-Luc and Gal4-DBD (Gal4) or Gal4-TF (2.1.6) and treated with 25 ng/mL TNF-α for 24 h (2.1.5).

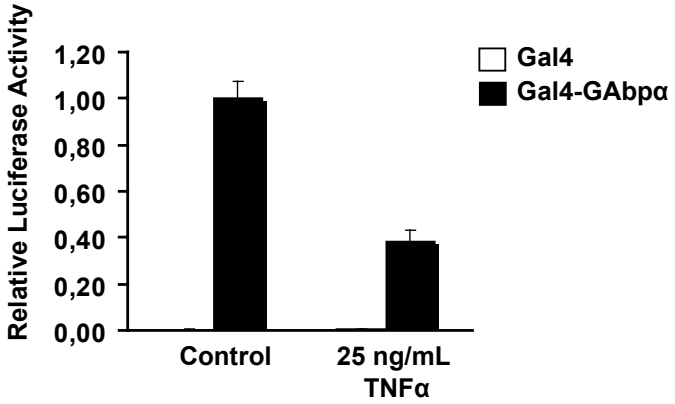

Figure 15: The relative luciferase activity of Gal4-GAbpα decreased upon stimulation with TNF-α in C2C12 cells. C2C12 cells were transfected with Gal4-Luc, CMV-ß-gal, and Gal4 or Gal4-GAbpα, respectively. Following this, cells were stimulated for 24 h with 25 ng/mL TNF-α and subjected to determination of relative luciferase activity. Relative luciferase activity was normalized to untreated control (N = 3, mean ± SEM, p = 0.025).

The transcriptional activity of Gal4-PSCP1 in C2C12 cells – as determined by the ability to induce reporter gene expression under basal conditions – were not higher than two-fold above background and hence almost not detectable (data not shown). Under

the same conditions, however, the basal transcriptional activity of Gal4-GAbpα was significantly detectable above background. Stimulation with TNF-α caused a decrease of relative luciferase activity (Figure 15). Again, the expression levels of Gal4 fusion proteins were analyzed via western-blot (2.6.3). Upon transfection of C2C12 cells under assay conditions, cells were stimulated for 24 h with 10 or 100 ng/mL TNF-α, or left untreated (2.1.5). As control, overexpression levels of Gal4-PSPC1 were also analyzed in C2C12 cells. Despite the fact, that no transcriptional activity of Gal4-PSPC1 was detectable in C2C12 cells, the PSPC1 protein was identified at protein levels (Figure 16). The protein levels of Gal4-GAbpα were not altered upon stimulation with TNF-α.

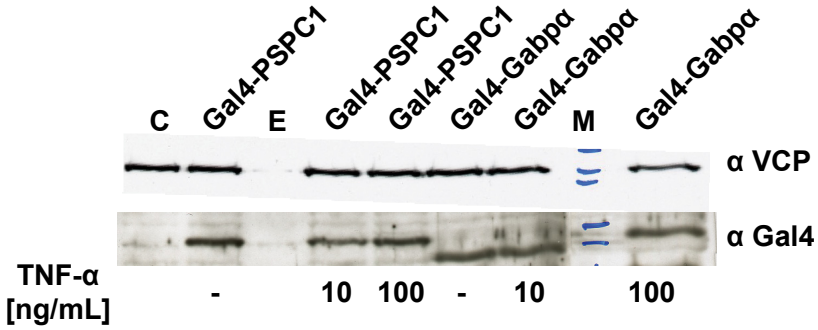

Figure 16: Western-blot analysis of overexpressed Gal4 fusion protein levels in C2C12 cells. Cells were transfected with no DNA at all (C), pGal4-PSPC1 or pGal4-GAbpα. Then, cells were stimulated with 10 or 100 ng/ mL TNF-α, or left untreated. Whole cell extracts were prepared and analyzed for protein overexpression by western-blot with the anti-Gal4 antibody or anti-VCP as loading control (2.6.6). (E: empty lane; M: Marker (protein ladder); C: Control)

These data suggest that the transcriptional activity of GAbpα is decreased in a pro-inflammatory condition. Furthermore, GAbpα has been described to be crucial for several pathways which so far had not been addressed in the context of muscle atrophy. Following the initial discovery of this transcriptional regulator to activate transcription from viral promoters, the transcription of several mitochondrial respiration genes and sub-synaptic genes at the NMJ is likewise activated by GAbp (Rosmarin et al. 2004).

3.1.4 TNF-α Does Not Regulate the Activity of GAbpα on the Expression Level in C2C12 Cells

In solution GAbpα dimerizes with GAbpβ thereby forming the transcriptional active heterodimeric GAbp. A diminished expression of GAbpβ upon TNF-α signalling might

also cause a decreased transcriptional activity of GAbpα, since GAbpβ mediates the protein-protein interactions to the basal transcription machinery. Therefore, the expression of GAbpβ was analyzed via qRT-PCR. C2C12 myoblasts were allowed to differentiate into C2C12 myotubes and then stimulated overnight with 5 ng/mL or 25 ng/mL TNF-α. These cells were then harvested, targeted to RNA extraction (2.5.1), cDNA synthesis (2.4.9) and qRT-PCR analysis (2.4.2.2). GAbpβ mRNA levels were not changed upon TNF-α treatment of C2C12 cells, while transcript levels of GAbpα were slightly downregulated upon treatment with TNF-α (Figure 17).

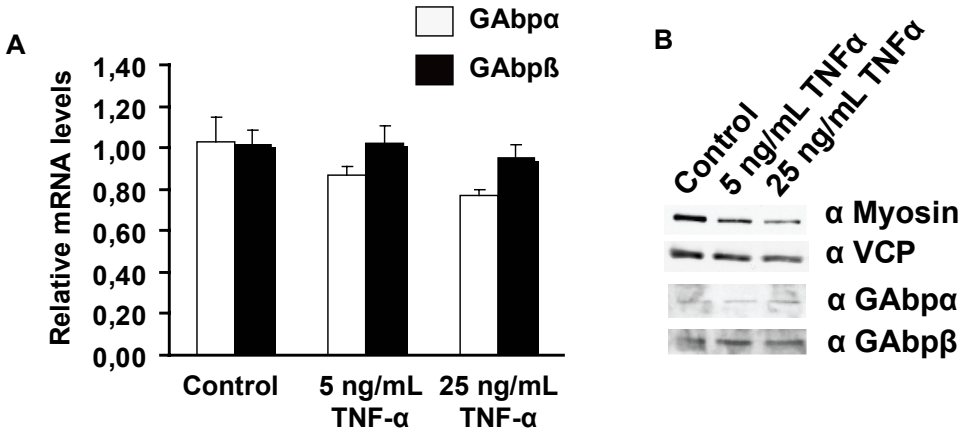

Figure 17: Analysis of relative mRNA levels and protein levels GAbp in C2C12 myotubes.

A) Relative quantification of mRNA levels of GAbpα and GAbpβ in C2C12 cells by qRT-PCR analysis. C2C12 myoblasts were allowed to differentiate for ~ 4 days into C2C12 myotubes. Fully differentiated myotubes were then stimulated overnight with 5 ng/mL or 25 ng/mL TNF-α. RNA was extracted, cDNA synthesis carried out and the mRNA levels of GAbpα and GAbpβ detected by qRT-PCR (N = 1, mean ± STDEV, STDEV represents variation from PCR replicates).

B) Western-Blot of endogenous proteins in TNF-α stimulated C2C12 myotubes. Myotubes were stimulation overnight with 5 or 25 ng/mL TNF-α and subjected to preparation of native protein extracts.

Along with this experiment, the endogenous protein levels of GAbpα and GAbpβ were also analyzed in C2C12 myotubes. For this purpose, cells were seeded on 6-well plates, and allowed to differentiate into myotubes. Following this, cells were stimulated overnight with 5 or 25 ng/mL TNF-α and subjected to preparation of native protein cell extracts. These extracts were then analyzed by western-blot. While the protein levels of myosin again decreased upon TNF-α treatment, the levels of GAbpα and GAbpβ remained unaltered under these conditions (Figure 17). In conclusion, TNF-α signalling in C2C12 does not regulate the activity of GAbp on the expression level.

Overall, Gal4-GAbpα was identified as a novel transcriptional regulator with dysregulated activity in TNF-α treated HEK293T and C2C12 cells.

3.2 Knock-Down of GAbpα in C2C12 Cells by Lentiviral Delivery of a GAbpα-specific miRNA

The physiological importance of GAbpα in muscle cells was addressed by a transient knock-down of GAbpα in C2C12 cells. As described previously, the whole-body knock-out of GAbpα and conditional knock-down in muscle-tissue have already underlined the physiological importance of GAbpα in the context of the NMJ (de Kerchove D'Exaerde et al. 2002; Ristevski et al. 2004). However, transient loss-of-function studies of GAbpα in muscle tissue have not been examined so far. The advantage of transient loss-of-function studies is that they mimic acute effects, which are of interest especially in the context of a chronic inflammation process. In this study, the loss-of-function of GAbpα by lentiviral mediated delivery of an RNAi against GAbpα was addressed.

3.2.1 GAbpα Was Efficiently Knocked-Down by a miRNA

The effectors of RNAi mediated knock-down can either be small hairpin RNAs (shRNA) or micro-RNA (miRNA)-based shRNA. While shRNAs are transcribed from constitutive active pol III promoters (U6), miRNAs are transcribed from pol II promoters, which may be used also in a tissue-specific manner (Wiznerowicz et al. 2006). With the aim to knock-down GAbpα in C2C12 cells *in vitro* and eventually later on in muscle tissue, miRNAs were chosen as RNAi molecule. Since alternative splicing variants of GAbpα, which vary within the 5' untranslated region (UTR), have previously been described, miRNAs targeting the 3'UTR were designed (O'Leary et al. 2005).

For miRNA design, two different splice variants of GAbpα were used, which vary in the length of the 3'UTR (2.7.1). The GAbpα sequence with the Pubmed accession number NM008065 carries a ~ 1 kb longer 3'UTR than the GAbpα sequence with the accession number BC013562. Based on these sequences, the miRNA1256 was predicted to have the highest knock-down efficiency on GAbpα with the short 3`UTR, while miRNA4216

and miRNA4682 were predicted to have the highest knock-down efficiency on GAbpα with the accession number NM 008065. All three designed RNAi molecules were cloned into a miRNA expression vector, resulting in pcDNA6.2-GW/EmGFP-miRNA1256, -miRNA4216 and –miRNA4682 (2.7.2).

The knock-down efficiency of these designed RNAi molecules was tested thereafter by employing the "GeneEraser™ Luciferase Suppression-Test System". For this purpose, a vector carrying the targeted gene sequence of GAbpα had to be cloned into the 3´UTR of the luciferase gene (pTarget vector). Upon transfection into HEK293 cells, this vector expresses a luciferase-target gene mRNA reporter construct. This consisted of the coding region for the luciferase reporter enzyme, a translational stop codon, the target gene, and the 3`UTR of the luciferase. Co-expression of functional RNAi molecules causes degradation of the luciferase-target gene mRNA. Due to the length of the 3'UTR of GAbpα (~ 3 kb), two different pTarget vectors containing the miRNA target sites were cloned (2.7.3). The plasmid pTarget-GAbpα-ORF contained the complete open reading frame (ORF) (1106 bp) of GAbpα and a small portion of the 3'UTR (616 bp) and was targeted by miRNA1256. The ramaining part of the 3'UTR (2347 bp) was cloned into a second pTarget vector, pTarget-GAbpα-3'UTR, and targeted by miRNA4216 and -4682.

Following cloning, these plasmids were analysed in the pTarget system in HEK293 cells (2.7.4). The miRNA4216 and -4682 did not decrease reporter activity of the pTarget-GAbpα-3'UTR as compared to control miRNA, an unspecific miRNA sequence (miRNA NC), which served as negative control (data not shown). However, overexpression of miRNA1256 resulted in a dose-dependent decrease of reporter activity from the pTarget-Gabpα-ORF vector compared to control miRNA in HEK293 cells (Figure 18). Since a minimal amount of RNAi tested (1 ng miRNA) yielded still a knock-down effect of > 70%, this miRNA was found to be very effective. Thus, miRNA1256 targeted efficiently degradation of the GAbpα target gene.

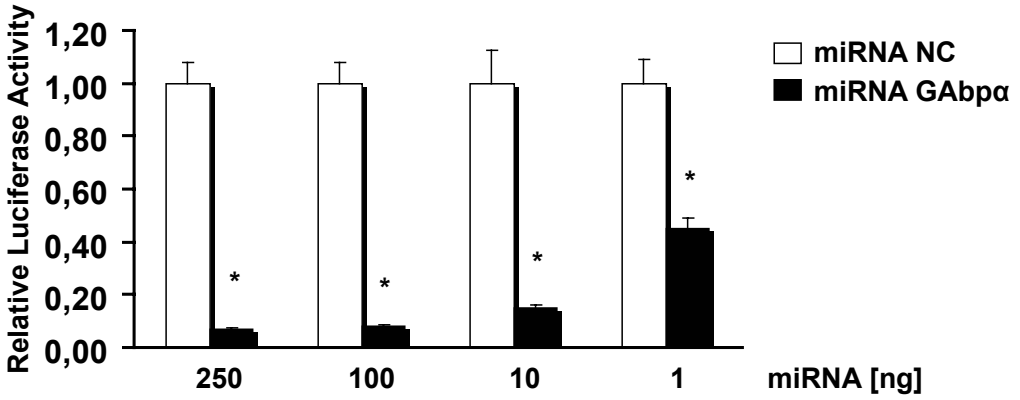

Figure 18: The miRNA1256 (miRNA GAbpα) was very efficient for knock-down of a luciferase-target gene mRNA reporter construct (pTarget-GAbpα-ORF) in HEK293 cells (2.7.4). Cells were transfected with 100 ng pTarget-GAbpα-ORF and indicated amounts of pCDNA6.2-GW/EmGFP-miRNA 1256 or – miRNA NC. Relative luciferase activity was determined as described in M X and normalized to the relative luciferase activity of miRNA NC. (N = 9, three independent experiments, mean ± SEM, * p< 0.0001, t test for comparison between miRNA GAbpα versus miRNA NC for each group separately)

Next, the knock-down efficiency of the miRNA1256 was tested on GAbpα protein levels by overexpression of the miRNA1256 vector along with an expression vector for GAbpα (2.7.5). For this purpose, an overexpression vector for GAbpα had to be cloned.

The coding sequence of GAbpα was obtained through restriction digest of the insert GAbpα-ORF from the pTarget-GAbpα-ORF vector by using *Not*I (2.4.3). Along with this, the pcDNA3.1(-) vector was subjected to digestion with *Not*I and then dephosphorylated (2.4.10). Both, insert and vector, were then ligated (2.4.7). Completion of the cloning procedure resulted in an expression vector for GAbpα (pcDNA3.1(-)GAbpα) (2.4.12).

HEK293T cells were transfected with 2 µg of pcDNA3.1-GAbpα (2.1.4.1). Concomitantly, cells were transfected with 0, 0.5, 1, 2 or 4 µg pcDNA6.2-GW/EmGFP-miRNA 1256. In a further transfection reaction, co-transfection with 4 µg pcDNA6.2-GW/EmGFP-miRNA NC served as negative control. Thereafter, whole cell extracts were prepared and analyzed for overexpression of GAbpα by western-blot (2.6.6). The loading control VCP confirmed uniform protein loading in each sample (Figure 19). The knock-down of overexpressed GAbpα was efficiently detected already at the minimal amount tested (0.5 µg miRNA1256). GAbpα protein levels were only slightly decreased by using the maximal amount of the unspecific miRNA (4 µg).

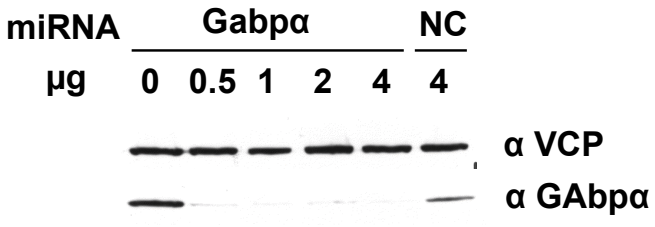

Figure 19: Overexpressed GAbpα protein levels in HEK293T cells were significantly decreased upon concomitant expression of the miRNA GAbpα. HEK293T cells were transfected with 2 µg pcDNA3.1-Gabpα in each experiment. In parallel, cells were transfected with 0 µg miRNA (first lane), 0.5, 1, 2 or 4 µg miRNA GAbpα (second, third, fourth and fifth lane respectively) or 4 µg miRNA NC. Thereafter, whole cell extracts wer prepared and overexpressed GAbpα protein levels assessed by western-blot. As loading control, VCP protein levels were analyzed.

Consequently, the miRNA 1256 (miRNA GAbpα) was used for knock-down of endogenous GAbpα in C2C12 cells via lentiviral delivery.

3.2.2 Infection of C2C12 Cells with Lentivirus containing a miRNA GAbpα Expression Cassette

The advantage of lentiviral gene delivery is a stable transduction even of non dividing and fully differentiated cells as well as long-term transgene expression, since the gene of interest is integrated into the host genome (Naldini 1998; Tiscornia et al. 2006). Delivery of the miRNA by transfection was not suitable in this setting due to the relatively low transfection efficiency of C2C12 cells. Therefore, a lentivirus vector system was chosen for the delivery of the miRNA into proliferating C2C12 myoblasts and differentiated C2C12 myotubes.

Based on the design and cloning of the miRNA by using the “Block-iT Pol II miR RNAi Expression Vector Kits” from Invitrogen, the “Lentiviral Pol II miR RNAi Expression System” was employed in this study for generation of the lentiviral destination vector (2.7.6). This vector contained the miRNA GAbpα expression cassette. Next, this destination vector was utilized for generation of lentivirus in 293FT cells (2.8.1). Co-cistronic expression of GFP from the pLenti6-GAbpα and -NC allowed for evaluation of lentivirus production in the packaging cell line 293FT via microscopic analysis. Over 90% of lentivirus producing cells showed GFP expression indicating a successful transfection of 293FT cells and lentivirus production with the pLenti6-GAbpα, -NC and helper plasmids (Figure 20).

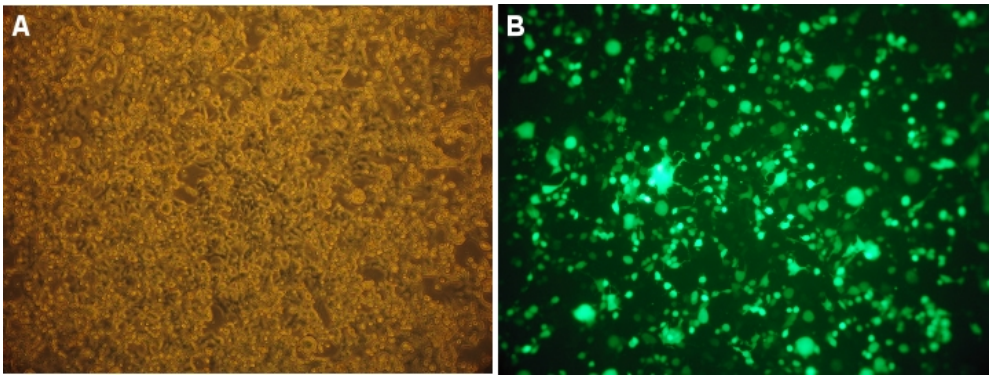

Figure 20: Production of lentivirus in HEK293FT cells. HEK293FT cells were transfected with helper plasmids and pLenti6-Gabpα as described in 2.8.1. The next day, co-cistronic GFP expression was analyzed by microscopic analysis. A) Phase Contrast B) GFP

The lentivirus containing supernatant was harvested and C2C12 cells transduced with virus using a dilution range of $1x10^{-2}$ to $1x10^{-6}$ (2.8.4). However, no GFP expression was detected in C2C12 cells by microscopic analysis (data not shown). Next, various variations from the protocol were tested to obtain efficiently transduced C2C12 cells. These were for instance production of lentivirus from more 293FT cells, harvest of virus containing supernatant on different days, transduction of C2C12 cells with a higher virus titer. Yet, no efficiently transduced C2C12 cells were detectable upon transduction with such prepared virus.

Based on these results, an alternative protocol for producing lentivirus was tested (2.8.2). This time, HEK293T cells were employed as packaging cell line and transfected for this purpose on 2x15cm dishes per miRNA (GAbpα and NC). Virus harvest was performed on day 3 after transfection. This virus was then diluted 1:2 and 1:5 for transduction of C2C12 cells and HEK293T cells, respectively. Transduction was performed during passaging by using polybrene (2.8.4). While ~ 100% of transduced HEK293T cells showed GFP expression, ~ 5% of transduced C2C12 cells were GFP positive. With the aim to concentrate lentivirus, an ultracentrifugation step was performed directly after the harvest of virus from the producer cell line (2.8.3). Such concentrated lentivirus was titered in C2C12 cells by using serial dilutions of the lentiviral stock which ranged from $1.5x10^{-4}$ to $1.5x10^{-8}$ (2.8.5). Cells were subjected to Blasticidin selection for the course of 10 days. Thereafter, surviving colonies were

detected by crystal violet staining, counted and in consideration of the virus titer expressed as transforming units (TU) per mL.

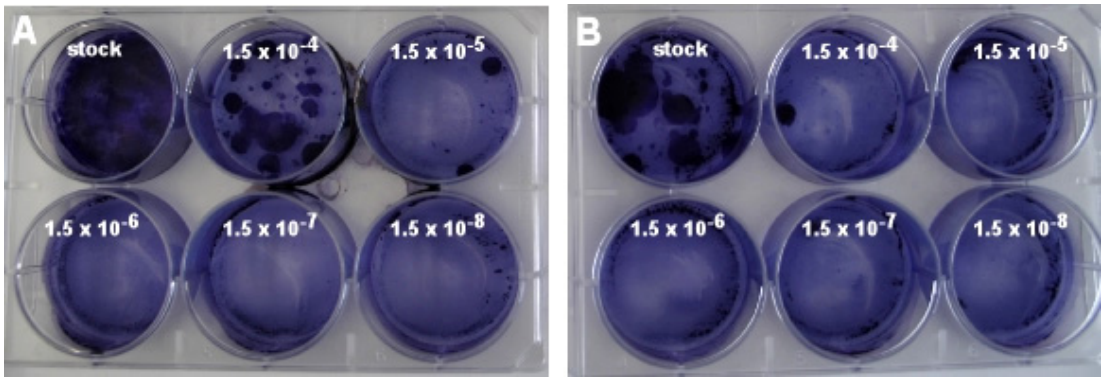

Figure 21: Determination of virus titer via crystal violet staining of transduced and blasticidin selected C2C12 cells (2.8.5). C2C12 cells were transduced with concentrated lentivirus (stock) that contained as transgene an expression cassette for the miRNA NC (A) or Gabpα (B). In parallel, serial dilutions of the lentiviral stock were prepared which ranged from $1.5x10^{2}$ to $1.5x10^{-7}$ and cells were also transduced with diluted lentivirus. Thereafter, cells were subjected to blasticidin selection for 10 days. Following this, surviving colonies were detected by crystal violet staining.

The titer of the lentivirus containing miRNA NC (Figure 21 A) and miRNA GAbpα (Figure 21 B) was determined to $3.3x10^{8}$ TU/mL and $2.6x10^{7}$ TU/mL, respectively. Following this, C2C12 cells were transduced using an MOI of 1 and 5 and such subjected to lysis for protein analysis (2.6.6). Protein samples were analyzed via western-blot for knock-down of GAbpα, however, no change in protein levels was detected in miRNA GAbpα versus miRNA NC cells (data not shown). Thus, the lentivirus generated in this study was obviously inefficient for transient transduction of C2C12 cells and transient knock-down of GAbpα protein levels.

Finally, stable transduced C2C12 cells were prepared (2.8.6). By using blasticidin selection, untransduced cells were eliminated and efficiently transduced cells enriched. The latter was allowed to differentiate and tested on protein and mRNA level for knock-down of GAbpα (Figure 22). The relative mRNA levels of GAbpα in miRNA NC containing C2C12 cell clones were slightly increased compared to the untreated control (C). In contrast, the transcript levels of GAbpα in miRNA GAbpα containing C2C12 cell clones remained unchanged (see for instance clone 1 and 5) or were not significantly decreased (clone 4 and 6). In addition, GAbpα protein expression was also

assessed by western-blot of stable transduced C2C12 cells (2.6.6). Samples 2 and 3 of miRNA NC containing C2C12 cells showed a protein decrease compared to sample 1 thus indicating unspecific effects. A similar observation was made with samples derived from miRNA GAbpα C2C12 cells. Here, samples 2 and 3 seemed to contain less GAbpα than sample 1. Similar results were obtained when analyzing samples 4-6 from miRNA NC or GAbpα (data not shown). To conclude, no miRNA GAbpα specific knock-down of GAbpα was detected in stable transduced C2C12 cells as compared to unspecific control (miRNA NC).

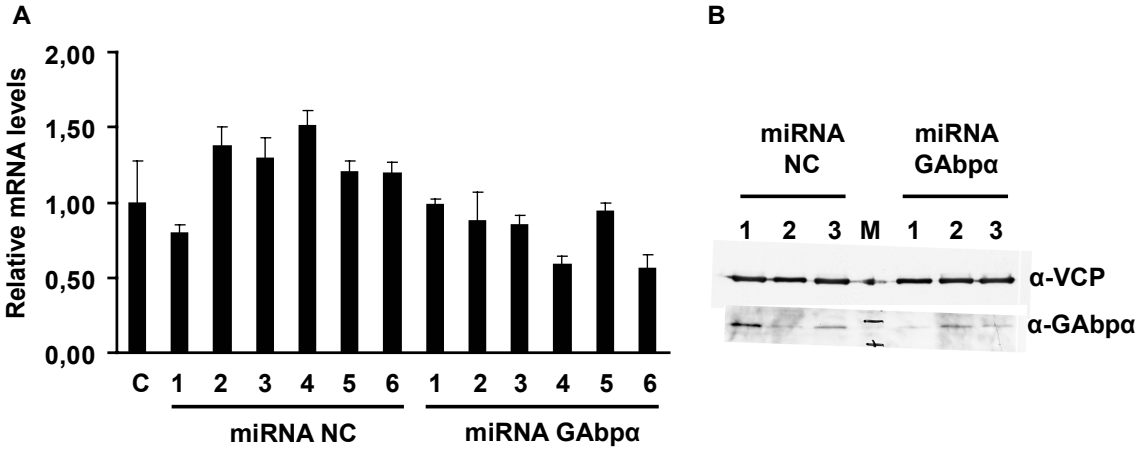

Figure 22: Stable transduced C2C12 myotubes showed no significant decreased of relative GAbpα mRNA or protein levels.

A) C2C12 myotubes stably expressing miRNA expression cassettes, Gabpα or NC, were taken for mRNA analysis. Normalization was carried out over untransduced C2C12 myotubes (C). (N = 1, mean ± STDEV, STDEV represents variation from PCR replicates)

B) Stable transduced C2C12 cells were prepared as described in the 2.8.6. These cells were then differentiated into C2C12 myotubes. Following this, native cell extracts were prepared and protein levels analyzed by western-blot. Shown are three representative cell clones per miRNA.

While establishing an RNAi-mediated knock-down system for GAbpα in C2C12 cells, two muscle-specific knock-out studies of GAbpα were published (Jaworski et al. 2007; O'Leary et al. 2007). These studies further supported the importance of this transcriptional regulator for the functional integrity of the NMJ. However, the molecular mechanisms underlying the transcriptional regulation of sub-synaptic target genes in muscle cells had not been addressed in these studies. Since the transcriptional regulation of GAbp was of novel interest, the elucidation of this mechanism was further addressed in this study.

3.3 The Transcriptional Active GAbp Heterodimer Dissociates in TNF-α Stimulated C2C12 Cells

3.3.1 TNF-α Treatment of C2C12 Cells Causes the Dissociation of the Heterodimeric GAbp

As shown before in this study, the transcriptional activity of overexpressed GAbpα decreased upon TNF-α stimulation of HEK293T and C2C12 cells in a mammalian one-hybrid assay. The altered transcriptional activity of GAbpα was not regulated by transcription as shown by determination of endogenous mRNA and protein levels of GAbpα and GAbpβ in C2C12 cells (Figure 17). Since the individual DNA-binding activity of GAbpα is not detectable by the mammalian one-hybrid assay - DNA-binding occurs in this assay exclusively via the Gal4 DNA-binding domain - a change in the DNA binding of GAbpα, which might also cause an alteration of transcriptional activity, could be ruled out. As another possibility for a diminished transcriptional activity, the dissociation of the GAbp complex was addressed. Since the transcriptional activation domain and DNA binding domain of GAbp are separated on two different proteins, GAbpα and GAbpβ, dissociation was predicted to lower the activity. A suitable tool for studying protein-protein interactions in cell culture is the mammalian two-hybrid assay. For this purpose, two fusion proteins are expressed, each containing a different tag. While one protein carries a DNA binding domain, for example Gal4, the other contains a transcriptional activation domain, for example Vp16. Upon co-transfection with a Gal4 driven luciferase reporter into a mammalian cell line, the interaction of these proteins is represented by an increased luciferase expression. Noteworthy, an increased luciferase activity stands for the close proximity of both proteins and not a transcriptional activity of the overexpressed proteins like it is detectable by the mammalian one-hybrid assay. Consequently, a diminished luciferase expression suggests that a dissociation of both proteins has occurred. Usually, the tags alone, Gal4 and Vp16 are used as negative control.

Since GAbpα was already available as fusion protein with the Gal4 DNA binding domain, a fusion protein of GAbpβ with Vp16 was cloned. The coding region of GAbpβ was amplified from the plasmid pcDNA3.1(-)GAbpβ by using the primer pair GAbpβ-Vp16-for and GAbpβ-Vp16-rev via PCR. The cloning procedure for pcDNA3.1(-

)Gabpβ is described in 3.4.1. Upon restriction digest of both vector and insert with *Kpn*I and *Nhe*I, the PCR product was then cloned into the pCMX-Vp16 vector. This Vp16-GAbpβ expression protein contained the Vp16 domain at the N-terminus. Following this, a mammalian two-hybrid assay was performed in C2C12 cells (2.1.6). As negative controls, Gal4 and Vp16 constructs were transfected while the interaction of GAbpβ and GAbpα was analyzed by transfection of Gal4-GAbpα and Vp16-GAbpβ (2.1.4.2). Transfected cells were stimulated for 48 h with 25 ng/mL TNF-α, or left untreated (2.1.5), and finally assayed for relative luciferase activity (2.6.5) (Figure 23).

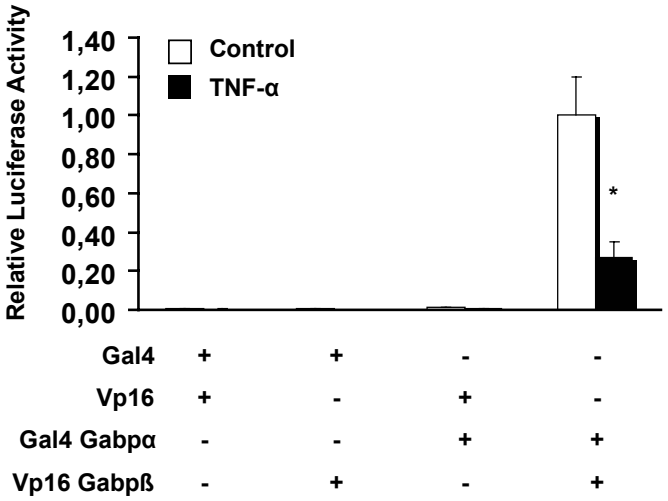

Figure 23: Gal4-GAbpα and Vp16-GAbpβ dissociate upon TNF-α treatment of C2C12 cells. For the mammalian two-hybrid assay, C2C12 cells were transfected with Gal4-Luc and CMV-ß-gal as well as indicated constructs and stimulated for 48 h with 25 ng/mL TNF-α or left untreated. Following this, relative luciferase activity was determined and normalized to untreated (control) co-expression of Gal4-GAbpα and Vp16-GAbpβ (N = 9, 3 independent experiments, mean ± SEM, * $p < 0.001$, t test. Usually, this transfection and stimulation experimental design requires a multifactorial ANOVA analysis. However, for simplicity a t test was performed. In addition, since the TNF-α effect in each transfection group individually was of interest, this statistical analysis method was found to be more adequate here).

No luciferase activity was detectable in the negative control settings. Thus, no interaction occurred between Gal4 with Vp16, Gal4 with Vp16-GAbpβ or Gal4-GAbpα with Vp16. Co-expression of Gal4-GAbpα with Vp16-GAbpβ induced, however, clearly the expression of the luciferase reporter via the Gal4 promoter, thus, underlying the specific protein-protein interaction between these proteins. Stimulation with TNF-α resulted in a significant reduction of reporter gene expression ($p < 0.001$). This decreased protein-protein interaction indicates a dissociation of the transcriptional active heterodimer due to the pro-inflammatory cytokine TNF-α.

In order to assess whether TNF-α mediated dissociation occurs in C2C12 cells on endogenous protein levels as well, a co-immunoprecipitation was performed (2.6.4). C2C12 myotubes were stimulated for 30 min with 25 ng/mL TNF-α (2.1.5) and then targeted to co-immunoprecipitation by using a polyclonal GAbpβ antibody. Immunoblotting with a polyclonal murine GAbpβ antibody confirmed that equal amounts of GAbpβ were pulled down in TNF-α treated and control C2C12 cells (2.6.3). Concomitantly, less GAbpα was detected in the eluate upon TNF-α treatment. This strengthens the finding from the mammalian two-hybrid assay and indicates the dissociation of endogenous proteins in response to TNF-α.

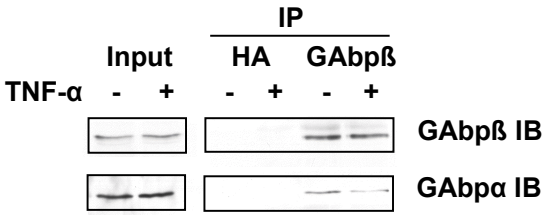

Figure 24: The heterodimeric GAbp complex dissociates upon TNF-α stimulation of C2C12 myotubes. Co-immunoprecipitation of GAbpβ and GAbpα was performed from extracts of C2C12 myotubes. Cells were allowed to differentiate, stimulated for 30 min with 25 ng/mL TNF-α, extracted and subsequently subjected to immunoprecipitation with an antibody against GAbpβ. The presence of GAbpα and GAbpβ was analyzed by western-blot in the input and eluate fractions (IP).

3.3.2 The Minimal Interaction Domains of GAbpα and GAbpβ are Sufficient for TNF-α Mediated Dissociation of the Complex

The dissociation of the GAbp complex might be caused by post-translational modifications (e.g. phosphorylations) or changes in protein-protein interactions with other transcriptional regulators or the basal transcriptional proteins. As mentioned earlier, several proteins have already been described to bind to GAbp, e.g. Sp1, HDAC, p300 (Rosmarin et al. 2004). Therefore, domain truncations of GAbpα and GAbpβ were cloned in order to identify those domains or post-translational modification sites required for TNF-α mediated dissociation via the mammalian two-hybrid assay. The domains crucial for the protein-protein interaction between GAbpα and GAbpβ were not modified to guarantee a functional protein-protein interaction in the mammalian two-hybrid assay. For this reason, all corresponding domain truncation constructs

carried the protein interaction domains, which are the C-terminal portion of GAbpα (aa 325-349) and the N-terminal portion of GAbpβ (aa 1-169).

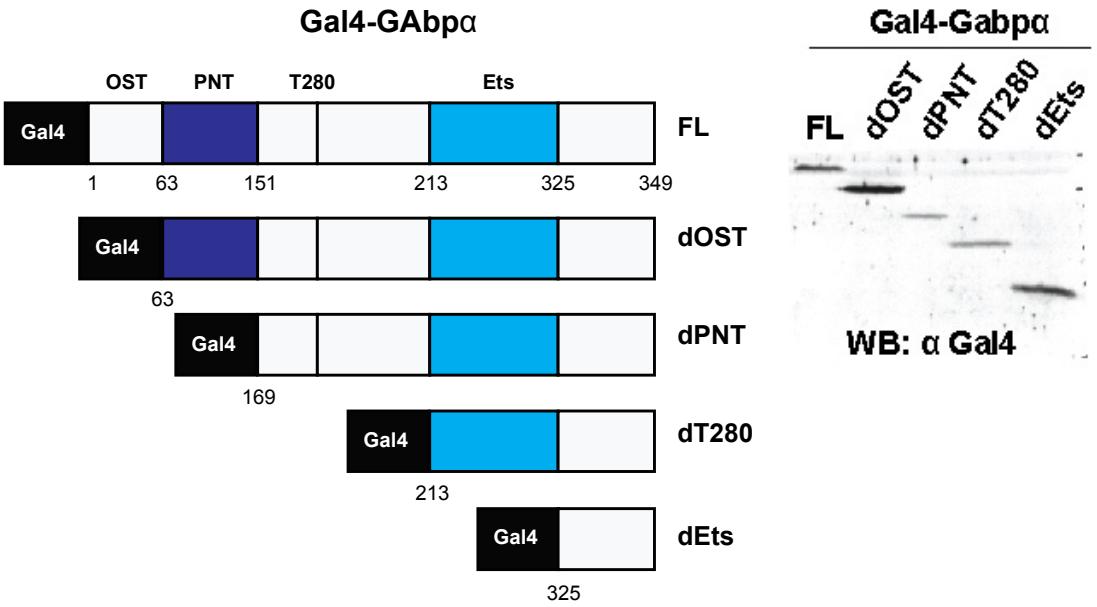

Figure 25: Illustration of cloned Gal4-GAbpα domain truncations (left) and overexpression analysis of corresponding fusion proteins in HEK293T cells (right). N-terminal domain deletions of GAbpα were cloned into the pGal4 vector. These Gal4-GAbpα fusion proteins were transfected into HEK293T cells for overexpression analysis. Whole cell extracts were performed and the fusion protein levels detected by western-blot using the Gal4 antibody.

For cloning of Gal4-GAbpα domain truncation constructs, four different PCR reactions were performed to amplify various N-terminal domain truncations based on the Gal4-GAbpα template (2.4.2.1). In all four PCR reactions the same reverse primer, GAbpα-AscI-rev, was used. Deletion of the first 63 amino acids resulted in Gal4-GAbpα dOST, which was amplified by using dOST-PacI-for as forward primer. Next, deletion of the pointed domain (PNT) yielded dPNT by using the primer dPNT-PacI-for. Gal4-GAbpα dT280 was obtained by deleting the phosphorylation site T280 and dEts by removing the Ets DNA binding domain. In the latter case dEts-PacI-for was used as forward primer while dT280-PacI-for was used to generate Gal4-GAbpα dT280. Each of these PCR products was then subjected to restriction digest with *Pac*I and *Asc*I (2.4.3). Ligation of each these constructs into an identically digested pGal4 vector resulted in Gal4 fusion proteins (2.4.7) (Figure 25). Confirmed plasmids were used for overexpression analysis in HEK293T cells via western-blot by using a Gal4 antibody

(2.6.6). The proteins migrated at expected size, thus, indicating a correct expression of the truncated Gal4-GAbpα proteins (Figure 25).

Next, Gal4-GAbpα domain truncation constructs were analyzed in a mammalian two-hybrid assay (2.1.6). C2C12 cells were transfected with pGal4-Luc, pCMV-ß-gal and pVp16-GAbpβ on each well. Along with this, six different Gal4 fusion proteins, Gal4, Gal4-GAbpα, dOST, dPNT, dT280, or dEts, were transfected on corresponding wells. Cells were stimulated with 25 ng/mL TNF-α and assayed thereafter for relative luciferase activity (2.6.7).

In this study, the Gal4-GAbpα fusion protein contained an N-terminal deletion of ~ 100 aa of GAbpα (Pubmed accession number BC013562). At the time-point of the screen, this part of the N-terminus of GAbpα (aa 1-63 of the BC013562) was not associated with any function. Later, structural characterization of GAbpα revealed that this domain folds into stable folded structure and was named OST domain (Kang et al. 2008). Upon deletion of the OST domain, PNT domain or T280 site, a decrease of relative luciferase activity was detected compared to the full length fusion protein. Hence, for these domain truncations of GAbpα the protein-protein interaction to Vp16-GAbpβ decreased ~ 40% compared to the full length Gal4-GAbpα. TNF-α stimulation caused a significant decrease of relative luciferase activity in the positive control, the full length fusion protein Gal4-GAbpα, and three consecutive domain truncation constructs, dOST, dPNT, and dT280. This means, that with all tested domain truncations of Gal4-GAbpα, the protein-protein interaction to Vp16-GAbpβ decreased. No basal transcriptional activity and hence no decrease upon TNF-α treatment was detectable by using Gal4 alone or the Gal4-GAbpα dEts protein. This finding is according to previous studies claiming that the presence of the C-Terminus as well as the Ets domain were required for GAbpα binding to GAbpβ. Furthermore, these results indicate that the minimal GAbpβ-binding domain of Gal4-GAbpα protein is sufficient for the TNF-α mediated dissociation.

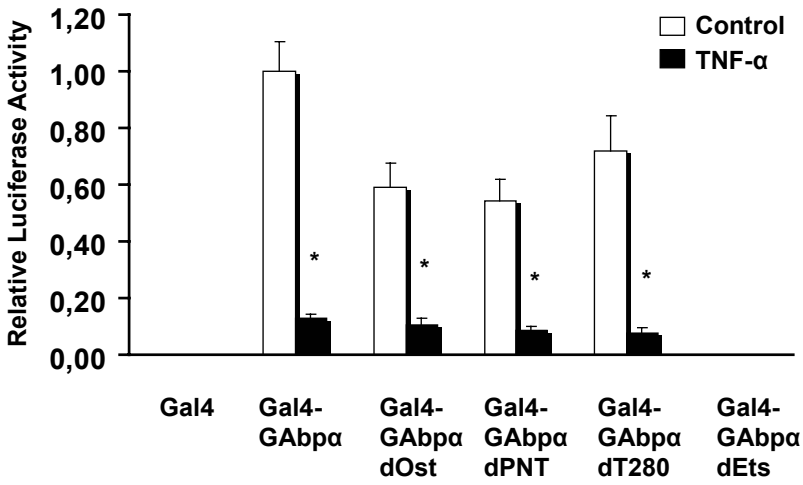

Figure 26: The protein-protein interaction between Vp16-GAbpβ and Gal4-GAbpα, dOST, dPNT, dT280 or dEts decreases upon stimulation with TNF-α. The mammalian two-hybrid assay was carried out in C2C12 cells, which were transfected with Gal4-Luc, CMV-ß-gal, and Vp16-GAbpβ as well as indicated Gal4 fusion proteins. Thereafter, cells were stimulated for 48 h with 25 ng/mL TNF-α or left untreated. Finally, relative luciferase activity was determined and normalized to untreated co-expression of Gal4-GAbpα and Vp16-GAbpβ. (N = 9, 3 independent experiments, mean ± SEM, * $p < 0.001$, t test, for details regarding the statistical analysis see Figure 23).

Domain deletions of GAbpβ were then cloned into the pCMX-Vp16 for subsequent analysis via the mammalian two-hybrid assay. While the leucine zipper domain (LeuZip) is required for homodimerization of GAbpβ, the transcriptional activation domain (TAD) is crucial for activation of transcription. The minimal construct (dPhoSit) contained only the ankyrin repeats (ANK). In addition, this construct differed from dTAD by two missing putative phosporylation sites, which had been mapped to S170 and T180 (Figure 27). The DNA for the domain truncation constructs was amplified via PCR from the pVp16-GAbpβ vector by using the same forward primer, GAbpβ-Vp16-for, in all PCR reactions (2.4.2.1). Three different PCR reactions were carried out by using reverse primers GAbpβ-dLeuZip-rev, GAbpβ-dTAD-rev and GAbpβ-dPhoSit-rev in order to obtain the dLeuZip, dTAD and dPhoSit constructs, respectively. These inserts were then double digested with *Kpn*I and *Nhe*I and each ligated into an identically digested pCMV-Vp16 vector (2.4.3, 2.4.7). The cloning procedure was finished as described in 2.4.12.

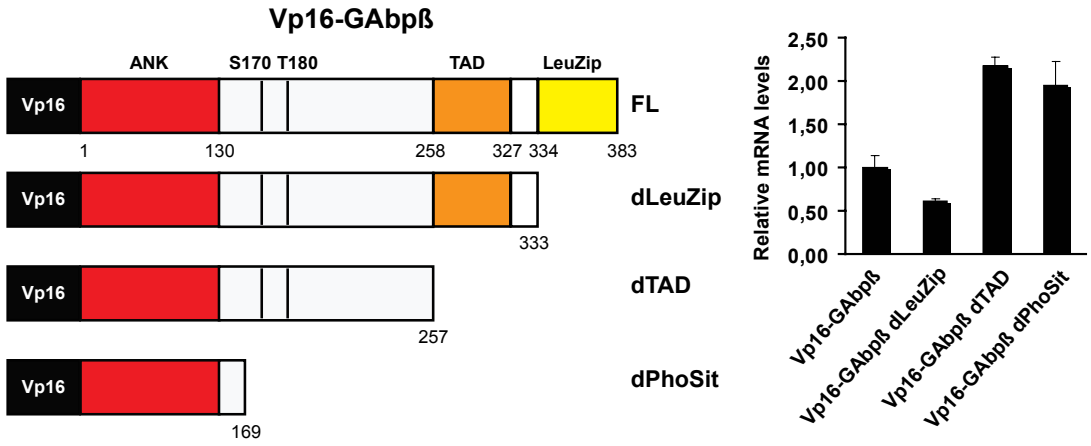

Figure 27: Scheme of Vp16-GAbpβ domain deletions and expression analysis. C-terminal domain deletions of GAbpβ were cloned into the pCMX-Vp16 vector. These Vp16-GAbpβ fusion proteins were analyzed via qRT-PCR upon transfection in C2C12 cells. Relative mRNA levels were normalized to the full length (Vp16-GAbpβ) protein. (mean + STDEV indicating pipetting errors)

Due to the fact that the protein expression from the pCMX-Vp16 vector results in relatively low overexpressed protein levels (data not shown), a qRT-PCR analysis of transfected C2C12 cells was performed instead. For the qRT-PCR analysis, a probe targeting the Vp16 domain was employed to guarantee the proper detection of all constructs. C2C12 cells were transfected under assay conditions with the constructs for the full length fusion protein (Vp16-GAbpβ) or the domain truncations (dLeuZip, dTAD, dPhoSit) (2.1.6). Cells were harvested and targeted to RNA extraction (2.5.1), cDNA synthesis (2.4.9) and qRT-PCR analysis (2.4.2.2). The relative mRNA levels were normalized to the full length protein. The relative mRNA level of the dLeuZip protein was slightly decreased, while the relative mRNA levels of the dTAD and dPhoSit protein were increased (Figure 27).

These Vp16-GAbpβ domain truncation proteins were then used in the mammalian two-hybrid assay. C2C12 cells were transfected with pGal4-Luc, pCMV-ß-gal, and pGal4-GAbpα on each well (2.1.6). Then, the different Vp16 constructs were tested by transfecting Vp16, Vp16-GAbpβ, dLeuZip, dTAD or dPhoSit. Following this, cells were stimulated for 48 h with 25 ng/mL TNF, or left untreated, and assessed for relative luciferase activity (2.1.5) (Figure 28).

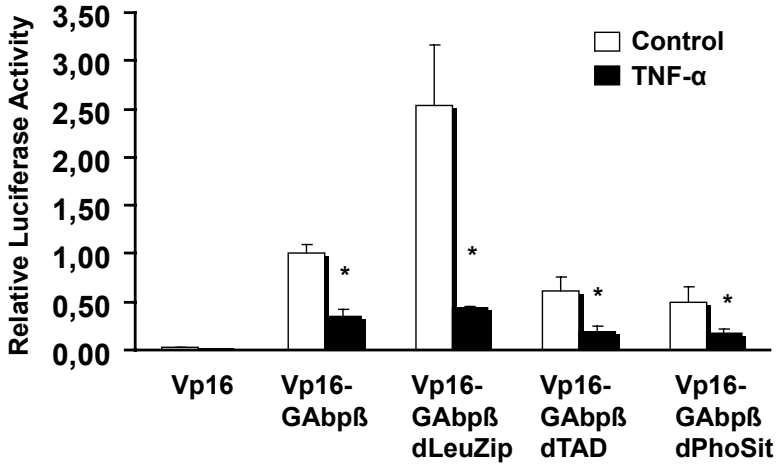

Figure 28: The protein-protein interaction between Gal4-GAbpα and Vp16-GAbpβ, dLeuZip, dTAD, and dPhoSit decreases upon stimulation with TNF-α. The mammalian two-hybrid assay was performed in C2C12 cells as follows. Cells were transfected with Gal4-Luc, CMV-ß-gal, and Gal4-GAbpα as well as indicated plasmids and stimulated for 48 h with 25 ng/mL TNF-α or left untreated. Finally, relative luciferase activity was determined and normalized to untreated co-expression of Gal4-GAbpα and Vp16-GAbpβ. (N = 9, 3 independent experiments, mean ± SEM, * $p < 0.05$, t test, for details regarding the statistical analysis see Figure 23).

Interestingly, deletion of the LeuZip domain caused an increase in relative luciferase expression hence indicating an increased protein-protein interaction compared to the full length fusion protein. However, deletion of both, the LeuZip and TAD domain in the dTAD protein resulted in a lower relative luciferase activity compared to the full length fusion protein. This was also true for the dPhoSit protein resulting from the simultaneous deletion of the LeuZip, TAD domain and phosphorylation sites, which gave rise to the dPhoSit protein. Despite the differing degree of protein-protein interaction of the tested domain deletion constructs, TNF-α treatment caused a significant decrease in relative luciferase activity upon overexpression of Gal4-GAbpα and Vp16-GAbpβ ($p< 0.001$), dLeuZip ($p = 0.0038$), dTAD ($p = 0.0021$), or dPhoSit ($p = 0.0282$). To conclude, the domain leading to TNF-α mediated dissociation of Gal4-GAbpα from Vp16-GAbpβ is the minimal binding domain of Vp16-GAbpβ.

Next, the minimal binding domains of Vp16-GAbpβ as well as Gal4-GAbpα were tested in the mammalian two hybrid assay for TNF-α mediated dissociation (2.1.6). C2C12 cells were transfected with Gal4-Luc, CMV-ß-gal, plus Vp16-GAbpβ dPhoSit and Gal4-GAbpα-dT280 and stimulated for 48 h with 25 ng/mL TNF-α (2.1.4.2, 2.1.5).

Thereafter, cells were lysed and targeted to determination of relative luciferase activity (Figure 29).

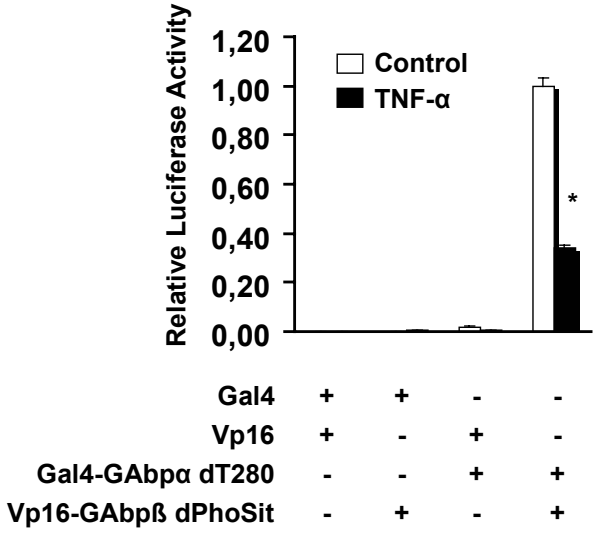

Figure 29: The minimal binding domains of Gal4-GAbpα (dT280) and Vp16-GAbpβ (dPhoSit) are sufficient for TNF-α mediated decrease of the protein-protein interaction. For the mammalian two-hybrid assay, cells were transfected with Gal4-Luc, CMV-ß-gal as well as indicated plasmids and stimulated for 48 h with 25 ng/mL TNF-α or left untreated. Finally, relative luciferase activity was determined and normalized to untreated co-expression of Gal4-GAbpα and Vp16-GAbpβ. (N = 9, 3 independent experiments, mean ± SEM, * $p < 0.001$, t test, for details regarding the statistical analysis see Figure 23).

Again, only co-expression of Vp16-GAbpβ dPhoSit and Gal4-GAbpα dT280 caused a detectable luciferase activity compared to negative control settings indicating a strong protein-protein interaction (Figure 29). The relative luciferase activity diminished significantly ($p < 0.001$) after TNF-α treatment. This result suggests that the minimal binding domains of GAbpβ and GAbpα are also sufficient for dissociation of the GAbp complex under pro-inflammatory conditions.

3.3.3 The Dissociation is Specific to TNF-α as Compared to Other Pro-Inflammatory Stimuli

Next, the specificity of this observation was addressed by testing other pro-inflammatory stimuli for their ability to diminish the protein-protein interaction of GAbpα and GAbpβ in the mammalian two-hybrid assay. As mentioned earlier, along with TNF-α, the implication of the other pro-inflammatory cytokines like IFN-γ, IL-1β and IL-6 has been described in different models of muscle atrophy. In addition,

lipopolysaccharides (LPS) were also analyzed in this study, since this bacterial endotoxin induces a strong immune response and activates tissue-residing macrophages *in vivo*. The latter can be mimicked *in vitro* by stimulating RAW cells, a mouse leukaemic monocyte macrophage cell line, with LPS and using such conditioned RAW medium (CM-RAW) for stimulation of other mammalian cells. Upon activation with LPS, RAW cells secrete pro-inflammatory cytokine, as for instance TNF-α. In this context, the conditioned RAW medium used in this study was analyzed by ELISA for presence of various cytokines. While IFN-γ and IL-1β were could not be detected, 2500 pg/mL IL-6 and 1050 pg/mL TNF-α were detected thus indicating that these pro-inflammatory are the predominant species in this medium (unpublished data).

C2C12 cells were transfected with Gal4-Luc, CMV-ß-gal and the minimal domains of Vp16-GAbpβ (dPhoSit) and Gal4-GAbpα (dT280) (2.1.6). Thereafter, cells were stimulated for 48 h with 25 ng/mL TNF-α, 100 U/mL IFN-γ, 10 ng/mL IL-1β, 20 ng/mL IL-6, 100 ng/mL LPS, conditioned or control RAW medium or left untreated (2.1.5). The concentrations of these stimuli represent standard concentrations which are routinely used to mimic a chronic inflammation in cell culture. Finally, relative luciferase activity was determined (Figure 30).

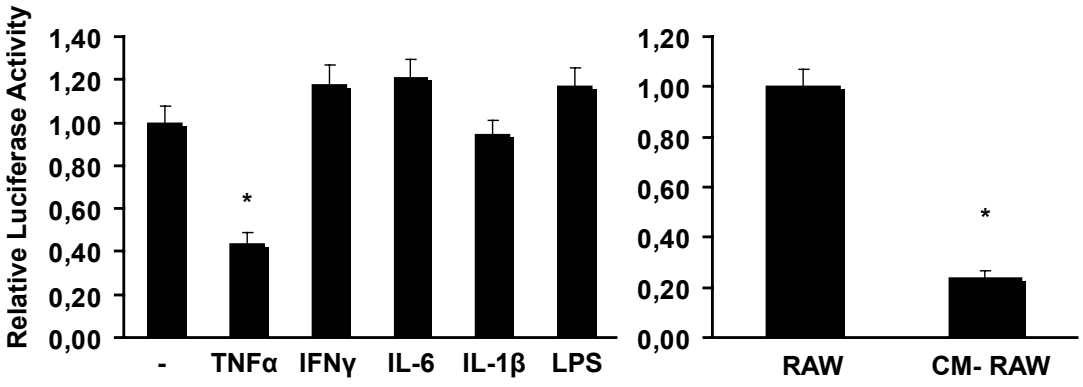

Figure 30: The dissociation of Gal4-GAbpα dT280 from Vp16-GAbpβ dPhoSit is specific to TNF-α. Conditioned RAW medium shows a similar effect as TNF-α alone. C2C12 cells were transfected with Gal4-Luc and CMV-ß-gal as well as Gal4-GAbpα dT280 and Vp16-GAbpβ dPhoSit and stimulated for 48 h with 25 ng/mL TNF-α, 100 U/mL IFN-γ, 20 ng/mL IL-6, 10 ng/mL IL-1β, or 100 ng/mL LPS or left untreated. In a parallel experiment, such transfected cells were stimulated for 48 h with control RAW medium or conditioned RAW medium (N = 9, 3 independent experiments, mean ± SEM, * $p < 0.01$, one-way ANOVA with Dunnett´s posttest comparing each treated group to the corresponding control group).

In this mammalian two-hybrid assay, no decreased relative luciferase activity was detected in IFN-γ, IL-1β, IL-6, or LPS treated C2C12 cells. Interestingly, conditioned RAW medium, however, caused a significant decrease ($p < 0.0001$) similar to the TNF-α effect. To conclude, the dissociation of the transcriptional active GAbp seems to be specific to TNF-α when compared to other pro-inflammatory cytokines. However, activated macrophages show the same effect.

3.3.4 The TNF-α Mediated Dissociation of the GAbp complex is triggered by the Induction of Reactive Oxygen Species

In the past, it was discovered that GAbp is subjected to redox regulation in 3T3 cells, thereby leading to changes GAbp-dependent gene expression (Martin et al. 1996). Furthermore, in a consecutive study, this effect was linked to GAbpα which carries four redox-sensitive cysteine residues within the Ets domain and the most C-terminal domain (Chinenov et al. 1998). Oxidation of these residues has been associated with a change in DNA binding and heterodimerization of both proteins (Chinenov et al. 1998). Since TNF-α is known to induce the production of reactive oxygen species (ROS), the redox regulation of GAbp heterodimerization was addressed in this study by the mammalian two-hybrid assay.

ROS are molecules formed as natural byproducts during cellular respiration and are characterized by the presence of unpaired valence shell electrons giving rise to their high reactivity (e.g. hydrogen peroxide H_2O_2). Usually, ROS are not harmful to mammalian cells due to the antioxidative function of vitamins (e.g. ascorbic acid), enzymes (e.g. superoxide dismutase, catalase) or small molecules (glutathione). On the contrary, some crucial signalling pathways depend on ROS (apoptosis, transcriptional activation of host defence genes). In addition, they are produced by some components of the immune system for destruction of invading microbes. Accumulation of these compounds may, however, cause oxidative stress resulting in serious tissue damage. Moreover, ROS have been described to have a causal role in two different *in vitro* models of insulin resistance, a pathology being linked to the Metabolic Syndrome (Houstis et al. 2006). In the corresponding study, two different antioxidative compounds were used for proving the causal link. While Mn(III)tetrakis(4-benzoic acid)porphyrin Chloride (MnTBAP) is a cell-permeable superoxide dismutase (SOD) mimetic and

thereby protects cells from the damaging effects of H_2O_2, *N*-acetylcysteine (NAC) has similar effects by inducing the formation of glutathione in cells.

Next, the question was addressed whether production of ROS was implicated in TNF-α mediated dissociation of GAbp. For this purpose, the mammalian two-hybrid assay was performed by using the full length fusion proteins of Gal4-GAbpα and Vp16-GAbpβ. C2C12 cells were transfected as described before (MX) and stimulated with 12.5 ng/mL TNF-α or 1 mM H_2O_2 for 48 h. Concomitantly, cells were targeted to increasing doses of MnTBAP (37.5 µM, 75 µM, and 150 µM) or NAC (1.25 mM, 2.5 mM, and 5 mM). Following this, the relative luciferase activity was determined (Figure 31). Interestingly, the relative luciferase activity decreased in H_2O_2 treated C2C12 cells suggesting a dissociation of Gal4-GAbpα and Vp16-GAbpβ under these conditions (Figure 31). The same was repeatedly true for TNF-α treated cells. Concomitant stimulation with H_2O_2 and NAC rescued significantly the decrease in luciferase activity at 2.5 mM NAC (60 % rescue) and 5 mM NAC (80 % rescue). This could also be observed by concomitant treatment with MnTBAP and TNF-α (~ 52 % rescue) already at the mid-range concentration of 75 µM MnTBAP. A rescue of 80 % was achieved by using 5 mM NAC and TNF-α.

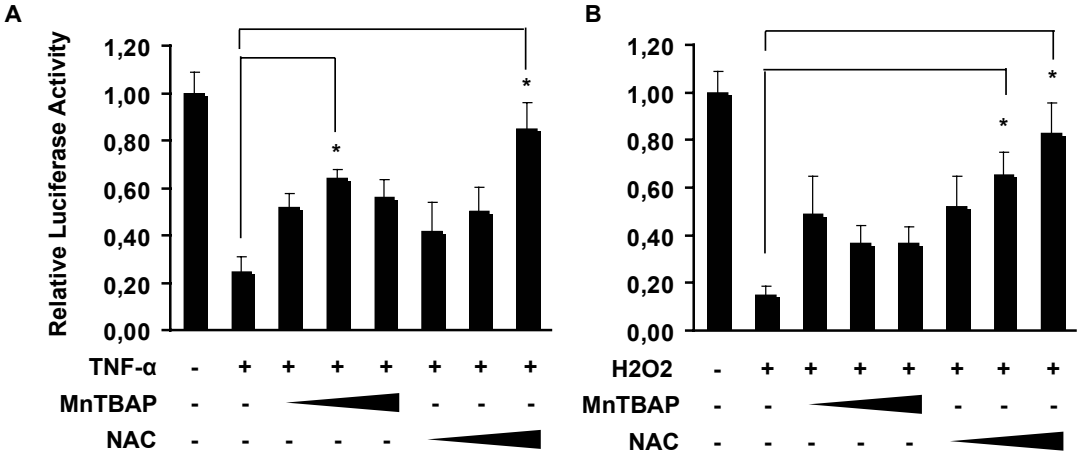

Figure 31: TNF-α or H_2O_2 mediated dissociation of GAbp in C2C12 cells is rescued by ROS inhibitors. C2C12 cells were transfected with pGal4-GAbpα, pVp16-GAbpβ, and pGal4-Luc. Thereafter, cells were stimulated with 25 ng/mL TNF-α or 1 mM H_2O_2. Concomitant treatment with ROS inhibitors was carried out by using 37.5 µM, 75 µM, 150 µM MnTBAP or 1.25 mM, 2.5 mM, or 5 mM NAC. Finally, relative luciferase activity was determined and normalized to untreated control. (N = 6, 2 independent experiments, mean ± SEM, * $p < 0.05$, One-way ANOVA with Dunnett´s posttest comparing each group treated with a ROS inhibitor to the group with TNF-α stimulation alone).

Taken together, TNF-α stimulation of C2C12 cells leads to the dissociation of GAbpα and GAbpβ with the minimal binding domains being sufficient. This altered functional interaction was found to be specific for TNF-α as compared to other pro-inflammatory cytokines. Moreover, oxidative stress of C2C12 cells causes likewise a dissociation of the transcriptional active heterodimer. ROS inhibitors efficiently rescued the dissociation in both conditions, TNF-α stimulation and oxidative stress.

3.4 TNF-α Inhibits Neuregulin Stimulated Expression of GAbp Target Genes in C2C12 Cells

Next, the question was addressed, which implication the TNF-α mediated dissociation of GAbp has on the transcription regulation of GAbp target genes in C2C12 cells The heterodimeric transcription factor GAbp has been described to activate transcription of various target genes in different tissues. In muscle cells, GAbp plays a role in the development and organization of target genes crucial for the neuromuscular junction (NMJ). The AChRε is a prominent example of a gene regulated in such a way (Mejat et al. 2003). Stimulation of C2C12 cells with Neuregulin (NRG), which is a growth factor secreted from nerve cells and therefore commonly used for mimicking the events at the NMJ *in vitro*, is known to cause an increase in AChRε-transcription. The compartmentalized transcription of sub-synaptic target genes is accomplished by the presence of the N-Box within corresponding promoter sequences. This N-Box represents the consensus-motif for binding of GAbp through its DNA binding component GAbpα. In this study, the impact of TNF-α mediated dissociation of GAbpα and GAbpβ was analyzed on putative target genes by using an artificial 3xNBox promoter and the natural AChRε promoter.

3.4.1 TNF-α inhibits the Activation of a 3xNBox Promoter by NRG

For the 3xNBox promoter study, C2C12 cells were transfected with the pCMV-ß-gal, p3xNBox promoter or control vector (pTAL-Luc) and stimulated for 48 h with 5 nM Neuregulin (NRG), 25 ng/mL TNF-α, NRG and TNF-α together, or left untreated (2.1.7, 2.1.5). Then, relative luciferase activity was determined and normalized to NRG stimulated cells (Figure 32).

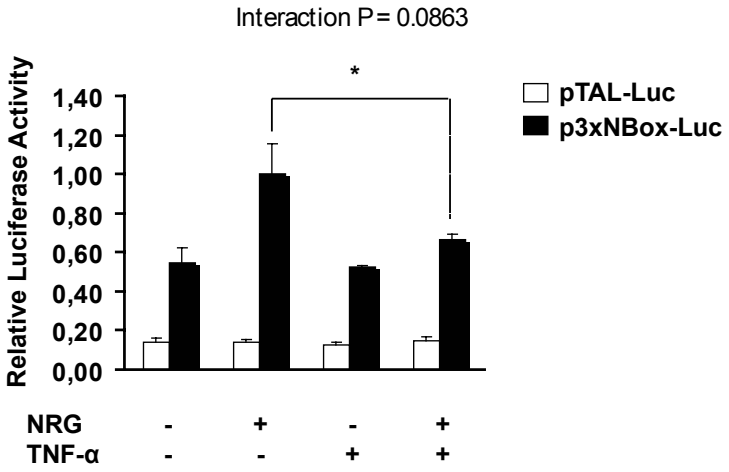

Figure 32: TNF-α inhibits NRG mediated induction of 3xNBox promoter activity. C2C12 cells were transfected with pCMV-ß-gal and pTAL-Luc or p3xNBox-Luc and stimulated for 48 h with 5 nM Neuregulin (NRG), 25 ng/mL TNF-α, NRG + TNF-α, or left untreated. Then, relative luciferase activity was determined and normalized to NRG stimulated cells (N = 9, 3 independent experiments, mean ± SEM, * $p < 0.01$, two-way ANOVA with Bonferroni posttests comparing vehicle versus NRG in the absence or presence of the TNF-α).

The promoter activity of the control vector (pTAL-Luc), which contains the backbone DNA sequence without the artificial 3xNBox consensus motif, did not change under these conditions. NRG stimulation caused an increase in 3xNBox-promoter activity of ~ 45%, while TNF-α stimulation treatment led to no significant alteration of promoter activity. However, NRG stimulation in the presence of TNF-α significantly inhibited the promoter activity. In this promoter assay, the interaction between NRG and TNF-α treatment was not significant (Interaction $p = 0.0863$). In summary, a trend towards an inhibition of NRG mediated activation of 3xNBox promoter activity in C2C12 cells was detectable upon concomitant treatment with TNF-α. In the next step, the function of GAbp on the natural AChRε promoter was elucidated.

3.4.2 Neuregulin Promoted Induction of AChRε Promoter Activity is inhibited in the Presence of TNF-α

In order to assess whether the TNF-α mediated dissociation of the heterodimeric GAbp complex plays a role in the expression of AChRε, an AChRε promoter assay was performed in C2C12 cells. For this purpose, an AChRε promoter driven luciferase plasmid was cloned. In this study, the promoter fragment ranging from 152 bp upstream of the transcription start site, which contains the N-Box, was used (Duclert et al. 1993).

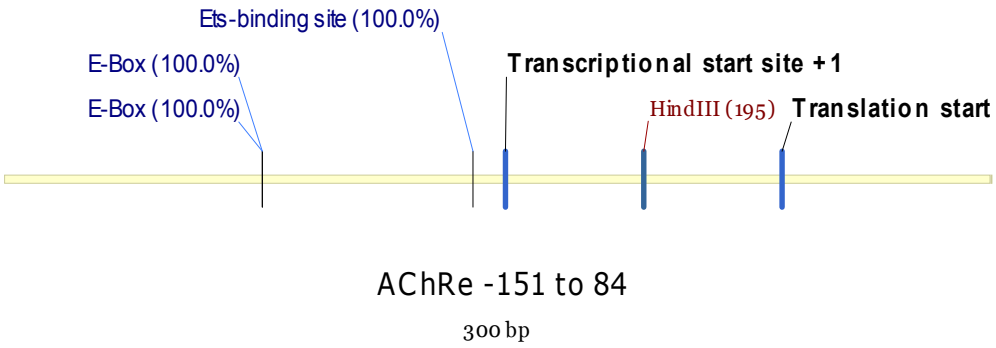

Figure 33: Illustration of the murine AChRε promoter. This promoter sequence was cloned resulting in pGL3-AChRε plasmid and was subsequently used in AChRε promoter studies in C2C12 cells. Muscle-specific transcription factors, from the MyoD protein family for instance, bind to the myogenic E-Box consensus motif (CAGCTG) thereby driving muscle-specific expression. Since this is a palindromic sequence two E-Boxes are indicated. The heterodimeric GAbp protein binds to the N-Box (CGGAA), an Ets-binding site.

This promoter fragment has previously been shown to be sufficient for local restricted expression of AChRε in the sub-synaptic muscle cells. In addition, this sequence contains an E-Box crucial for muscle-specific gene expression (Figure 33). The promoter fragment (~ 300 bp) was amplified via PCR from murine genomic DNA by using the AChRe-Mm-promoter-for and AChRe-Mm-promoter-rev primer pair (2.4.2.1). Following this, the promoter fragment and the vector pGL3 were double digested with *Kpn*I and *Nhe*I, ligated and the cloning procedure completed according to 2.4.12.

For corresponding promoter assays, an overexpression construct for GAbpβ was also required. The coding sequence of Gabpβ was amplified via PCR from a C2C12 cDNA pool by using primer Gabpβ-for and Gabpβ-rev, and subjected to restriction digest with *Nhe*I and *Xho*I along with the vector pcDNA3.1 (-) vector (2.4.2.1, 2.4.3). Upon completion of the cloning procedure, this overexpression plasmid for GAbpβ (pcDNA3.1(-)GAbpβ) was used in AChRε promoter assays. The cloning of the overexpression plasmid pcDNA3.1(-)GAbpα is described in 3.2.1. Next, the AChRε promoter fragment was tested in C2C12 cells. C2C12 myoblasts were transfected with pGL3-AChRε or the control plasmid (pGL3), CMV-ß-gal, pcDNA3.1(-)GAbpα, and pcDNA3.1(-)GAbpβ (2.1.7). Following this, cells were stimulated for 48 h with vehicle (PBS + 0.1% BSA) or 5 nM Neuregulin in the presence or absence of 25 ng/mL TNF-α (2.1.5). Finally, the relative luciferase activity was determined (Figure 34).

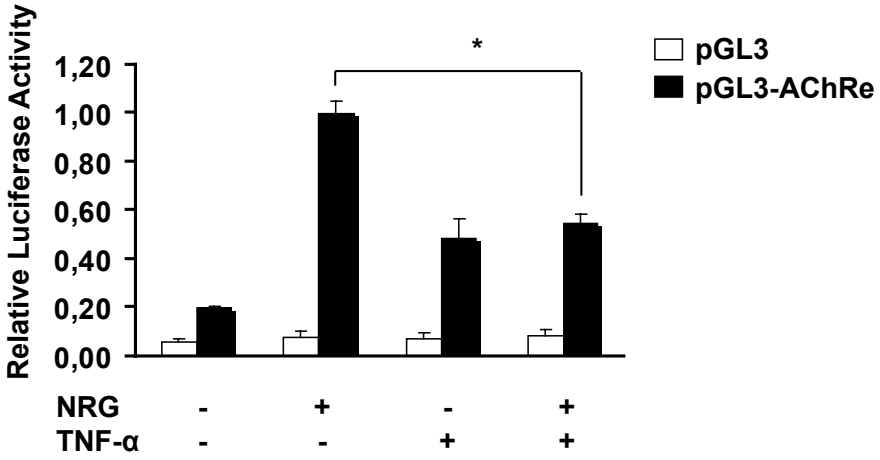

Figure 34: NRG mediated induction of the AChRε-promoter in C2C12 cells is inhibited by TNF-α. C2C12 cells were transfected with CMV-β-gal, pcDNA3.1(-)GAbpα, pcDNA3.1(-)GAbpβ and pGL3 or pGL3-AChRε and treated for 48 h with 5 nM NRG, 25 ng/mL TNF-α or both stimuli together. Thereafter, the relative luciferase activity was determined and normalized to NRG stimulation (N = 12, 4 independent experiments, mean ± SEM, * $p < 0.001$, two-way ANOVA with Bonferroni posttests comparing vehicle vs NRG in the absence or presence of the TNF-α).

The AChRε promoter activity was significantly induced upon stimulation with NRG. This effect was even greater (80% increase) than NRG mediated induction of the 3xNBox promoter (~ 45% increase). Also, treatment with TNF-α caused a slight increase in AChRε promoter activity when compared to untreated control. Yet, the presence of TNF-α caused a significant decrease in NRG-mediated induction of the promoter activity. Thereby, the interaction between NRG and TNF-α treatment was significant (Interaction $p < 0.0001$). The control promoter (pGL3) showed no altered transcriptional activity under these conditions, thus, supporting the notion that the effect observed here is specific to the AChRε promoter. Promoter analysis in C2C12 cells without concomitant overexpression of GAbp caused similar changes of promoter activity under these conditions (data not shown). However, since this was dependent on recruitment of endogenous GAbp, the extent of NRG-mediated induction and decrease by concomitant TNF-α treatment was lower. Based on this result, concomitant overexpression of GAbp was found to be more appropriate for promoter analysis.

In order to investigate, whether this effect was mediated by binding of GAbp to the N-Box, an N-Box mutant promoter was cloned by replacing the N-Box consensus motif through an *Eco*RI restriction site. This mutation strategy allowed for amplification of the upstream and downstream region of the N-Box by two PCR reactions and

subsequent ligation of correspondingly digested PCR fragments into the pGL3 vector. Therefore, two PCR primers were designed containing the mutated nucleotides in the middle and a complementary stretch of basepairs at the 5´- and 3´-ends. Following this, the sequence upstream and downstream of the mutated N-Box (N-Box*mut*) was amplified by two different PCR reactions using the pGL3-AChRε plasmid as template (2.4.2.1). The N-Box*mut* upstream region was amplified by combining the primer AChRe-Mm-prom-for with N-Boxmut-mAChRe-prom-rev for one PCR reaction, while the primer N-Boxmut-mAChRe-prom-for and AChRe-Mm-prom-rev were used for obtaining the N-Box*mut* downstream region. The upstream PCR fragment was digested with *Kpn*I and *Eco*RI, while *Eco*RI and *Nhe*I were taken for digestion of the downstream PCR fragment (2.4.3). Following this, these fragments were ligated to the accordingly with *Kpn*I and *Nhe*I digested pGL3 vector (2.4.7). The cloning procedure was completed as described in 2.4.12.

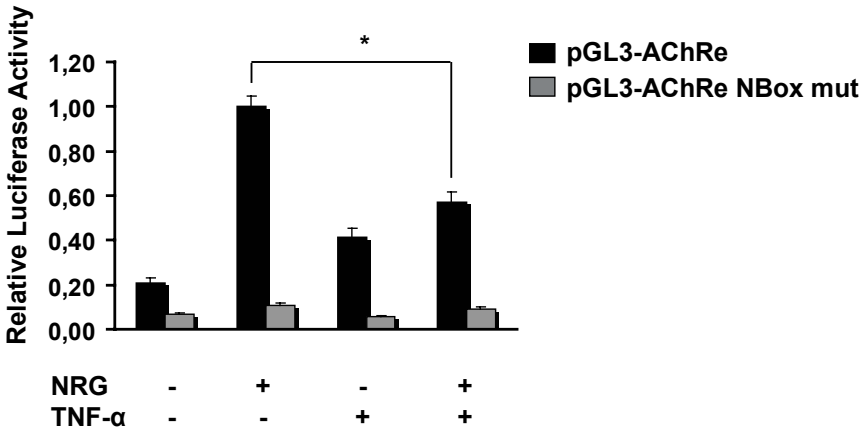

Figure 35: The basal promoter activity of the AChRε-Nbox*mut* promoter C2C12 cells was extremely low. Cells were transfected with CMV-β-gal, pcDNA3.1(-)GAbpα, pcDNA3.1(-)GAbpβ and pGL3-AChRε or pGL3-AChRε-NBox*mut* and treated for 48 h with 5 nM NRG, 25 ng/mL TNF-α, or both stimuli together. Thereafter, the relative luciferase activity was determined and normalized to NRG stimulation of the control vector (pGL3-AChRε) (N = 12, 4 independent experiments, mean ± SEM, * $p < 0.001$, two-way ANOVA with Bonferroni posttests comparing vehicle vs NRG in the absence or presence of the TNF-α).

The promoter plasmid pGL3-AChRε-NBox*mut* was then tested in a promoter assay in C2C12 cells (2.1.7). As a control, the AChRε promoter plasmid containing the intact N-Box was used (pGL3-AChRε). Deletion of the N-Box resulted in a significantly lower basal AChRε promoter activity compared to the promoter containing the intact N-Box (Figure 35). In addition, NRG mediated stimulation was much less pronounced. Based

on this relatively low basal as well as induced promoter activity, this experiment was found to be unsuitable for analyzing an implication of the NBox in TNF-α dependent decrease.

3.4.3 Implication of Pro-Inflammatory Cytokines in Inhibition of NRG Mediated Induction of AChRε Promoter Activity and Gene Expression

Next, the specificity of this TNF-α dependent decrease of AChRε promoter activity under pro-inflammatory conditions was addressed by comparison to other cytokines. AChRε promoter studies were performed as described before (2.1.7).

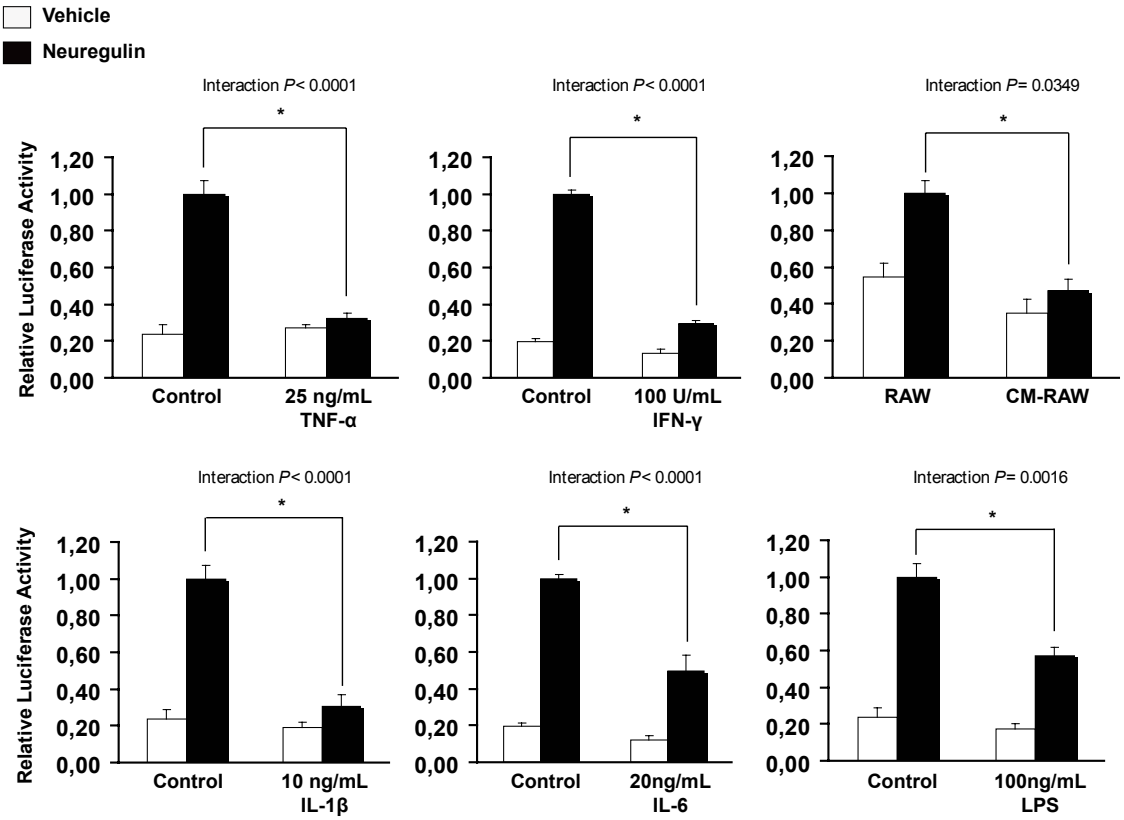

Figure 36: TNF-α, IL-1β and conditioned RAW medium (CM-RAW) inhibited NRG mediated activation of the AChRε promoter in C2C12 cells. Cells were transfected with CMV-β-gal, pcDNA3.1(-)GAbpα, pcDNA3.1(-)GAbpβ and pGL3-AChRε and stimulated for 48 h with vehicle or 5 nM NRG plus 25 ng/mL TNF-α, 50 U/mL IFN-γ, 100 ng/mL LPS, 20 ng/mL IL-6, 10 ng/mL IL-1β (N = 9, 3 independent experiments) or conditioned RAW medium (N = 6, 2 independent experiments). Relative luciferase activity was measured thereafter and normalized to NRG stimulated AChRε promoter activity (mean ± SEM, * $p < 0.05$, two-way ANOVA with Bonferroni posttests comparing vehicle vs NRG in the control setting or presence of a pro-inflammatory stimulus).

C2C12 cells were stimulated for 48 h with vehicle or 5 nM NRG and concomitantly treated with 25 ng/mL TNF-α, 50 U/mL IFN-γ, 100 ng/mL LPS, 20 ng/mL IL-6, or 10 ng/mL IL-1β (Figure 36) (2.1.5). The basal (unstimulated) promoter activity was diminished slightly by IFN-γ, CM-RAW or IL-6, while it was not altered by TNF-α or IL-1β. Again, concomitant treatment with TNF-α and NRG caused a diminished AChRε promoter activity (70% decrease) as compared to NRG stimulation in the absence of TNF-α (Interaction $p < 0.0001$) (Figure 36). A similar effect was detected by concomitant treatment with IFN-γ (Interaction $p < 0.0001$) or IL-1β (Interaction $p < 0.0001$), both cytokines causing a 70% decrease of AChRε promoter activity. Co-treatment with conditioned RAW medium (Interaction $p < 0.05$), IL-6 (Interaction $p < 0.0001$) or LPS (Interaction $p = 0.0019$) resulted in only 50 % decrease of AChRε promoter activity.

The results suggest that the decrease of AChRε promoter activity is not specific to TNF-α. However, the various pro-inflammatory cytokines tested here have a different impact on decreasing AChRε promoter activity. Usually, promoter activity assays by overexpression of a promoter fragment display only those events occurring on the selected promoter fragment. Moreover, the *in vivo* events are ideally analyzed by expression analysis of the corresponding gene. Therefore, the endogenous expression levels of AChRε were analyzed in C2C12 myotubes for diminished expression during NRG expression in the presence of various pro-inflammatory cytokines. C2C12 cells were seeded on individual wells of 6-well plates, differentiated into myotubes, and stimulated on day 3 for 16 h with two different concentrations per cytokine in the presence of 5 nM NRG or vehicle (2.1.5). In a parallel experiment, conditioned RAW medium was used as a stimulus. Following this, RNA was isolated (2.5.1), cDNA synthesis (2.4.9) performed and relative transcript levels of AChRε measured by qRT-PCR (2.4.2.2).

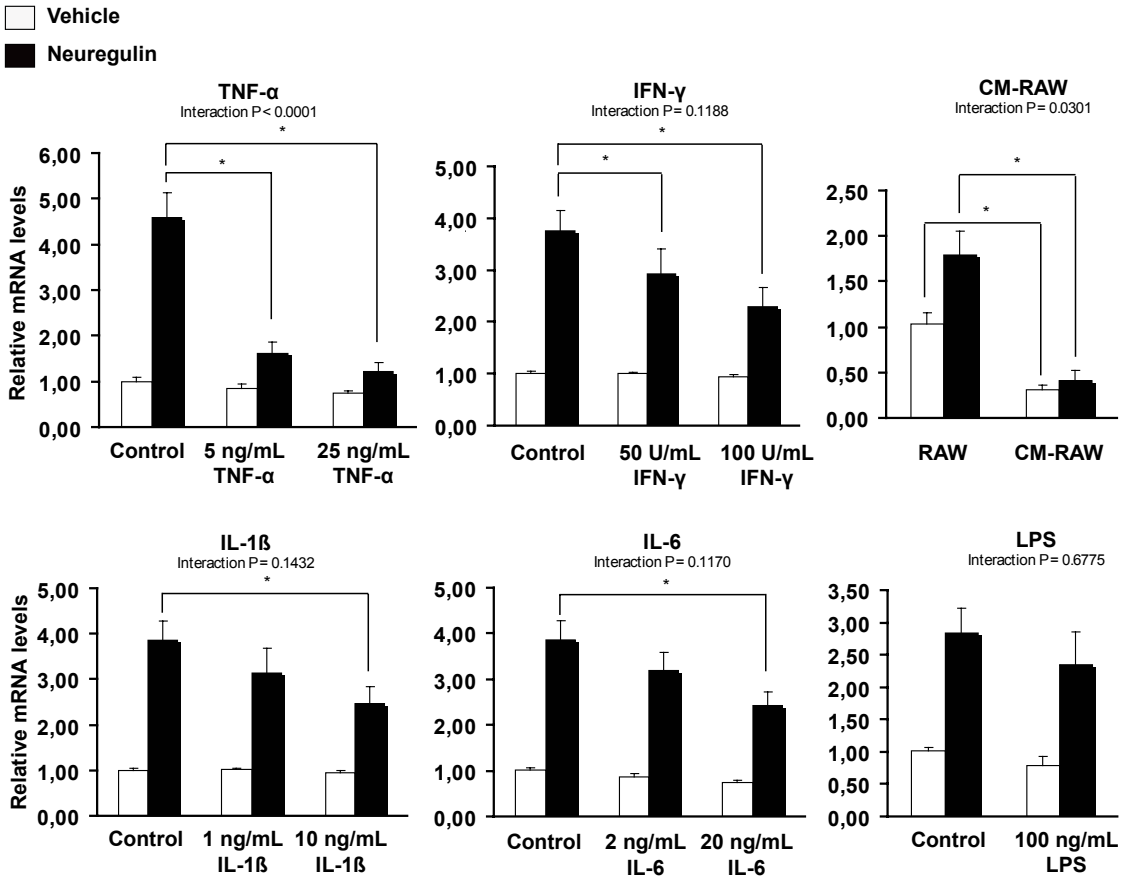

Figure 37: NRG induction of relative AChRε mRNA levels in C2C12 myotubes was most dramatically inhibited in the presence of TNF-α or conditioned RAW medium (CM-RAW). C2C12 cells were differentiated into myotubes and subsequently stimulated for 16 h as indicated. RNA was extracted, cDNA synthesized and relative mRNA levels of AChRε determined by qRT-PCR. Relative mRNA levels were normalized to unstimulated control setting (N = 6, three independent experiments, mean ± SEM, * $p < 0.05$, Two-way ANOVA with Bonferroni posttests comparing vehicle vs NRG in the control setting or presence of a pro-inflammatory stimulus).

AChRε gene expression was on average induced ~ 4 fold by NRG treatment (Figure 37). This induction was, however, less (~ 2 fold) in the presence of RAW control medium. Only treatment with CM-RAW resulted in a significant decrease of basal AChRε transcript levels (70% decrease). These levels were not altered by single-treatment with TNF-α, LPS, IL-6, IL-1β, or IFN-γ. The interaction between NRG treatment and LPS (Interaction $p = 0.6775$), IL-6 (Interaction $p = 0.1170$), IFN-γ (Interaction $p = 0.1188$), or IL-1β (Interaction $p = 0.1432$) treatment were statistically not significant. Posttesting revealed that the greatest decrease of NRG mediated AChRε gene expression was 37%, 36% and 33% in the presence of 20 ng/mL IL-6, 10 ng/mL IL-1β, and 100 U/mL IFN-γ respectively. However, TNF-α (Interaction $p < 0.0001$) and conditioned RAW medium (Interaction $p = 0.00301$) had both a significant impact on

decreasing NRG mediated gene expression of AChRε. In these cases, the interaction between these treatments was also significant. Noteworthy, TNF-α did efficiently inhibit NRG mediated gene expression by 64% in the presence of the lowest concentration tested (5 ng/mL TNF-α). The highest concentration TNF-α (25 ng/mL TNF-α) caused a similar strong decrease (73%) like conditioned RAW medium (77% decrease) of relative mRNA levels.

The results demonstrate that NRG mediated induction of endogenous AChRε gene expression was similarly strong inhibited by TNF-α alone or CM-RAW, while other pro-inflammatory cytokines did not have any significant impact in this study. Furthermore, CM-RAW caused already a significant decrease of basal AChRε gene expression.

3.4.4 ROS are implicated in TNF-α Mediated Inhibition of NRG Dependent AChRε Gene Expression

As shown before, TNF-α mediated dissociation of GAbpα and GAbpβ was caused by ROS. In order to investigate, whether ROS were similarly implicated in the regulation of AChRε gene expression under pro-inflammatory conditions, C2C12 myotubes were stimulated as described before in the presence of ROS inhibitors. These cells were then subjected to analysis of relative AChRε mRNA levels.

C2C12 cells were differentiated to myotubes and stimulated for 18 h with 5 nM NRG, 25 ng/mL TNF-α, or both stimuli together (2.1.5). In a parallel experiment, cells were also stimulated with 1 mM H_2O_2. This ROS inducing agent was also used in a co-stimulation experiment with NRG. Concomitant with the co-stimulation conditions (TNF-α + NRG and H_2O_2 + NRG), cells were also treated with 150 µM MnTBAP or 5 mM NAC. Thereafter, RNA was extracted (2.5.1), cDNA synthesis carried out (2.4.9), and relative AChRε mRNA levels detected by qRT-PCR (2.4.2.2).

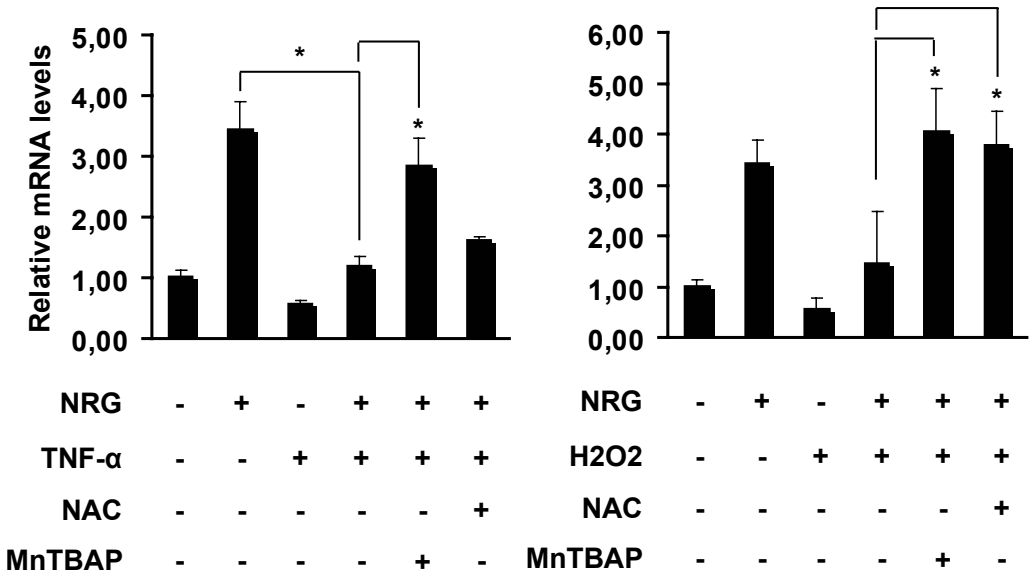

Figure 38: Relative mRNA levels of AChRε in C2C12 myotubes as measured by qRT-PCR. C2C12 cells were allowed to differentiate into myotubes and subsequently stimulated as indicated for 18 h with 5 nM NRG, 25 ng/mL TNF-α, 1 mM H_2O_2, 150 µM MnTBAP or 5 mM NAC (N = 4, two independent experiments, mean ± SEM, one-way ANOVA with Bonferroni´s multiple comparison test).

Again, NRG stimulation of C2C12 myotubes caused a ~ 3.5 fold increase in relative mRNA levels of AChRε. Gene expression of AChRε was not significantly altered by single treatment with TNF-α or H_2O_2. Repeatedly, NRG-mediated increase of AChRε mRNA levels was significantly decreased in the presence of TNF-α. Interestingly, H_2O_2 did also inhibit NRG mediated AChRε gene expression, however, not significantly due to the relatively high standard error mean (Figure 38). Concomitant stimulation of NRG plus TNF-α with MnTBAP did significantly rescue (73% rescue) a decrease in relative AChRε mRNA levels. The inhibition of NRG induced AChRε expression by H_2O_2 was even rescued > 100% by both ROS inhibitors, MnTBAP and NAC.

Taken together, inhibition of NRG mediated AChRε gene expression by TNF-α or H_2O_2 in C2C12 cells is caused by intracellularly activated ROS.

3.5 Expression of Sub-Synaptic Genes is Decreased in a Mouse Model for Cancer Cachexia

The Colon26 mouse model has been employed by A. Vegiopoulos (DKFZ) as *in vivo* model for Cancer Cachexia (Tanaka et al. 1990; Tsuruo et al. 1983). All experiments were performed according to 2.9. Upon tumour injection, affected mice undergo

significant muscle loss. In this study, skeletal muscle tissue of these animals was investigated for alterations of sub-synaptic gene expression. RNA was extracted from gastrocnemius muscle (2.5.2), targeted to cDNA synthesis (2.4.9) and qRT-PCR analysis of sub-synaptic genes (2.4.2.2). While the expression of the ubiquitin ligase MuRF1 was significantly induced in Colon25 bearing mice, the expression of GAbp was slightly upregulated (Figure 39). In contrast, AChRe and AChR-Esterase (AChREst)-expression was significantly decreased, and the expression of AChR delta-subunit (AChRδ), utrophin, and MuSk were slightly downregulated.

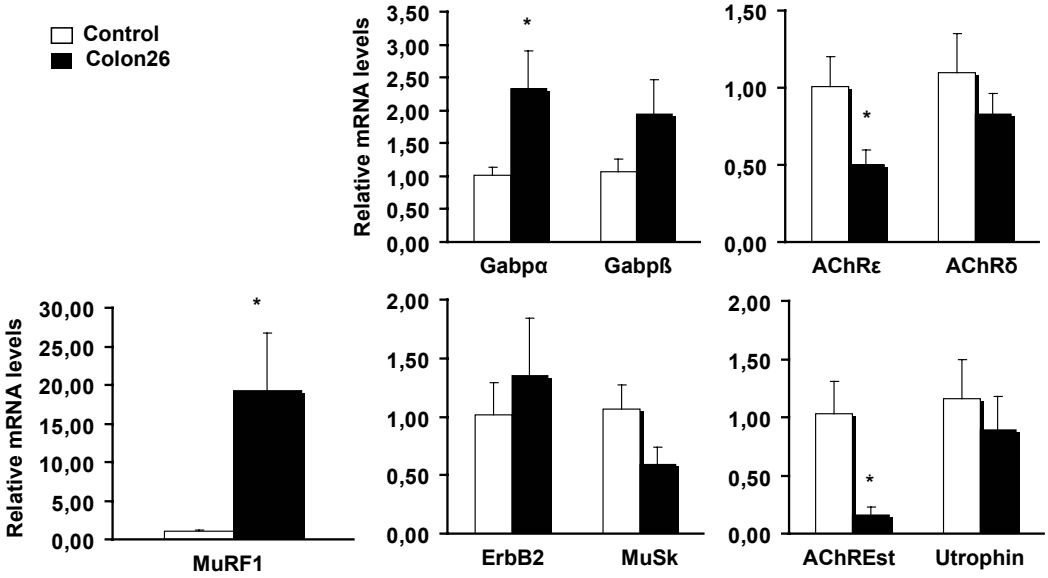

Figure 39: Expression analysis of sub-synaptic genes from gastrocnemius skeletal muscle tissue of Colon26 bearing tumor mice. Mice were treated and sacrificed as described in 2.9. Relative mRNA levels were normalized to GAPDH. (* $p < 0.05$, mean ± SEM).

In brief, these findings suggest, that the expression of GAbp target genes is similarly regulated in this *in vivo* model for cancer cachexia as compared to C2C12 muscle cells exposure to atrophic stimulation.

4 Discussion

This study presents the identification of GAbp as novel transcriptional regulator with dysregulated transcriptional activity under pro-inflammatory conditions in muscle cells. Furthermore, the dysregulated transcriptional activity is caused by dissociation of the DNA-binding component (GAbpα) and transcriptional activation component (GAbpβ) in the presence of TNF-α or conditioned macrophage medium. This pro-inflammatory signalling causes formation of reactive oxygen species and links GAbp dissociation to decreased gene expression of GAbp sub-synaptic target genes in muscle cells.

4.1 A Screen Approach to Identify Novel Transcriptional Regulators with Dysregulated Activity in Response to Atrophic Stimulation

In this study, a cell-based high-throughput screen was employed to find novel transcriptional regulators with dysregulated transcriptional activity in atrophic signalling. Previously, the transcription factor Foxo was discovered in muscle dysfunction accompanying muscle atrophy to up-regulate ubiquitin ligases, which target the degradation of muscle proteins (Sandri et al. 2004, Stitt et al. 2004). Thereby, the analysis of protein expression levels in different *in vivo* models for muscle atrophy paved the way for finding new targets in atrophic signalling (Bodine et al. 2001). Despite this work in elucidating the molecular mechanisms in muscle atrophy, it seems plausible that also other transcription factors are involved in the gene expression changes which accompany muscle dysfunction. Furthermore, the screen presented in this study, expands the search for novel targets to a more global and unconfined perspective by monitoring changes in protein activity of transcriptional regulators downstream of atrophic signalling pathways.

The screen design entailed two major constrains. First, the library of transcriptional regulators consisted of fusion proteins each with an N-terminal Gal4 DNA binding domain. This may modify the protein folding process or even mask certain protein-protein interaction domains. Second, due to the ease of transfection, the screen was

performed in HEK293T cells, a human mammalian cell line. Due to the low transfection efficiency of C2C12 cells, this cell line was not appropriate for this screen. The cellular environment of HEK293T cells provided the proteins from the basal transcriptional machinery being as well as co-regulators, which may by subjected to tissue-specific expression. Therefore, potential transcriptional interaction partners might be missing in HEK293T cells, and, thus, will not show up as hits in the screen. The fact, that 40% of the murine and 60% of the human factors showed an alteration of transcriptional activity, suggests that a human cell environment slightly favours functional interactions amongst proteins from the same species. Moreover, the changes of transcriptional activity were also greater for human factors compared to murine factors.

More factors showed an altered transcriptional activity upon treatment with TNF-α (40%) than with Dex (26%). The canonical glucocorticoid pathway requires the presence of the glucocorticoid receptor (GR) and converges within the nucleus in transcriptional control of target genes. The fact that HEK293T cells lack the GR allowed for screening of transcriptional regulators, which are influenced in their activity by other glucocorticoid mediated signalling pathways (Beck et al. 2008). For instance, the family of Foxo transcription factors was previously discovered and implicated in glucocorticoid mediated muscle atrophy without a functional interactions with the GR (Accili & Arden 2004). In this study, novel transcription factors with altered activity in Dex treated cells were not found, probably because the majority of intracellular signalling pathways triggered by Dex required the presence of GR.

TNF-α induces the transcriptional activity of NF-κB which in turn interacts with diverse proteins thereby influencing probably other pathways (Bouwmeester et al. 2004). In this study, TNF-α caused a change of transcriptional activity in more transcriptional regulators and induced also the greatest fold changes of transcriptional activity of individual transcriptional regulators as compared to the unstimulated setting. Overall, these fold changes were lower when compared to an alternative screen design, in which along with the Gal4 fusion proteins another protein was overexpressed (Amelio et al. 2007). In the latter scenario, the functional interaction of the overexpressed protein with individual factors from the screen is focus of interest. In this context, GR co-

transfection with individual Gal4 fusion proteins from the screen led to stronger fold changes of relative luciferase activity (data not shown). However, this screen design limits the interactions of individual Gal4 fusion protein to those occurring with the overexpressed protein of interest and is therefore not ideal when seeking for novel transcriptional regulators. In summary, the recruitment of endogenous proteins by Dexamethasone or TNF-α triggered signalling induces a relatively low change of transcriptional activity as compared to parallel overexpression of GR or NF-κB but broadens also the list of emerging targets.

Retesting of putative TNF-α targets from the screen revealed that the alterations of relative luciferase activity for the majority of targets could not be reproduced. The reason for this may be either clonal variations in the cell line used for the screen and for retesting, or that some of the TNF-α targets were false positives. Among those tested, two targets, Gal4-GAbpα and Gal4-PSPC1, showed reproducible alterations of transcriptional activity in HEK293T cells. Upon validation of these targets in the murine muscle cell line C2C12, no transcriptional activity was detected for PSPC1. The human PSPC1 protein shares ~ 98.3% consensus positions with the murine PSPC1 protein. This should theoretically allow functional interaction of the human PSCP1 protein to murine proteins in C2C12 cell. However, while GAbpα is ubiquitously expressed, PSPC1 shows strong expression in testis and moderate expression in lung, spleen and ovary. Thus, PSPC1 might not play a crucial role in muscle tissue and hence lack transcriptional activity in muscle cells. Interestingly, the transcriptional activity of GAbpα was similarly altered in the human HEK293T and the murine C2C12 cell line, respectively. The human and murine GAbpα protein shares 97.8% consensus positions, thus allowing for functional interactions of proteins from different species. Therefore, this protein was identified as novel transcriptional regulator with dysregulated activity in TNF-α signalling.

To date, the transcriptional activity of GAbpα in the context of pro-inflammatory signalling has not been investigated. As mentioned before, GAbpα is the DNA-binding component of the heterodimeric Gabp complex, which activates genes of the respiratory chain as well as sub-synaptic target genes (Rosmarin et al. 2004, Virbasius, 1993 #33,

Yang, 2007 #35, Xue, 2007 #34). Moreover, it seemed appealing to investigate, whether altered gene expression patterns of these target genes in muscle cells under pro-inflammatory signalling contribute to the functional disturbances observed in muscle atrophy. While respiratory chain proteins are correlated with energy production through oxidation of sugar or fats, sub-synaptic target genes are crucial for the innervation of muscle cells by the nervous system. A malfunction of oxidative phosphorylation may cause an accumulation of ROS within the cell and thereby cause tissue damage (Giorgio et al. 2007). Likewise, denervation of muscle tissue is known to cause muscle atrophy (Bodine et al. 2001).

4.2 The Transcriptional Active GAbp Heterodimer Dissociates under Pro-Inflammatory Conditions

Regulation of transcriptional activity can be accomplished on the protein level, by protein activity, by functional interaction with other transcriptional regulators or proteins of the basal transcription machinery, or by binding to DNA. In fact, while the DNA binding of GAbpα, and the protein-protein binding between GAbpα and GAbpβ are specific, a multitude of other proteins of the transcription complex can bind in a tissue-specific manner to GAbp (Rosmarin et al. 2004). The Pointed and OST domain of GAbpα are both involved in such interactions (Kang et al. 2008). Also, the N-terminal Ankyrin repeat domain of GAbpβ represents a classical protein-protein interaction domain. In addition, posttranslational modifications are likewise a plausible way to regulate the transcriptional activity of a transcriptional regulator. In this respect, two phosphorylation sites had previously been determined for GAbpα being targeted by Erk and Jnk MAP kinases in NRG stimulated muscle cells (Fromm & Burden 2001).

Due to experimental design, the regulation of GAbp transcriptional activity by DNA-binding could be ruled out, since DNA-binding in the mammalian one-hybrid assay and, hence, also under screen conditions occurred exclusively via the Gal4 DNA binding domain. Equally important for the analysis of the altered transcriptional activity of GAbpα was GAbpβ, since the transcriptional activation domain of the transcriptional active GAbp heterodimer resides on this protein component (Batchelor et al. 1998). Interestingly, the interaction of GAbpα and GAbpβ decreased significantly upon TNF-α

stimulation providing the first hint for the mechanism of TNF-α regulating the transcriptional activity of GAbp. In the past, the domain structure of both GAbpα and GAbpβ has been investigated in detail, thus, providing a useful orientation about defined folding domains of both proteins, which were targeted while preparing corresponding domain deletions (Kang et al. 2008). Deletion of the N-terminally located OST domain of GAbpα caused a decreased interaction of Gal4-GAbpα with Vp16-GAbpβ protein as compared to the full length Gal4-GAbpα protein (Figure 40). This might be explained by other proteins potentially binding to this domain and, thereby, enhancing the binding to GAbpβ. In a recently published study, binding of the histone acetyltransferase CBP/p300 to this domain has been presented (Kang et al. 2008). It is tempting to speculate, whether this component of the basal transcriptional machinery binds in parallel to GAbpβ, thereby, stabilizing the transcriptional active GAbp heterodimer. A similar observation, decreased interaction, was detected upon further deletion of the pointed domain (PNT) and phosphorylation site T280 of Gal4-GAbpα. In addition, truncation of the leucine zipper domain (LeuZip) plus transcriptional activation domain (TAD) and phosphorylation sites (S170, T180) of the Vp16-GAbpβ protein caused likewise a decreased interaction compared to the full length Vp16-GAbpβ protein. A complete loss of the interaction was detected upon deletion of the OST, PNT, and Ets domain together in the Gal4-GAbpα protein. As mentioned earlier, this finding is according to previous studies in which the C-terminus plus the Ets domain of GAbpα were shown to be required for GAbpβ binding (Chinenov et al. 2000). Deletion of the Leucine Zipper domain (LeuZip) in the Vp16-GAbpβ protein increased the interaction to Gal4-GAbpα implying that the binding between both proteins is stronger when homodimerization of GAbpβ is inhibited. Potentially, the direct binding of GAbpα and GAbpβ might be weaker in the heterotetramer due to sterical hindrance.

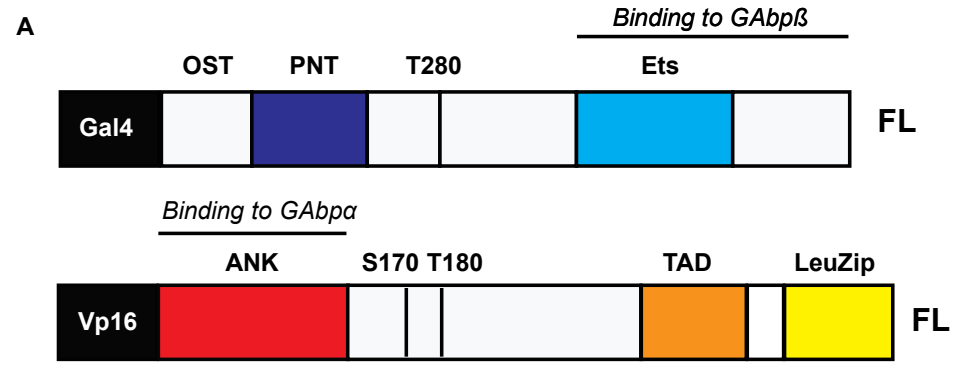

B

	PPI		PPI
Gal4-GAbpα FL	1	Vp16-GAbpß FL	1
Gal4-GAbpα dOST	0.6	Vp16-GAbpß dLeuZip	2.5
Gal4-GAbpα dPNT	0.55	Vp16-GAbpß dTAD	0.6
Gal4-GAbpα dT280	0.7	Vp16-GAbpß dPhoSit	0.5
Gal4-GAbpα dEts	0		

Figure 40: Domain structure of Gal4-GAbpα and Vp16-GAbpβ (A) and alterations of interaction (PPI) detected for corresponding domain deletions via the mammalian two-hybrid assay as compared to the full length protein (B).

TNF-α mediated reduction of the functional interaction occurred with all tested domain deletions of Gal4-GAbpα as well as Vp16-GAbpβ, thus, suggesting that the minimal binding domains are also sufficient for TNF-α mediated dissociation. In addition, phosphorylation was not implicated in this dissociation. This is also in accordance with two recent studies, in which the phosphorylation of GAbpα and GAbpβ were both shown to be dispensable for NRG mediated transcription of AChR (Sunesen et al. 2003, Herndon, 2008 #46).

Importantly, the dissociation of GAbpβ and GAbpα was specific to TNF-α, since other pro-inflammatory cytokines like IFN-γ, IL-6, IL-1β did not decrease the interaction between the minimal binding domains of Vp16-Gabpβ (dPhoSit) and Gal4-GAbpα (dT280). Only conditioned RAW medium decreased this functional interaction to a similar extent as TNF-α alone, thus suggesting that TNF-α release from conditioned macrophages is the specific stimulus for dissociation of the transcriptional active GAbp protein. In summary, the dissociation of GAbpβ and GAbpα represents a novel finding of regulating the transcriptional activity of GAbp under pro-inflammatory conditions in

muscle cells. In addition, the finding that the GAbp complex dissociates upon oxidative stress has not been addressed muscle cells so far. In previous studies the DNA binding activity of GAbp was inhibited by pro-oxidant conditions in 3T3 cells (Martin et al. 1996). In addition, modification of Cys421 in GAbpα was identified to inhibit dimerization with GAbpβ *in vitro*; however, GAbp dissociation has not been addressed by *in vivo* techniques (Chinenov et al. 1998). Therefore, this is the first report of redox regulated GAbp activity in muscle cells. This finding is of major interest, since ROS have been suggested to mediate the intracellular signalling pathways of TNF-α and modulate many inflammation-induced alterations of muscle function (Garg & Aggarwal 2002, Supinski, 2007 #68). In addition, ROS are implicated in skeletal muscle insulin resistance, which is in turn accompanied by oxidative stress and low-grade inflammation (Wei et al. 2008). Consequently, the identification of GAbp dissociation under pro-inflammatory conditions in muscle cells involving the action of ROS may provide a novel link between inflammatory mediators and the subsequent alteration in muscle specific gene expression.

4.3 Expression of Sub-synaptic Genes is altered Under Pro-Inflammatory Conditions

Ets transcription factors are downstream targets of signalling pathways and can interact with a multitude of proteins of the transcription complex in a cell-type specific manner (Sharrocks 2001). This characteristic is highlighted by ubiquitous expression of GAbp; however, liver, muscle and hematopoietic cells represent the major tissue sites for GAbp (Rosmarin et al. 2004). In muscle tissue, GAbp organizes the neuromuscular junction (NMJ) by activating transcription of sub-synaptic genes in the innervated muscle cell (Briguet & Ruegg 2000). The presence of the NBox, a consensus-motif for binding of GAbp, in the promoter sequences of these genes drives the compartmentalized transcription of AChRε for instance. Consequently, it was of specific interest to analyze whether GAbp dissociation under pro-inflammatory conditions finally results in a reduced expression of sub-synaptic target genes in muscle cells.

Analysis of an artificial 3xNBox promoter in C2C12 cells confirmed the previously described NRG mediated induction of NBox containing promoter activity (Lee et al. 2004). Since GAbp was identified as the protein binding component of the NBox, it is plausible that induction of NBox containing promoter activity occurs through recruitment of endogenous GAbp to the NBox consensus motif (Schaeffer et al. 1998).

Stimulation with TNF-α alone did not alter the promoter activity, probably because under basal conditions the endogenous complex is not bound to DNA and hence a dissociation of the complex in solution does not have an impact on gene expression. As alternative explanation, the endogenous GAbp complex might be stabilized by other proteins of the basal transcription complex in TNF-α treated cells. Under the same conditions, the access of these proteins in the mammalian two-hybrid assay might be sterically hindered due to the Gal4 and Vp16 tags. Interestingly, NRG treatment in the context of the mammalian two-hybrid assay did not increase the interaction between GAbpα and GAbpβ (data not shown), which is in accordance with a previous study proposing that both subunits form a stable heterodimer in solution (Chinenov et al. 2000). However, NRG stimulation in the presence of TNF-α did significantly restrict 3xNBox-promoter activity, even though the significance test for interaction between both parameters (NRG and TNF-α stimulation) was not significant (Interaction P = 0.0863) probably due to low sample number. In this scenario, NRG drives probably the recruitment of the GAbp complex to NBox consensus motif while TNF-α counteracts this transcriptional activation process by causing a dissociation of both proteins.

This finding is highlighted by promoter assays in C2C12 cells using the natural AChRε promoter, where TNF-α efficiently restricts NRG mediated increase of AChRε promoter activity. In this case, the NRG-mediated induction of promoter activity was even more pronounced, thus, suggesting, that further regulatory motifs in the promoter sequence and/or further transcriptional regulators and proteins of the basal transcription machinery modulate promoter activity. Surprisingly, TNF-α treatment alone caused an upregulation of AChRε promoter activity. As mentioned before, this can be explained by the fact, that a 300 bp AChRε promoter fragment contains even more regulatory sequences (for example the E-Box), which contribute to AChRε promoter activity, than

the artificial 3xNBox promoter. Alternatively, NRG-mediated AChRε-expression has been previously correlated with activation of the c-JUN N-terminal kinase (JNK) (Si et al. 1999). Since TNF-α can likewise activate JNK, this may explain the relatively mild activation of AChRε-promoter activity by TNF-α treatment (Kamata et al. 2005).

Thereafter, the specificity of this finding was addressed by comparison with other pro-inflammatory cytokines. While IFN-γ and IL-1β did significantly inhibit NRG induced AChRε-promoter activity, the corresponding AChRε mRNA levels were not dramatically altered in C2C12 myotubes. Analysis of LPS and IL-6 led so similar results. Moreover, the interaction between cytokine and NRG was significant for all cytokines tested in the AChRε promoter studies, but failed to obtain significance status in the corresponding qRT-PCR analysis. In the latter, the interaction was only significant for TNF-α and CM-RAW. Thus, IFN-γ, IL-1β, LPS, and IL-6 have less impact on inhibiting NRG mediated increase of AChRε mRNA levels. TNF-α treatment alone did not alter AChRε mRNA levels but blocked efficiently NRG mediated increase in AChRε mRNA levels. Interestingly, CM-RAW did not only inhibit NRG mediated increase of AChRε mRNA levels to a similar extent like TNF-α, but decreased the very same also in the absence of NRG. In short, CM-RAW and TNF-α do efficiently block NRG mediated increase of AChRε gene expression. This is in accordance with the above described finding from the mammalian two-hybrid assay, where TNF-α stimulation alone likewise contributed significantly to GAbp dissociation as the treatment with CM-RAW. Most importantly, oxidative stress decreased also AChRε mRNA levels in C2C12 myotubes. Despite the fact, that this change was not significant due to a relatively high standard error mean, the trend is a novel finding. Concomitant treatment with ROS inhibitors dramatically rescued this inhibition as well as the TNF-α mediated decrease of AChRε mRNA levels, thus linking pro-inflammatory conditions to decreased gene expression of sub-synaptic GAbp target genes by activation of ROS. Interestingly, the activity of an artificial GAbp responsive promoter was decreased in 3T3 cells upon depletion of the ROS-scavenging peptide glutathione supporting the finding presented in this study in muscle cells (Martin et al. 1996). Strikingly, expression levels of mitochondrial GAbp target genes, which function in the oxidative phosphorylation (i.e. ATP synthase, cytochrome oxidase subunits IV and Vb), were not

altered under these settings (data not shown) suggesting that the transcriptional activity of GAbp is subjected to context- and tissue-specific regulation.

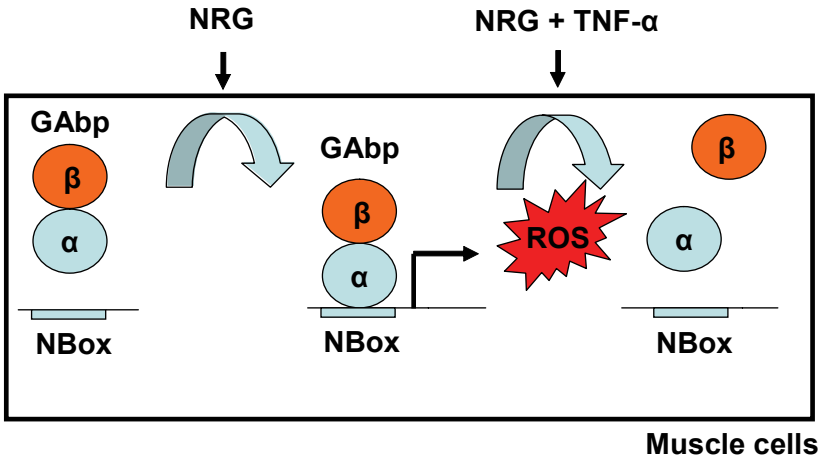

Figure 41: Proposed model of regulation of transcriptional activity of GAbp by ROS in muscle cells under pro-inflammatory conditions. NRG stimulation causes binding of GAbp to NBox consensus motifs within promoter sequences of sub-synaptic target genes and increases thereby the transcription of the these genes. This expression is significantly decreased in muscle cells during pro-inflammatory stimulation through activation of ROS and concomitant dissociation of GAbp.

To summarize, this study gives rise to following molecular model for linking pro-inflammatory conditions to novel altered gene expression pathways in muscle cells. Stimulation of muscle cells with TNF-α decreases expression of GAbp sub-synaptic target genes by activation of ROS, and dissociation of the transcriptional active GAbp heterodimer (Figure 41). As mentioned before, the activity of Foxo proteins is regulated by phosphorylation thereby targeting the up-regulation of ubiquitin ligases in different models of muscle atrophy (Sandri et al. 2004; Stitt et al. 2004). The redox regulation of the Ets transcription factor GAbp and concomitant altered expression of sub-synaptic target genes will contribute to the elucidation of the molecular mechanisms in atrophic signalling. Thereby, this study extends the previous discovery of muscle proteins being targeted in muscle atrophy (i.e. myosin, MyoD) to those proteins crucial for the proper innervation of muscle tissue, a yet unknown link.

So far, no study has addressed the NRG mediated formation of the transcriptional active heterodimer or heterotetramer on NBox containing DNA sequences *in vivo*. Preliminary chromatin immunoprecipitation experiments in C2C12 myotubes, which have been

performed in this study (data not shown) to investigate the dissociation of GAbp on the AChRε promoter in C2C12 myotubes under pro-inflammatory conditions, suggest a link of GAbp dissociation to AChRε gene expression. However, due to the low abundance of GAbpα and GAbpβ in muscle cells, enrichment of GAbpβ binding upon NRG treatment was very low (~ 1.5-fold). Despite this fact, less GAbpβ binding was detectable by co-stimulation with NRG plus TNF-α treatment, thus providing a link between GAbp dissociation and altered AChRε gene expression. In addition, a direct evidence for the implication of GAbp dissociation in reduction of AChRε gene expression in muscle cells under pro-inflammatory conditions can be investigated by overexpression of TNF-α resistant GAbp in muscle cells. In this context, the presence of redox sensitive Cys-residues within the N-terminal binding domain of GAbpα suggests that these residues maybe targeted by ROS (Chinenov et al. 1998).

In the past, NF-κB and activator protein (AP)-1 have already been identified as redox regulated transcription factors (Sen & Packer 1996). While redox sensitive Cys residues of GAbpα are implicated in heterodimerization with GAbpβ, this redox regulation has never been investigated in muscle cells. A decreased expression of sub-synaptic target genes in muscle cells, which is described in this study, suggests that inflammatory conditions may cause denervation of muscle cells through induction of ROS species and subsequent dissociation of the transcriptional active GAbp heterodimer. Unbalanced ROS levels cause damage to cells by oxidation of DNA, protein and membrane damage. In this context, ROS are probably implicated in Duchenne muscular dystrophy (DMD), a degenerative neuromuscular disease (Whitehead et al. 2006). Interestingly, transcript levels of AChRε were found to be significantly decreased in the skeletal tissue from of Colon26 mice, a model for cancer cachexia, thus, supporting the finding presented in this study from cell culture experiments. Finally, it is tempting to speculate, that muscle wasting, which is also observed in elderly people, arises from accumulation of ROS during ageing and concomitant denervation by above mentioned molecular pathway.

5 References

Accili, D. & Arden, K. C. 2004 FoxOs at the crossroads of cellular metabolism, differentiation, and transformation. *Cell* **117**, 421-6.

Acharyya, S., Ladner, K. J., Nelsen, L. L., Damrauer, J., Reiser, P. J., Swoap, S. & Guttridge, D. C. 2004 Cancer cachexia is regulated by selective targeting of skeletal muscle gene products. *J Clin Invest* **114**, 370-8.

Amelio, A. L., Miraglia, L. J., Conkright, J. J., Mercer, B. A., Batalov, S., Cavett, V., Orth, A. P., Busby, J., Hogenesch, J. B. & Conkright, M. D. 2007 A coactivator trap identifies NONO (p54nrb) as a component of the cAMP-signaling pathway. *Proc Natl Acad Sci U S A* **104**, 20314-9.

Batchelor, A. H., Piper, D. E., de la Brousse, F. C., McKnight, S. L. & Wolberger, C. 1998 The structure of GABPalpha/beta: an ETS domain- ankyrin repeat heterodimer bound to DNA. *Science* **279**, 1037-41.

Beck, I. M., Vanden Berghe, W., Vermeulen, L., Bougarne, N., Vander Cruyssen, B., Haegeman, G. & De Bosscher, K. 2008 Altered subcellular distribution of MSK1 induced by glucocorticoids contributes to NF-kappaB inhibition. *Embo J* **27**, 1682-93.

Beutler, B. & Cerami, A. 1986 Cachectin and tumour necrosis factor as two sides of the same biological coin. *Nature* **320**, 584-8.

Bodine, S. C., Latres, E., Baumhueter, S., Lai, V. K., Nunez, L., Clarke, B. A., Poueymirou, W. T., Panaro, F. J., Na, E., Dharmarajan, K., Pan, Z. Q., Valenzuela, D. M., DeChiara, T. M., Stitt, T. N., Yancopoulos, G. D. & Glass, D. J. 2001 Identification of ubiquitin ligases required for skeletal muscle atrophy. *Science* **294**, 1704-8.

Bouwmeester, T., Bauch, A., Ruffner, H., Angrand, P. O., Bergamini, G., Croughton, K., Cruciat, C., Eberhard, D., Gagneur, J., Ghidelli, S., Hopf, C., Huhse, B., Mangano, R., Michon, A. M., Schirle, M., Schlegl, J., Schwab, M., Stein, M. A., Bauer, A., Casari, G., Drewes, G., Gavin, A. C., Jackson, D. B., Joberty, G., Neubauer, G., Rick, J., Kuster, B. & Superti-Furga, G. 2004 A physical and functional map of the human TNF-alpha/NF-kappa B signal transduction pathway. *Nat Cell Biol* **6**, 97-105.

Briguet, A. & Ruegg, M. A. 2000 The Ets transcription factor GABP is required for postsynaptic differentiation in vivo. *J Neurosci* **20**, 5989-96.

Cai, D., Frantz, J. D., Tawa, N. E., Jr., Melendez, P. A., Oh, B. C., Lidov, H. G., Hasselgren, P. O., Frontera, W. R., Lee, J., Glass, D. J. & Shoelson, S. E. 2004 IKKbeta/NF-kappaB activation causes severe muscle wasting in mice. *Cell* **119**, 285-98.

REFERENCES

Calle, E. E. & Kaaks, R. 2004 Overweight, obesity and cancer: epidemiological evidence and proposed mechanisms. *Nat Rev Cancer* **4**, 579-91.

Chinenov, Y., Henzl, M. & Martin, M. E. 2000 The alpha and beta subunits of the GA-binding protein form a stable heterodimer in solution. Revised model of heterotetrameric complex assembly. *J Biol Chem* **275**, 7749-56.

Chinenov, Y., Schmidt, T., Yang, X. Y. & Martin, M. E. 1998 Identification of redox-sensitive cysteines in GA-binding protein-alpha that regulate DNA binding and heterodimerization. *J Biol Chem* **273**, 6203-9.

Clarke, B. A., Drujan, D., Willis, M. S., Murphy, L. O., Corpina, R. A., Burova, E., Rakhilin, S. V., Stitt, T. N., Patterson, C., Latres, E. & Glass, D. J. 2007 The E3 Ligase MuRF1 degrades myosin heavy chain protein in dexamethasone-treated skeletal muscle. *Cell Metab* **6**, 376-85.

de Kerchove D'Exaerde, A., Cartaud, J., Ravel-Chapuis, A., Seroz, T., Pasteau, F., Angus, L. M., Jasmin, B. J., Changeux, J. P. & Schaeffer, L. 2002 Expression of mutant Ets protein at the neuromuscular synapse causes alterations in morphology and gene expression. *EMBO Rep* **3**, 1075-81.

del Aguila, L. F., Claffey, K. P. & Kirwan, J. P. 1999 TNF-alpha impairs insulin signaling and insulin stimulation of glucose uptake in C2C12 muscle cells. *Am J Physiol* **276**, E849-55.

Duclert, A., Savatier, N. & Changeux, J. P. 1993 An 83-nucleotide promoter of the acetylcholine receptor epsilon-subunit gene confers preferential synaptic expression in mouse muscle. *Proc Natl Acad Sci U S A* **90**, 3043-7.

Fromm, L. & Burden, S. J. 2001 Neuregulin-1-stimulated phosphorylation of GABP in skeletal muscle cells. *Biochemistry* **40**, 5306-12.

Garg, A. K. & Aggarwal, B. B. 2002 Reactive oxygen intermediates in TNF signaling. *Mol Immunol* **39**, 509-17.

Giorgio, M., Trinei, M., Migliaccio, E. & Pelicci, P. G. 2007 Hydrogen peroxide: a metabolic by-product or a common mediator of ageing signals? *Nat Rev Mol Cell Biol* **8**, 722-8.

Goldberg, A. L. 1969 Protein turnover in skeletal muscle. II. Effects of denervation and cortisone on protein catabolism in skeletal muscle. *J Biol Chem* **244**, 3223-9.

Gomes, M. D., Lecker, S. H., Jagoe, R. T., Navon, A. & Goldberg, A. L. 2001 Atrogin-1, a muscle-specific F-box protein highly expressed during muscle atrophy. *Proc Natl Acad Sci U S A* **98**, 14440-5.

Guttridge, D. C., Mayo, M. W., Madrid, L. V., Wang, C. Y. & Baldwin, A. S., Jr. 2000 NF-kappaB-induced loss of MyoD messenger RNA: possible role in muscle decay and cachexia. *Science* **289**, 2363-6.

REFERENCES

Hotamisligil, G. S. 2006 Inflammation and metabolic disorders. *Nature* **444**, 860-7.

Houstis, N., Rosen, E. D. & Lander, E. S. 2006 Reactive oxygen species have a causal role in multiple forms of insulin resistance. *Nature* **440**, 944-8.

Jaworski, A., Smith, C. L. & Burden, S. J. 2007 GA-binding protein is dispensable for neuromuscular synapse formation and synapse-specific gene expression. *Mol Cell Biol* **27**, 5040-6.

Kamata, H., Honda, S., Maeda, S., Chang, L., Hirata, H. & Karin, M. 2005 Reactive oxygen species promote TNFalpha-induced death and sustained JNK activation by inhibiting MAP kinase phosphatases. *Cell* **120**, 649-61.

Kang, H. S., Nelson, M. L., Mackereth, C. D., Scharpf, M., Graves, B. J. & McIntosh, L. P. 2008 Identification and structural characterization of a CBP/p300-binding domain from the ETS family transcription factor GABP alpha. *J Mol Biol* **377**, 636-46.

Langen, R. C., Van Der Velden, J. L., Schols, A. M., Kelders, M. C., Wouters, E. F. & Janssen-Heininger, Y. M. 2004 Tumor necrosis factor-alpha inhibits myogenic differentiation through MyoD protein destabilization. *Faseb J* **18**, 227-37.

Lee, H. H., Choi, R. C., Ting, A. K., Siow, N. L., Jiang, J. X., Massoulie, J. & Tsim, K. W. 2004 Transcriptional regulation of acetylcholinesterase-associated collagen ColQ: differential expression in fast and slow twitch muscle fibers is driven by distinct promoters. *J Biol Chem* **279**, 27098-107.

Li, Y. P., Schwartz, R. J., Waddell, I. D., Holloway, B. R. & Reid, M. B. 1998 Skeletal muscle myocytes undergo protein loss and reactive oxygen-mediated NF-kappaB activation in response to tumor necrosis factor alpha. *Faseb J* **12**, 871-80.

Livak, K. J., Flood, S. J., Marmaro, J., Giusti, W. & Deetz, K. 1995 Oligonucleotides with fluorescent dyes at opposite ends provide a quenched probe system useful for detecting PCR product and nucleic acid hybridization. *PCR Methods Appl* **4**, 357-62.

Ma, K., Mallidis, C., Bhasin, S., Mahabadi, V., Artaza, J., Gonzalez-Cadavid, N., Arias, J. & Salehian, B. 2003 Glucocorticoid-induced skeletal muscle atrophy is associated with upregulation of myostatin gene expression. *Am J Physiol Endocrinol Metab* **285**, E363-71.

Martin, M. E., Chinenov, Y., Yu, M., Schmidt, T. K. & Yang, X. Y. 1996 Redox regulation of GA-binding protein-alpha DNA binding activity. *J Biol Chem* **271**, 25617-23.

McKay, L. I. & Cidlowski, J. A. 1999 Molecular control of immune/inflammatory responses: interactions between nuclear factor-kappa B and steroid receptor-signaling pathways. *Endocr Rev* **20**, 435-59.

REFERENCES

McKinnell, I. W. & Rudnicki, M. A. 2004 Molecular mechanisms of muscle atrophy. *Cell* **119**, 907-10.

Medzhitov, R. 2008 Origin and physiological roles of inflammation. *Nature* **454**, 428-35.

Mejat, A., Ravel-Chapuis, A., Vandromme, M. & Schaeffer, L. 2003 Synapse-specific gene expression at the neuromuscular junction. *Ann N Y Acad Sci* **998**, 53-65.

Naldini, L. 1998 Lentiviruses as gene transfer agents for delivery to non-dividing cells. *Curr Opin Biotechnol* **9**, 457-63.

O'Leary, D. A., Koleski, D., Kola, I., Hertzog, P. J. & Ristevski, S. 2005 Identification and expression analysis of alternative transcripts of the mouse GA-binding protein (Gabp) subunits alpha and beta1. *Gene* **344**, 79-92.

O'Leary, D. A., Noakes, P. G., Lavidis, N. A., Kola, I., Hertzog, P. J. & Ristevski, S. 2007 Targeting of the ETS factor GABPalpha disrupts neuromuscular junction synaptic function. *Mol Cell Biol* **27**, 3470-80.

Ohno, K., Anlar, B. & Engel, A. G. 1999 Congenital myasthenic syndrome caused by a mutation in the Ets-binding site of the promoter region of the acetylcholine receptor epsilon subunit gene. *Neuromuscul Disord* **9**, 131-5.

Oliff, A., Defeo-Jones, D., Boyer, M., Martinez, D., Kiefer, D., Vuocolo, G., Wolfe, A. & Socher, S. H. 1987 Tumors secreting human TNF/cachectin induce cachexia in mice. *Cell* **50**, 555-63.

Popkin, B. M. 2007 Understanding global nutrition dynamics as a step towards controlling cancer incidence. *Nat Rev Cancer* **7**, 61-7.

Renz, H., Henke, A., Hofmann, P., Wolff, L. J., Schmidt, A., Ruschoff, J. & Gemsa, D. 1992 Sensitization of rat alveolar macrophages to enhanced TNF-alpha release by in vivo treatment with dexamethasone. *Cell Immunol* **144**, 249-57.

Ristevski, S., O'Leary, D. A., Thornell, A. P., Owen, M. J., Kola, I. & Hertzog, P. J. 2004 The ETS transcription factor GABPalpha is essential for early embryogenesis. *Mol Cell Biol* **24**, 5844-9.

Rosmarin, A. G., Resendes, K. K., Yang, Z., McMillan, J. N. & Fleming, S. L. 2004 GA-binding protein transcription factor: a review of GABP as an integrator of intracellular signaling and protein-protein interactions. *Blood Cells Mol Dis* **32**, 143-54.

Sacheck, J. M., Ohtsuka, A., McLary, S. C. & Goldberg, A. L. 2004 IGF-I stimulates muscle growth by suppressing protein breakdown and expression of atrophy-related ubiquitin ligases, atrogin-1 and MuRF1. *Am J Physiol Endocrinol Metab* **287**, E591-601.

REFERENCES

Sandri, M., Sandri, C., Gilbert, A., Skurk, C., Calabria, E., Picard, A., Walsh, K., Schiaffino, S., Lecker, S. H. & Goldberg, A. L. 2004 Foxo transcription factors induce the atrophy-related ubiquitin ligase atrogin-1 and cause skeletal muscle atrophy. *Cell* **117**, 399-412.

Schaeffer, L., Duclert, N., Huchet-Dymanus, M. & Changeux, J. P. 1998 Implication of a multisubunit Ets-related transcription factor in synaptic expression of the nicotinic acetylcholine receptor. *Embo J* **17**, 3078-90.

Sen, C. K. & Packer, L. 1996 Antioxidant and redox regulation of gene transcription. *Faseb J* **10**, 709-20.

Sharrocks, A. D. 2001 The ETS-domain transcription factor family. *Nat Rev Mol Cell Biol* **2**, 827-37.

Si, J., Wang, Q. & Mei, L. 1999 Essential roles of c-JUN and c-JUN N-terminal kinase (JNK) in neuregulin-increased expression of the acetylcholine receptor epsilon-subunit. *J Neurosci* **19**, 8498-508.

Stitt, T. N., Drujan, D., Clarke, B. A., Panaro, F., Timofeyva, Y., Kline, W. O., Gonzalez, M., Yancopoulos, G. D. & Glass, D. J. 2004 The IGF-1/PI3K/Akt pathway prevents expression of muscle atrophy-induced ubiquitin ligases by inhibiting FOXO transcription factors. *Mol Cell* **14**, 395-403.

Strassmann, G., Patil-Koota, V., Finkelman, F., Fong, M. & Kambayashi, T. 1994 Evidence for the involvement of interleukin 10 in the differential deactivation of murine peritoneal macrophages by prostaglandin E2. *J Exp Med* **180**, 2365-70.

Sunesen, M., Huchet-Dymanus, M., Christensen, M. O. & Changeux, J. P. 2003 Phosphorylation-elicited quaternary changes of GA binding protein in transcriptional activation. *Mol Cell Biol* **23**, 8008-18.

Tanaka, Y., Eda, H., Tanaka, T., Udagawa, T., Ishikawa, T., Horii, I., Ishitsuka, H., Kataoka, T. & Taguchi, T. 1990 Experimental cancer cachexia induced by transplantable colon 26 adenocarcinoma in mice. *Cancer Res* **50**, 2290-5.

Tintignac, L. A., Lagirand, J., Batonnet, S., Sirri, V., Leibovitch, M. P. & Leibovitch, S. A. 2005 Degradation of MyoD mediated by the SCF (MAFbx) ubiquitin ligase. *J Biol Chem* **280**, 2847-56.

Tiscornia, G., Singer, O. & Verma, I. M. 2006 Production and purification of lentiviral vectors. *Nat Protoc* **1**, 241-5.

Tisdale, M. J. 2002 Cachexia in cancer patients. *Nat Rev Cancer* **2**, 862-71.

Tsuruo, T., Yamori, T., Naganuma, K., Tsukagoshi, S. & Sakurai, Y. 1983 Characterization of metastatic clones derived from a metastatic variant of mouse colon adenocarcinoma 26. *Cancer Res* **43**, 5437-42.

REFERENCES

Wei, Y., Chen, K., Whaley-Connell, A. T., Stump, C. S., Ibdah, J. A. & Sowers, J. R. 2008 Skeletal muscle insulin resistance: role of inflammatory cytokines and reactive oxygen species. *Am J Physiol Regul Integr Comp Physiol* **294**, R673-80.

Whitehead, N. P., Yeung, E. W. & Allen, D. G. 2006 Muscle damage in mdx (dystrophic) mice: role of calcium and reactive oxygen species. *Clin Exp Pharmacol Physiol* **33**, 657-62.

Witzemann, V., Schwarz, H., Koenen, M., Berberich, C., Villarroel, A., Wernig, A., Brenner, H. R. & Sakmann, B. 1996 Acetylcholine receptor epsilon-subunit deletion causes muscle weakness and atrophy in juvenile and adult mice. *Proc Natl Acad Sci U S A* **93**, 13286-91.

Wiznerowicz, M., Szulc, J. & Trono, D. 2006 Tuning silence: conditional systems for RNA interference. *Nat Methods* **3**, 682-8.

Yaffe, D. & Saxel, O. 1977 Serial passaging and differentiation of myogenic cells isolated from dystrophic mouse muscle. *Nature* **270**, 725-7.

6 Materials

6.1 Instruments

Product	Distributor
Centrifuge (Super T 21)	Sorvall
Centrifuge (Minifuge, RF)	Heraeus
Centrifuge (Mikro 22R)	Hettich GmbH & Co KG
Centrifuge (Labofuge 400R)	Heraeus
Centrifuge (Biofuge pico)	Heraeus
Centrifuge (Biofuge fresco)	Heraeus
CO_2 Incubators	SANYO
Elektrophoresis *Power Supply*, *Power Pac HC/Basic*	Bio-Rad
Gel Doc Apparatus	Bio-Rad
Gene Pulser II	Bio-Rad
iCycler Thermal Cycler	Bio-Rad
SDS Gel Apparatus	Bio-Rad
Table Centrifuge (miniSpin plus)	Neolab
Thermomixed comfort	Eppendorf
Real time PCR System 7300	Applied Biosystems
SW28 Ti rotor	Beckman
TissueLyser	QIAGEN
NanoDrop, ND-1000 Spectrophotometer	Peqlab
Microscope, Axiovert 40 CFL	Carl Zeiss
Multidrop 384	Thermo Scientific
Luminometer *microplate* Mithras LB 940	Berthold technologies
Sonifier W-250	Branson
1430 ultra(HTS) microplate Imager ViewLux System	PerkinElmer
Ultracentrifuge XL-70	Beckman
Ultrospec 3000pro UV/Visible Spectrophotomoeter	GE Healthcare Life Sciences

6.2 Consumables

Product	Distributor
Tissue Culture Plates (12-well plates)	Nunc
Tissue Culture Plates (10 cm, 15 cm, 6-well)	Falcon
96-well plates (black, transparent)	Nunc

6.3 Chemicals & Cytokines

All routinely used chemicals were purchased from Roth.

Product	Distributor
Agrin, recombinant rat C-terminal	R&D Systems
Albumin, Bovine Fraction V solution (30%), sterile filtered	Sigma
Ampicillin	Sigma
Bio-Rad Protein Assay (Bradford Reagent)	Bio-Rad
BrightLite	PerkinElmer
Bovine Serum Albumine (BSA), 10 mg/ mL	NEB
Centrifuge tubes, Polyallomer quickseal	Beckman Coulter
Chloramphenicol	Sigma
Calf Intestine Phosphatase (CIP)	NEB
Crystal Violet Solution	Sigma
Dexamethasone	Sigma
DMEM, 4500 mg/L D-Glucose, with Glutamine	Invitrogen
DNase/RNase free Water	Invitrogen
DNase set	QIAGEN
Fetal Calf Serum (FCS)	Invitrogen
Gene Ruler™ 1kb DNA Ladder	Fermentas
Geneticin	Invitrogen
Hyperfilm™ ECL	GE Healthcare, Amersham
Hyperfilm™ ECL Western Blotting Detection Reagents	GE Healthcare, Amersham
IgG-HRP (anti-mouse, anti-rabbit)	Bio-Rad
Interferon-γ, recombinant, mouse (mIFN- γ)	Roche Diagnostics
Interleukin 1 beta, recombinant, mouse	USBiological
Interleukin 6, recombinant, mouse	USBiological
T4 DNA-Ligase (400 kU/ mL)	NEB

Kanamycin	Sigma
L-Glutamine	Invitrogen
Lipofectamine™ Reagent	Invitrogen
Lipopolysaccharides *E.coli*	Sigma
Luciferin	Sigma
Mass Ruler™ Low range DNA Ladder	Fermentas
MEM Non-Essential Amino Acids	Invitrogen
Neuregulin, human NRG-β1/HRG-β1 EGF domain	R&D Systems
Nitrocellulose Membrane (0,45 µm)	Schleicher und Schuell
o-Nitrophenyl-β-D-galactopyranosid (ONPG)	Sigma
Nonidet NP40 (equivalent to Igepal)	Sigma
NZY Medium	Roth
Opti-MEM I	Invitrogen
Orange G	Sigma
Page Ruler™ Unstained Protein Ladder	Fermentas
Penicillin/Streptomycin (P/S)	Invitrogen
Pepstatin	Sigma
Phusion™ High-Fidelity DNA Polymerase (2 U/ mL)	Finnzymes
Platinum® Quantitative PCR SuperMix	Invitrogen
PMSF	Sigma
Polybrene (Hexadimethrine Bromide)	Sigma
Protein A/G PLUS-Agarose	SCBT
Protein A Agarose/ Salmon Sperm DNA	Upstate
QIAshredder Column	QIAGEN
QIAZOL	QIAGEN
Restriction Enzymes	NEB
RNaseZAP®	Sigma
Sodium Pyruvate (100 mM), sterile filtered	Sigma
Tissue Culture dishes/plates	Falcon
TNF-α, human recombinant	Alexis Biochemicals
TNF-α, murine recombinant	Biomol
Trypsine-EDTA (0.25%)	Invitrogen
Zeocin™	Invitrogen

6.4 Kits

Product	Vendor
2-D Quant Kit	Amersham
Block-iT™ Lentiviral Pol II miR RNAi Expression System	Invitrogen
Block-iT™ Pol II miR RNAi Expression Vector Kits	Invitrogen
First Strand cDNA Synthesis Kit	Fermentas
Gene Eraser™ Luciferase Suppression-Test System	Stratagene
PureLink7™ HiPure Plasmid FP Maxiprep Kit	Invitrogen
Qiaprep Plasmid Miniprep Kit	QIAGEN
QIAquick PCR Purification Kit	QIAGEN
Qiaquick Gel Extraction Kit	QIAGEN
RNeasy Mini Kit	QIAGEN

6.5 Bacterial Cells

E.coli	Source/Origin
XL1-blue	Stratagene
OneShot Stbl3	Invitrogen
OneShot TOP10	Invitrogen
XL10-Gold	Stratagene

6.6 Mammalian Cell Lines

Cell Lines	Source/Origin
C2C12 LP	L. Puri, Burnham Institute
C2C12 S	Sigma
RAW 264.6	R. Zawatzky, DKFZ
HEK293FT	Invitrogen
HEK293T	S. Herzig, DKFZ
HEK293	S. Herzig, DKFZ

6.7 Antibodies

Antibody	Final Dilution	Species	Company	Cat. No #
Gabpa (G-1)	1:200 – 1:1000	Mouse monoclonal	SCBT	Sc-28312
Gabpa (H-180)		Rabbit polyclonal	SCBT	Sc-22810
GAbpb2 (A01)	1:200 – 1:1000	Mouse polyclonal	Abnova	H00002553-A01

GAL4 (DBD)	1:500	Rabbit polyclonal	SCBT	Sc-577
GAL4, DNA binding domain mouse mAB (8C-1)	1:2000	Mouse monoclonal	Calbiochem	345766
Myosin skeletal (fast) clone MY-32	1:5000	Mouse monoclonal	Sigma	M 4276
VCP	1:10000	Mouse monoclona	abcam	Ab11433

6.8 Oligodesoxyribonucleotides

6.8.1 Oligodesoxyribonucleotides for plasmid cloning

Primer Name	**Oligonucleotide**	**Resulting Plasmid**
Gabpα pos447 for	TTTTTGCGGCCGCATGACTAAGAGAGAAGCAGAAGAG	pTarget-Gabpα-ORF
Gabpα pos2401 rev	TTTTTGCGGCCGCAATAGTGGTTTGAGTTAAGCCAGC	
Gabpα pos2443 for	TTTTTGCGGCCGCTTATTCATTATGTCAAGCCAAGGTC	pTarget-Gabpα-3'UTR
Gabpα pos4767 rev	TTTTTGCGGCCGCTCCCTTCTACAAAAGACTCAAGAG	
AChRe Mm promoter for	TTTTTGGTACCGCCTTGTGGATTACAGAACTGGCTGAAACC	pGL3-AChRe
AChRe Mm promoter rev	TTTTTGCTAGCCTGACCCCTGTACCCTACCAAAGAGTGTCAGG	
N-Box mut mAChRe prom for	CAGTCCCCAAACCTAGCGGATCCCTAACACCC	pGL3-AChRe-NBox*mut*
N-Box mut mAChRe prom rev	GAAGGGGAGGAGGGTGTTAGGGATCCGCTAGGTTTG	
GAbpβ for	TTTTTGCTAGCGTAATGTCCCTGGTAGATTTGGGGAAG	pcDNA3.1 (-)Gabpβ
GAbpβ rev	TTTTTCTCGAGCTAAACGGCTTCTTTGTTGGTCTGG	
GAbpβ Vp16 for	TTTTTGGTACCTCCCTGGTAGATTTGGGGAAGAAG	Vp16-Gabpβ
GAbpβ Vp16 rev	TTTTTGCTAGCCTAAACGGCTTCTTTGTTGGTCTG	

GAbpβ dLeuZip rev	TTTTTGCTAGCCTCCGGGTTGGTGTTGATTTGGTTC	dLeuZip
GAbpβ dTAD rev	TTTTTGCTAGCTTCAATTTCTGCACATTCCACCCG	dTAD
GAbpβ dPhoSit rev	TTTTTGCTAGCCTGACCCCCTGAGCTAACTACTTGCTG	dPhoSit
Gabpa AscI rev	TTTTTGGCGCGCCAATCTCTTTGTCTGCCTGTAGAGAG	Gal4-Gabpα deletions
dOST for PacI Gal4-Gabpa	TTTTTTTAATTAACTGGGCTGCTGCACTGGAAGGCTAC	dOST
dPNT for PacI Gal4-Gabpα	TTTTTTTAATTAACATTCCAGCCTCAGTGCCTCCCGC	dPNT
dT280 for PacI Gal4-Gabpα	TTTTTTTAATTAACAACAATGGTCAGATCCAACTATGG	dT280
dEts for PacI Gal4-Gabpα	TTTTTTTAATTAACCGGATGCAGCTGCATGGGATTGCC	dEst

6.8.2 Oligodesoxyribonucleotides for sequencing of plasmids

Oligonucleotide	**Sequenced Plasmid**
CAGCTCTTAAGGCTAGAGTA	pGAL4 for
TGCTCGAAGCATTAACCCTC	pGAL4 rev
CTAGCAAAATAGGCTGTCCC	pGL3 for
CTTTATGTTTTTGGCGTCTTCC	pGL3 rev
GGCCGACTTCGAGTTTGAGC	pVp16 for
CATTGACGTCAATGGGAG	pcDNA3.1(-) for

6.8.3 Oligodesoxyribonucleotides for miRNA cloning

Oligonucleotide	**miRNA ID**
CCTGTAAAGGTTAGAAAAGCTTGGTCAGTCAGTGGCCAAAACCAAGCTT TGCTCTAACCTTTAC	1256 bottom
TGCTGTAAAGGTTAGAGCAAAGCTTGGTTTTGGCCACTGACTGACCAAG CTTTTCTAACCTTTA	1256 top
CCTGACTACAGGCTATCAGACCTGTCAGTCAGTGGCCAAAACAGGTCTG AGCTAGCCTGTAGTC	4216 bottom
TGCTGACTACAGGCTAGCTCAGACCTGTTTTGGCCACTGACTGACAGGTC TGATAGCCTGTAGT	4216 top
CCTGAAGACATTAAGAGTCACAGGTCAGTCAGTGGCCAAAACCTGTGAC	4682 bottom

TGACTTAATGTCTTC
TGCTGAAGACATTAAGTCAGTCACAGGTTTTGGCCACTGACTGACCTGTG 4682 top
ACTCTTAATGTCTT

6.8.4 Plasmids

Plasmid DNA	**Source/Origin**
pCMV ßGal	A. Vegiopoulos, DKFZ
pGAL4 DBD	M.D. Conkright, Scripps
pGAL4 Luc	M.D. Conkright, Scripps
pGAL4 p65	Lienhard Schmitz, University of Bern
pGAL4 GR	S. Stoney Simsons, NIDDK
pGAL4 GAbpa	M.D. Conkright, Scripps
pGAL4 Gabpa dOST	A.M. Gail, DKFZ
pGAL4 Gabpa dPNT	A.M. Gail, DKFZ
pGAL4 Gabpa T280	A.M. Gail, DKFZ
pGAL4 Gabpa Ets	A.M. Gail, DKFZ
pGL3	Promega
pGL3 AChRe	A.M. Gail, DKFZ
pGL3 AChRe Nbox mut	A.M. Gail, DKFZ
pcDNA3.1(-)	Invitrogen
pcDNA3.1(-)GAbpa	A.M. Gail, DKFZ
pcDNA3.1(-)Gabpb1	A.M. Gail, DKFZ
pCMX Vp16	S. Herzig, DKFZ
pVp16 Gabpb	A.M. Gail, DKFZ
pVp16 Gabpb dLeuZip	A.M. Gail, DKFZ
pVp16 Gabpb dTAD	A.M. Gail, DKFZ
pVp16 Gabpb dPhoSit	A.M. Gail, DKFZ
pTarget MCS	Stratagene
pTarget Gabpa ORF	A.M. Gail, DKFZ
pTarget Gabpa 3'UTR	A.M. Gail, DKFZ
pcDNA6.2	Invitrogen
pcDNA6.2 miRNA 1256	A.M. Gail, DKFZ
pcDNA6.2 miRNA 4216	A.M. Gail, DKFZ
pcDNA6.2 miRNA 4682	A.M. Gail, DKFZ
pcDNA6.2 miRNA NC	A.M. Gail, DKFZ
pLenti	Invitrogen
pLenti miRNA GAbpa	A.M. Gail, DKFZ
pLenti miRNA NC	A.M. Gail, DKFZ

pMDL g/p RRE	G. Schütz, DKFZ
pMD2.G	G. Schütz, DKFZ
pRSVrev	G. Schütz, DKFZ

6.8.5 Taqman Probes

Gene Name/Symbol	**ID**
AchRd, Chrnd	Mm00445545_m1
AchRe, Chrne	Mm00437411_m1
ErbB2	Mm00648541_m1
GAbpa	Mm00484598_m1
Gabpb1	Mm00487471_m1
GAPDH	Mm99999915_g1
Musk	Mm00448006_m1
TBP	Mm00446973_m1
Utrophin	Mm01168858_m1

6.9 Media

Differentiation Medium for C2C12 cells	DMEM + 2% FCS + 1% Penicillin-Streptomycin
Freezing Medium for tissue culture	DMEM + 10% DMSO + 20% FCS
Growth Medium for C2C12 cells	DMEM + 20% FCS + 1% Penicillin-Streptomycin
Growth Medium for HEK293 and HEK293T cells	DMEM + 10% FCS + 1% Penicillin-Streptomycin
Growth Medium for HEK293FT cells	DMEM + 10% FCS + 1% Penicillin-Streptomycin + 500µg/mL Geneticin + 0.1 mM MEM Non-Essential Amino Acids + 1 mM Sodium Pyruvate + 6 mM L-glutamine

6.10 Recipes

(if not otherwise indicated, the buffers, media etc. were prepared in the solvent water)

Assay Buffer	15 mM K_3PO_4

	1 mM DTT 2 mM ATP in Gly-Gly Working Solution pH 7.8
2x BBS	50 mM BES 280 mM NaCl 1.5 mM Na_2HPO_4 pH 6.95 with NaOH
Blocking Buffer	PBST + 5% non-fat dry milk
Bromophenolblue (BPB) stock solution	150 mg BPB 90 mg Tris
Ethidium bromide stock solution	10 mg/mL
Gly-Gly Working Solution pH 7.8	25 mM Gly-Gly 15 mM $MgSO_4$ 4 mM EGTA
IP-Buffer (Hardy)	20 mM HEPES/KOH pH 7.4 125 mM NaCl 0.1% Igepal 0.5 mM EDTA 1x PIC
IP-Buffer (Larry)	20 mM HEPES/KOH pH 7.5 150 mM NaCl 1% Triton X-100 1mM EGTA 1.5 mM $MgCl_2$ 10% Glycerol + 1x PIC + 50 mM NaF + 1 mM Na_3VO_4
Harvest Buffer for Luciferase- and ßGalactosidase-Assay	Gly-Gly Working Solution pH 7.8 + 1% Triton X-100 + 1 mM DTT
LB medium	10 g/L Trypton 5 g/L Yeast Extract 10 g/L NaCl pH 7.0
Low salt LB medium	10 g/L Trypton 5 g/L Yeast Extract 5 g/L NaCl pH 7.5
Luciferase-Buffer	Gly-Gly Working Solution pH7.8 + 11.1% (v/v) Luciferase-Mix
Luciferase-Mix	1 mM Luciferin 10 mM DTT
Lysis Buffer for genomic DNA extraction	10 mM Tris pH 8.0

	100 mM NaCl 15 mM EDTA 0.5% SDS 0.5mg/mL Proteinase K
10x MOPS buffer	200 mM MOPS 50 mM NaAc 10 mM EDTA pH 7 ad 1 L RNase free water
ONPG Buffer	0.1 M Sodium phosphate pH 7.5 1 mM $MgCl_2$ 10 mM KCl 1 mg/mL ONPG
6x Orange G DNA loading buffer	10 mM EDTA 70% Glycerol a pinch Orange G
1x PBS	140 mM NaCl 1.5 mM KH_2PO_4 11.3 mM Na_2HPO_4 2.7 mM KCl
1x PBST	PBS 0.1% Tween 20
50x Protease Inhibitor Cocktail (PIC)	50 mM PMSF 50 mM NaF 0.5 mg/mL Leupeptin 0.5 mg/mL Aprotinin 0.5 mg/mL Pepstatin in ethanol
RNA Denaturing Buffer (indicated volumes refer to one RNA sample)	0.5 mg/mL ethidium bromide 0.5x MOPS buffer 66.6% formamide 8.9% formaldehyde 1x loading dye ad 10 µL RNase free water
SDS Running Buffer	25 mM Tris 190 mM Glycine 1% SDS 0.45% HCl
2x SDS Reducing buffer	120 mM Tris/HCl pH6.8 4% (w/v) SDS 20% Glycerol 200 mM DTT 0.01% BPB (1mg/mL)
2x SDS sample buffer + 8 M Urea	8 M Urea 200 mM DTT 120 mM Tris 4% SDS 20% Glycerol

	0.01% Bromphenolblue
Sodium Phosphate (0.1 M pH 7.5)	41 mL of 0.2 M $Na_2HPO_4*2H_2O$ 9 mL 0f 0.2 M $NaH_2PO_4*2\ H_2O$ ad 100 mL H_2O
1x TBE Buffer	45 mM Tris 44 mM Boric Acid 1 mM EDTA
1x TE Buffer	10 mM Tris 1 mM EDTA
1x Transfer Buffer	25 mM Tris 192 mM Glycine 0.01% SDS 20% Methanol